

Enhancing stem cell engraftment and function following corneal stem cell transplantation

A thesis submitted to the Division of Infection and Immunity of
University College London for the degree of Doctor of Philosophy.

Harley James Buck

June 2021

Primary Supervisor: Prof. Emma Morris

DECLARATION

I, Harley James Buck confirm that the work presented in this thesis is my own. Where information has been derived from other sources, I confirm that this has been indicated in the thesis.

Harley Buck

ABSTRACT

Transplantation of limbal epithelial stem cells (LESCs) can be an effective treatment for patients with Limbal Stem Cell Deficiency (LSCD), a condition where loss or damage of corneal stem cells results in painful inflammation and blindness. However, failure rates of both auto- and allografted cultured LESCs are high despite systemic immune suppression, for which the reasons are unclear. This project aimed to investigate variables important for successful engraftment, including graft stem cell composition, the graft bed inflammatory microenvironment, and the role of the immune system in corneal epithelial graft rejection.

We developed a mouse model of LSCD induced by chemical injury, able to accurately recapitulate features of the LSCD phenotype seen in human patients including corneal haze, epithelial defects, and neovascularisation accompanied by significant cellular infiltration into the cornea. We also demonstrated successful regeneration of the LSCD injury by transplanting sheets of corneal epithelium containing LESCs, while tracking engraftment and growth kinetics during wound healing.

Transplant of allogeneic donor derived epithelial grafts demonstrated characteristic signs of graft rejection including significant cellular infiltration into the cornea and expression of inflammatory cytokines and chemokines. Adoptive transfer of fluorescently labelled purified allogeneic immune cell subsets, including CD4⁺ and CD8⁺ T cells, to immunodeficient transplant recipients demonstrated their effect on stable epithelial grafts *in vivo*.

This project also aimed to develop strategies for the isolation and enrichment of LESC from primary human corneas. Several methods of tissue digestion and LESC isolation were compared, and the inflammatory chemokine and cytokine profile of primary human corneal epithelial and stromal cells was investigated *in vitro*.

IMPACT STATEMENT

The surface of the eye is covered by several different types of cells, each with its own role to play in vision. These cells can continuously regenerate themselves thanks to a small number of stem cells located within the limbal region of the cornea. Exposure to chemicals and a variety of diseases can damage these corneal stem cells leading to a condition known as limbal stem cell deficiency. As a result, such patients cannot regenerate the surface of the eye and suffer from blindness and severe discomfort.

The development of better treatments for these patients was identified as a number 1 ranked priority for corneal research in Fight for Sight recent priority setting partnership with the James Lind Alliance, and it was reported by the European Medicines Agency in 2015 that around 15,000 patients suffered from LSCD at that time. More recent studies estimate around 240 new cases per year in the UK. This disease has a vast impact on patients, with corneal diseases representing a major cause of blindness worldwide, second only to cataracts.

Currently the only treatment able to restore sight in these patients is a corneal stem cell transplant, but outcomes are highly variable. The success rate of a first-time corneal stem cell transplant using the patient's own cells (taken from the fellow healthy eye) is 68% at 10 years, however for stem cells taken from an unrelated donor, which is more often the case, is as low as 25% at 3 years. One major reason for this difference is the fact that donor stem cells may be rejected by the immune system, despite treatment with immune suppression drugs, meaning that there must be other factors that determine the success of such stem cell transplants.

The development of a mouse model of LSCD, and subsequent cornea regeneration through transplantation of donor stem cells during this project has potential benefits in both academia and a clinical context. Publication of this model in an internationally recognised research journal in the next year will allow researchers to effectively explore the role of the immune system in graft rejection. Data detailing the inflammatory response to corneal injury provides useful information for

researchers to develop treatment strategies to treat or inhibit this inflammation. Furthermore, several strategies to isolate corneal stem cells from donor tissue have been investigated, which, with further research may eventually lead to improved clinical practice in generating the stem cell grafts used to treat patients.

ACKNOWLEDGEMENTS

I am sincerely grateful for the invaluable advice and guidance provided by my supervisor Prof. Emma Morris, and would like to thank her for continuous patience and understanding throughout this PhD. I also owe thanks and gratitude to Dr. Pervinder Sagoo, Dr. Alex Shortt, and Prof. Hans Stauss for their input and support on this project. I would also like to thank all members of the Stauss/Morris research groups for their constant help and technical expertise, as well as the Moorfields Eye Charity for funding this research at UCL. Finally, my appreciation goes out to my friends and family for all their constant love and encouragement over the last few years.

TABLE OF CONTENTS

Declaration	2
Abstract	3
Impact statement	4
Acknowledgements	6
Table of contents	7
Chapter 1. Introduction	10
1.1 Anatomy of the cornea.....	10
1.2 Limbal epithelial stem cells	11
1.3 Limbal epithelial stem cell niche	13
1.4 Limbal stem cell deficiency and transplantation.....	15
1.5 Corneal immunity	18
1.6 Corneal allograft rejection.....	24
1.7 Aims	30
Chapter 2. Materials and Methods	31
2.1 Human limbal epithelial cell culture	31
2.1.1 Human corneal tissue.....	31
2.1.2 Collagenase digest.....	31
2.1.3 Alternative collagenase digest	32
2.1.4 Dispase digest.....	32
2.1.5 Trypsin digest	32
2.1.6 Explant culture	32
2.1.7 Culture conditions.....	33
2.1.8 GFP transduction.....	33
2.2 Enrichment strategies	34
2.2.1 Percoll.....	34

2.2.2	MACS positive selection.....	34
2.2.3	MACS depletion.....	34
2.2.4	Cell sorting.....	35
2.2.5	Flow Cytometry	35
2.2.6	Colony Forming Efficiency (CFE) Assay	35
2.2.7	RNA isolation and qPCR	36
2.2.8	Multiplex cytokine & chemokine profiling.....	36
2.3	Mouse model of LSCD and LESC transplantation	37
2.3.1	Animals:.....	37
2.3.2	Epithelial sheet preparation.....	37
2.3.3	LESC fibrin gel preparation.....	37
2.3.4	LSCD and LESC transplantation	38
2.3.5	Intravital multiphoton imaging	38
2.3.6	2C-TCR graft rejection	38
2.3.7	dsRed T cell graft rejection	39
2.3.8	CFP T cell graft rejection	40
2.3.9	BMDC T cell preparation:	40
Chapter 3. Establishing A Mouse Model of LSCD and LESC Transplantation		43
3.1	Experimental chemical injury to the mouse cornea recapitulates clinical features of LSCD.....	44
3.2	The corneal response to chemical injury is an acute inflammatory episode characterized by a stromal & epithelial wound healing response.	51
3.3	Development and optimisation of a protocol for LESC transplantation.....	60
3.4	Limbal epithelial stem cell transplantation prevents and reverts the LSCD phenotype.....	65
3.5	Summary.....	69

Chapter 4. Determining the Role of the Innate and Adaptive Immune Responses in LESC transplant rejection	70
4.1 Transplantation of allogeneic LESC into an immunocompetent mouse model of LESC results in graft rejection.	71
4.2 2C-TCR+ T cell mediated graft rejection.....	79
4.3 CD8+ T cell mediated graft rejection.....	84
4.4 CD4+ T cell mediated graft rejection.....	89
4.5 CD8+ and CD4+ T cell mediated graft rejection	91
4.6 Summary.....	101
Chapter 5. Optimising culture, identification, and isolation of human LESC	102
5.1 Primary human corneal tissue digestion and culture	103
5.2 Primary human corneal epithelial cell inflammatory profile	106
5.3 Enrichment of human corneal epithelial cells.....	110
5.3.1 Percoll density gradient centrifugation	110
5.3.2 Magnetic activated cell sorting.....	114
5.3.3 Fluorescence activated cell sorting.....	116
5.4 Development of a humanised mouse model of LESC transplantation	118
5.5 Summary.....	127
Chapter 6. Discussion	128
6.1 Establishing a mouse model of LSCD and LESC transplantation	128
6.2 Determining the role of the innate and adaptive immune response in LESC transplant rejection.....	130
6.3 Optimising culture, identification, and isolation of human LESC.....	136
Chapter 7. Conclusions	141
Chapter 8. Bibliography.....	143

CHAPTER 1. INTRODUCTION

1.1 Anatomy of the cornea

The transparency and integrity of the cornea, the clear window at the front of the eye, is vital for normal vision and protection from external pathogens through its barrier function and its antiangiogenic and immunomodulatory effects [1, 2]. Along with the anterior chamber and lens, the cornea serves to refract light toward the retina. Changes in lens shape allow the refocusing of incoming light to bring objects into focus, while the shape and focus of the cornea is fixed. In order to maintain transparency, the cornea is avascular, and so oxygen diffuses through the corneal tissue which has an average thickness of 0.5mm in the centre and slightly thicker, 0.7mm, at the peripheral edge. Despite lacking blood vessels, it is one of the most highly enervated tissues in the body with an estimated 300-600 times more sensory nerve endings than in the skin [3]. The human cornea is composed of several layers: corneal epithelium, Bowman's layer, corneal stroma, Descemet's membrane, and the corneal endothelium. The three main layers of the cornea derive from different germ layers during embryonic development; the endothelium and stroma emerge from the mesenchyme, while the epithelial layer

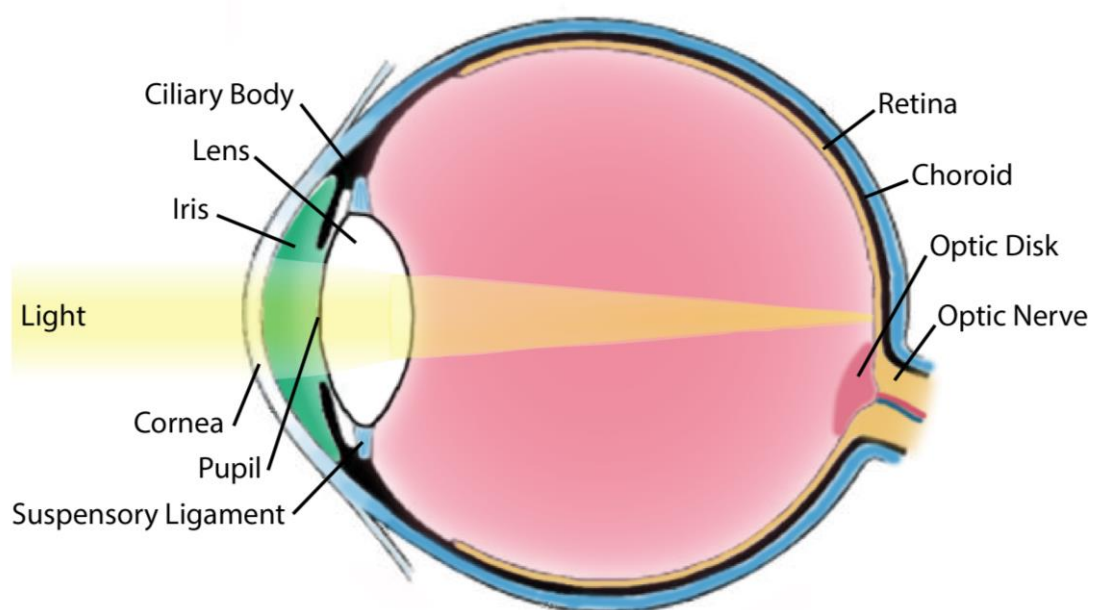


Figure 1.1 Diagram of the healthy human eye

develops from the ectoderm. This epithelial layer resides on Bowman's membrane and in a healthy adult human eye is only 6-8 cells thick, so most of the cornea thickness is contributed by the stroma. The epithelium continues to be renewed throughout adult life; however, the endothelium stops replicating after birth and loses cellularity at a rate of 0.56% cells per year [2].

The cells of the corneal epithelium have a high turnover rate, with terminally differentiated cells replenished by a small population of stem cells located in the limbus at the periphery of the cornea. This self-renewal rate can be defined by the equation $X + Y = Z$, (X =basal cell proliferation, Y =cells migrating centripetally from the periphery, Z =epithelial loss from the corneal surface). This renewal rate is normally stable during homeostasis, however, is capable of rapidly increasing in response to wound healing requirements [4].

1.2 Limbal epithelial stem cells

The limbal epithelial stem cells (LESC) reside in the basal layer of the limbus, a 1.5-2mm wide ring of tissue found at the junction of the cornea and the opaque conjunctiva. They are found in specialised pigmented niches termed palisades of Vogt where they are maintained in an undifferentiated state but proliferate to produce the transient amplifying cells (TAC) which migrate centripetally across the cornea [5]. These cells differentiate as they migrate from the basal layer towards the surface of the cornea, forming layers of stratified epithelium which act as a barrier to protect the eye. The nature of palisades of Vogt is still being determined, although several recent studies have illuminated the 3D structure through confocal and electron microscopy [5]. This series of radially oriented ridges of fibrovascular tissue within the limbus is highly variable between individuals, and believed to be as individual as fingerprints [6]. The interpalisade crypts at the basal cell level are part of the specialised niche of LESL. They are found at higher densities in the superior and inferior regions of the eye where cells are more protected by the

eyelids compared to the temporal or nasal regions, where the limbus is more exposed to degradation by ultraviolet light [5].

Several studies have demonstrated the importance of hypoxia in maintaining stem cells in their 'stem' phenotype, including LESC of the cornea. This is explored in a 2013 article from Bath *et al.* which showed that the cells were maintained at oxygen concentrations of 2-5%, reflecting the theoretical pericellular oxygen concentration of the human limbal basement membrane. Increasing this concentration to 10%, similar to that of the central cornea, *in vitro* resulted in differentiation to a TAC phenotype, as detected by changes in cytokeratin expression, loss of clonogenicity, and increases in ABCG2 [7].

LESCs comprise a very small population of cells in the cornea, and it has been shown that only 0.3-0.5% of cells from freshly isolated human limbal tissue are identified as LESCs[8]. They are classically characterised by their small cell size, an average of 10µm in diameter; slow cycling side population, as evidenced by label retention following pulse chase with a DNA marker such as bromodeoxyuridine (BrdU); slow proliferation during homeostasis; high proliferation potential in culture, or after wounding *in vivo*; the ability to form holoclones when cultured *in vitro* (colonies of cells with high proliferative potential); and expression of markers of differentiation such as Keratin-3 and -12 (differentiated epithelium) Keratin -19 (conjunctival epithelium), connexin-43, and involucrin [9-12].

Currently LESC can only be identified by these indirect methods, and as no positive markers have been unequivocally demonstrated, identifying LESCs precisely is more difficult. Undifferentiated cells of the basal limbal epithelium are known to express integrin $\alpha 9$, Keratin 19, vimentin, ABCG2, N-cadherin, PAX6, and $\Delta Np63\alpha$ [11, 13-16]. The p63 nuclear transcription factor has been demonstrated to be a marker for LESC, in particular the $\Delta Np63\alpha$ isoform. It has been shown in both *in vitro* and *in vivo* studies to be a specific marker, as it is highly expressed by holoclone forming cells of the limbal basal epithelium, and is also expressed by the TAC in their earliest stage of proliferation before loss through differentiation [16].

ATP-binding cassette subfamily G, member 2 (ABCG2) is more commonly known as a marker of haematopoietic stem cells, however corneal research has shown it is also present in the membrane and cytoplasm of limbal basal epithelium but not supra basal or corneal basal epithelium. As it is expressed by 2.5-3% of limbal epithelial cells, this is a useful marker of limbal basal cells however they lack the high colony forming efficiency (CFE) associated with true LESC [15]. A similar marker, ABCB5, was also recently published as a novel specific cell surface marker of LESC in the cornea, however evidence is not yet conclusive. It is present in both corneal epithelial embryonic development and adult surface epithelial repair, however despite being well localised with p63, ABCB5 knockout mice remained able to develop a corneal epithelium with the capacity to repair central injuries. This suggests that any corneal abnormalities arising from ABCB5 deficiency may be due to the antiapoptotic role of the protein [17]. Recent publications have indicated CD200 (also known as OX-2) as a novel cell surface marker of LESC[18]. CD200 is a transmembrane glycoprotein which transmits an immune-regulatory signal through its receptor to attenuate inflammatory reactions and promote immune tolerance[19]. Unfortunately many of these markers are also expressed by TACs or require intracellular staining making cell selection protocols for true LESC a particular technical challenge.

1.3 Limbal epithelial stem cell niche

Hypoxia is just one of several important conditions of the limbal niche microenvironment which are essential for the survival and maintenance of LESC. Molecular and soluble signalling from surrounding cells and nearby vasculature, or from the extracellular matrix (ECM) microenvironment are believed to provide the differential triggers which control stem cell homeostasis or activation [20]. The chemical and physical signals exchanged between the structures of the ECM, resident cells, and their local microenvironment allow molecular interactions which are critical for regulating LESC function. Limbal basal melanocytes provide

the pigmentation which give the limbus its darker appearance compared to the central cornea, and are believed to provide protection against ultraviolet radiation and oxidative DNA damage. In addition to this protective function it has been suggested that melanocytes play a role in the maintenance of a stem phenotype, with reports of co-localisation between N-cadherin positive melanocytes and limbal basal epithelial cells, and the non-uniform distribution around the limbus; where there are high levels found in crypts containing LSCs [21, 22]. Furthermore, Nakatsu et al. showed that several protein markers including vimentin, CD34, N-cadherin, and CD105 positivity in limbal mesenchymal cells were also involved in supporting the proliferation of LSCs at the same efficiency *in vitro* as 3T3 feeders. This indicates that the limbal stroma includes a heterogeneous population of potential candidates for the maintenance of LSCs. Sonic hedgehog, Wnt/ β -catenin, Notch, and TGF- β /BMP signalling pathways have all been implicated in the maintenance and self-renewal of LESC in the limbal niche, as well as cell-cell contact, cell-matrix contact, and paracrine signalling.

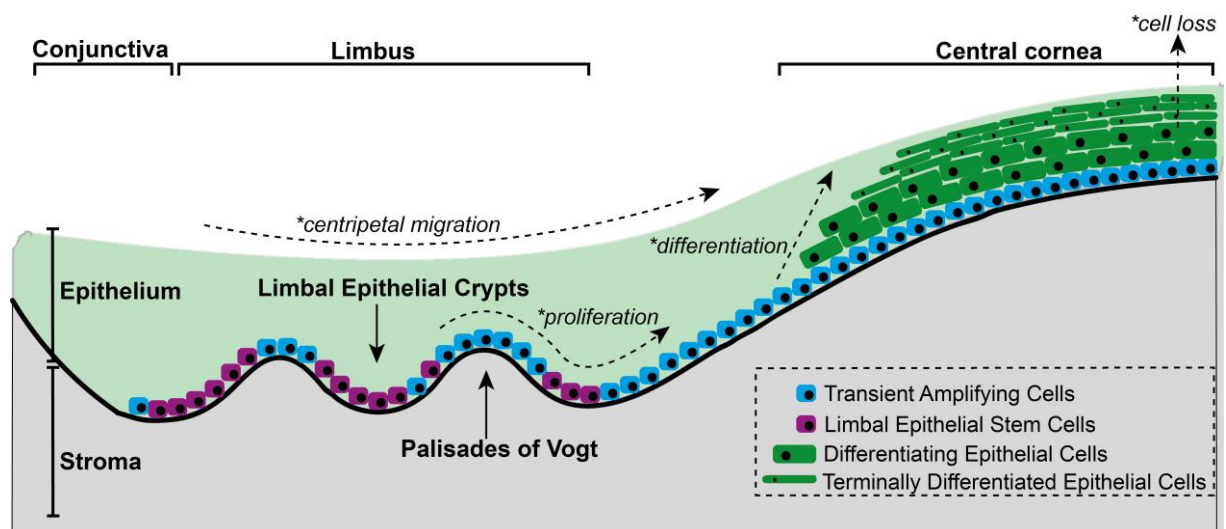


Figure 1.2 Diagram of human cornea and limbal structure

1.4 Limbal stem cell deficiency and transplantation

Damage to these stem cells results in the development of limbal stem cell deficiency (LSCD). This occurs most commonly through chemical or thermal burns, but also due to chronic inflammation, penetrating injury, chemotherapy, and certain rare genetic conditions including Stevens-Johnson syndrome, ocular cicatricial pemphigoid, and aniridia [23]. This damage causes remodelling of the corneal tissue through conjunctival epithelial outgrowth into the central cornea to replace lost corneal epithelium, corneal neovascularisation, and chronic inflammation, which together lead to painful ulceration and blindness. Compromising the borders of the ocular microenvironment results in a loss of immune privilege and onset of an inflammatory environment. Few epidemiological studies of LSCD have been performed, and due to subjective grading, differences in diagnosis, and the existence of various aetiologies, determining incidence numbers and global impact proves difficult to accurately estimate. It was reported by the European Medicines Agency (EMA) in 2015 that corneal lesions with associated LSCD due to ocular burns affected approximately 0.3 in 10,000 people in the EU, equivalent to around 15,000 people at that time [24]. A 2017 study of LSCD cases in Australia and New Zealand reported only 14 cases over the course of 1 year [25], while a more recent review estimates the incidence to be around 240 new cases per year in the UK [26].

For those patients with only single eye involvement, termed unilateral LSCD, an autologous graft to restore the LESC population is the best therapeutic option. This differs from corneal transplantation (keratoplasty) in which the full thickness central cornea is replaced by donor tissue, and is one of the most successful forms of solid organ transplant, even without HLA matching or systemic immune suppression, with allografts having a 90% first year survival rate [27]. During CLET a 2x2mm biopsy is taken from the limbus of the patient's healthy eye and expanded *ex vivo* either by culturing the intact explant until confluent outgrowth of epithelial cells is achieved, or by digesting the explant into a single cell suspension and culturing to confluence [28]. The use of *ex vivo* expanded

autologous human corneal epithelial sheets containing stem cells, under the name Holoclar[®], was approved in 2015 by the European Medicines Agency (EMA) for the treatment of patients with moderate or severe LSCD caused by burns. Holoclar is a cell sheet cultured from autologous LESC and containing a heterogeneous population of stem cells and their progeny at various stages of differentiation, containing 1-9% LSCs [29]. There are several alternative treatment protocols with varying success rates, but the absence of large scale double blinded clinical trials and inconsistencies in reporting and classification by clinicians, it is difficult to directly compare methods. While CLET is the most common procedure for LSCD treatment, there are similar older methods still in use. Conjunctival-limbal autograft (CLAU) has been used successfully since the 1980's, in which a larger biopsy is taken from the conjunctival-limbal region of the healthy eye and directly sutured to the injured eye with amniotic membrane. This is a simple procedure which can be performed with complex or costly laboratory equipment, however it is less effective and carries a much greater risk of damaging the donor eye [30]. Simple limbal epithelial transplant (SLET) was described in 2012, as very similar to the in-use CLAU procedure but using a much smaller biopsy, divided up into small sections on amniotic membrane and spread over the damaged eye [31].

Limbal epithelial cells are fastidious and difficult to culture *ex vivo* without the presence of a feeder layer. In the healthy eye, the growth factors and cytokines required for survival and proliferation are secreted from the tear film, aqueous fluid, and stromal cells[32]. *In vitro*, this can be reproduced through the use of human amniotic membrane (HAM) as a substrate for culture and transfer back to the eye during surgery, or, by seeding the digested limbal biopsy onto a feeder layer of growth arrested 3T3 mouse fibroblasts. This method of cultured limbal epithelial transplant (CLET) using HAM is preferable to the older but simpler method of directly suturing the biopsied segment of limbus onto the recipient cornea, because antigen presenting macrophages do not survive the process of *ex vivo* culture and so the risk of immune activation is reduced [33].

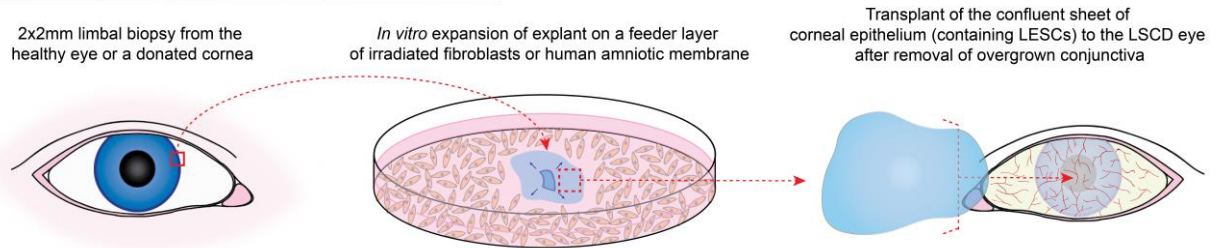
Cultured Limbal Epithelial Transplantation (CLET)

Figure 1.3 Illustration of the basic protocol for *in vitro* generation of corneal epithelial sheets.

Once the sheet of cultured limbal epithelial cells reaches confluency, it can then be transplanted onto the LSCD eye. Outcomes following this procedure in unilateral LSCD are reasonably good, with 68% of autografts surviving longer than 10 years [34]. For patients with bilateral LSCD the biopsy must be taken from cadaver-derived donor tissue which has far worse outcomes when transplanted, with only 25% of grafts surviving longer than 3 years despite systemic immunosuppression [35]. Clinical indications vary between practitioners, but the use of peri-operative topical steroids and broad-spectrum antibiotics were reported in all clinical studies evaluated by Shortt *et al.* (2010). Despite the absence of clear evidence for the benefit of immunosuppression in CLET, most patients who receive allogeneic cells are treated with cyclosporin A although treatment length, dose strength, and effectiveness vary between reported usage [36]. The use of steroids in patient care may predispose graft recipients to infection by opportunistic pathogens common in allograft recipients. Tissue matching strategies may also be considered by the treating physician in an attempt to improve outcomes, although there is no direct evidence of a benefit when using living related conjunctival limbal tissue, keratolimbal tissue, or *ex vivo* cultured LESC cells. Several studies have investigated this variable, however as of yet no clear conclusions can be drawn. There is also a further possibility of late failure, such as that reported in a recent publication which

showed evidence of limbal allograft rejection up to 8 years after transplantation[37].

The pathophysiology for this high degree of failure is believed to be due to immune-mediated allograft rejection, however given that almost a third of autografts also fail there is likely other intrinsic and extrinsic factors which can determine outcomes [35]. Examples may include the number and purity of stem cells within the grafts, inflammation in the graft bed, and damage or destruction of the LESC niche. During further analysis of these autologous transplants, Rama *et al* (2010) found that 78% of the successfully regenerated corneas had used grafts generated from cultures containing greater than 3% LESC, as indicated by p63 staining and holoclone formation[38]. In contrast, grafts from cultures containing less than 3% stem cells were only successful in 11% of patients. Despite this study, there is currently no data determining the most effective therapeutic dose or ratio of cell types within the graft to deliver optimal graft survival and function. The difficulty in studying these cells and their contribution towards graft outcome is further compounded by the lack of consensus on the optimal marker to select and use for graft preparation despite several markers for LESC being described.

Several animal models of LSCD and limbal allograft transplantation have previously been described, involving species ranging from rodents and rabbits to bovine, pigs, dogs, and goats [39-44]. A range of methods of transplantation were used, for example suturing a whole segment of donor limbus directly to the surface of the injured recipient cornea, however this is not an accurate representation of the CLET procedure performed in humans. Furthermore, limited investigations into parameters promoting optimal LESC engraftment and the immune mechanisms of limbal allograft failure have been undertaken.

1.5 Corneal immunity

The immune system is composed of two functionally distinct components: the innate immune system and the adaptive T cell-dependent immune system.

Pathogen invasion in the body is countered by both systems working in tandem. The cells and proteins of the innate system play a crucial role in the initiation and subsequent activation of the T and B cell response of the adaptive immune system, as well contributing to the removal of pathogens targeted by that response. The innate immune system is mainly composed of physical epithelial barriers, antigen presenting cells (APCs), phagocytic leukocytes, mast cells, and natural killer (NK) cells. It is characterised by its recognition of toll-like receptors (TLRs) and pathogen-associated molecular patterns (PAMPs) expressed on various microorganisms. Langerhaan cells (LCs) are an innate immune cell population found in epithelial tissues including the cornea, limbus, and conjunctiva [45]. Once believed to be dendritic cell prototypes, the current theory is that they belong to a subgroup of tissue resident macrophages and function as APCs [46].

One major cellular component of the immune system are T lymphocytes, which play an important role in the normal immune responses, homeostasis, and immunological memory, as well as being key driving factors in many inflammatory and autoimmune diseases. Originating from haematopoietic stem cells in the bone marrow, they migrate to the thymus to undergo maturation, selection, and transport to the periphery, where they form several differentiated subsets. These include naïve T cells, which respond to novel detected antigens, memory T cells which are residual cells left over from previous immune responses to maintain long term immunity, and regulatory T cells which assist in modulating immune responses. T cell responses vary depending on the location in the body as well as stage of the hosts development and maturity. While they populate nearly every organ and tissue of the body, they are predominantly clustered within lymphoid tissue, mucosal sites, and the skin.

Protein complexes on the T cell known as T cell antigen receptors (TCR) are the defining feature of T cells and consist of six different polypeptides, which form a transmembrane heterodimer consisting of either an $\alpha\beta$ chain or a $\delta\gamma$ chain, linked by a disulphide bond. Through complementary determining regions (CDRs), the TCR allows T cells to recognise foreign bodies and pathogens, and determine the antigen

to which the TCR will bind. In contrast to antibodies, T cell receptors (TCR) cannot directly bind antigen and so it requires broken down antigen peptides to be presented to the T cell. This function is performed by major histocompatibility complexes (MHC) on APCs; with MHC class I presenting antigen to CD8+ cytotoxic T cells, and MHC class II presenting to CD4+ T cells, also known as T helper cells [47]. While MHC class I is expressed on all nucleated cells of the body, Class II MHC molecules are only found on B cells, dendritic cells, and macrophages, and class III involved in the complement system [48]. TCR signalling alone is insufficient for complete T cell activation and can lead to a state in which T cells no longer respond to antigen stimulation. While the MHC-antigen complex binds to the TCR, the process also requires other co-stimulatory molecules such as CD28, CD2, and CD45 in order to promote activate T cells from a quiescent state and trigger proliferation and differentiation, apoptosis, or cytokine release [49].

When CD8+ T cells recognise peptides presented by MHC class I, the normal response against intracellular pathogens and tumour detection is summarised by three main mechanisms of action: 1) secretion of cytokines TNF- α and IFN- γ for their anti-microbial, anti-viral, and anti-tumour effects; 2) production and release of cytotoxic granules containing perforin which generates a pore in the target cell membrane allowing granzymes to enter and cleave intracellular proteins, resulting in apoptosis of the infected or malignant cell; 3) activated CD8+ T cells express Fas ligand on their surface which binds to its receptor Fas on the target cell which triggers activation of the caspase cascade resulting in apoptosis [50].

This differs to the CD4+ T cell response which recognises peptides presented by MHC class II on APCs such as dendritic cells or macrophages. This triggers naïve CD4+ to begin differentiating into multiple different lineages depending on the cytokine milieu of the microenvironment, as well as the type of APC and co-stimulation detected during activation. T helper type 1 (Th1) cells mainly induce cell mediated immunity through cytokine secretion to increase macrophage recruitment and phagocytosis, and are able to stimulate CD8+ cytotoxic T cell responses. Th2 cells are required for the production of antibodies including IgE and IgG, and so mainly

involved in the humoral response against parasites and allergic responses. Studies are continuing to identify further specialised subsets of CD4+ helper T cells including T follicular helper cells (Tfh) and T regulatory cells (Tregs), responsible for stimulating B cell maturation and protection against autoimmunity respectively [51].

The absence of blood and lymphatic vessels in the cornea is part of an important condition of the eye termed immune privilege. There are three main mechanisms thought to be involved in the complex system of immune privilege in the eye: (i) cellular, anatomical, and molecular barriers within the eye; (ii) an immunosuppressive microenvironment; and (iii), the phenomenon known as anterior chamber associated immune deviation (ACAID). An avascular cornea provides protection from angiogenic factors responsible for promoting neovascularisation, and the absence of a corneal lymphatic system inhibits APC channelling to the regional lymph nodes where they would activate alloantigen or pathogen specific T cells. The blood-ocular barrier comprises of tight junctions of the pigmented epithelial cell layer of the uveal track, the avascular cornea, and the retinal capillary endothelial cells. This enclosed space gives rise to a microenvironment to regionally suppress local inflammatory activation and to control the functionality of immune cells present. Membrane bound and soluble factors produced by the pigmented epithelial cells and contained within the aqueous humour are members of a defined group of proteins and biochemicals which make the ocular microenvironment highly anti-inflammatory [52]. Other immunosuppressive factors of this group include calcitonin gene related peptide, cytokines, neuropeptides, complement inhibitors, melanocyte stimulating hormone, and macrophage inhibitory factor. Stromal cells of the retina, iris, and ciliary body, and retina are able to convert T cells to regulatory T cells, while death inducing molecules such as Fas ligand (FasL) are expressed in the peripheral regions of the eye such as the stroma [53]. These induce apoptosis without inflammation or presence of any immune cells which cross ocular boundaries [54, 55].

Originally believed to be part of an aberrant immune response, Peter Medawar and colleagues in the 1940s demonstrated the indefinite survival of skin allografts

placed in the anterior chamber of the eye, in contrast to the rapid rejection in other tissues such as the skin [56]. Under these conditions antibody responses are preserved, whereas cellular responses such as cytotoxic T lymphocyte infiltration or delayed type hypersensitivity are suppressed. The anterior chamber contains transforming growth factor β (TGF- β), thrombospondin-1 (TSP-1), and antigen presenting cells (APCs). TGF- β inhibits the proliferation of cells, promotes apoptosis, and induces differentiation while TSP-1 has an inhibitory effect on angiogenesis which prevents peripheral T cells accessing the tissue through the vasculature. As the blood brain barrier does not prevent T-cell migration into the eye there are several mechanisms which regulate T cell activity, and antigen-activated effector T cell mediated immune responses become suppressed in the presence of aqueous humour [57]. Eye-derived APCs such as macrophages are able to migrate from the eye to the spleen where they stimulate production of TGF- β , CXCL2, and macrophage inflammatory protein-2 (MIP) and attract activated APCs in the bloodstream attract and bind to natural killer T cells (NKT). These NKT cells then generate increased levels of TGF- β , CCL5, and TSP-1 which results in T cell clustering and the subsequent differentiation into regulatory T cells, also known as ACAID-induced-T regulatory cells. CD4⁺ ACAID-Treg inhibit Th1 differentiation in the lymph nodes, while CD8⁺ ACAID-Treg inhibit Th1 and Th2 effector function in the eye [58]. Induction of ACAID after corneal transplantation when the graft antigens on the endothelial surface of the cornea are taken up by eye-derived APCs and transported to the spleen causing inhibition of the allo-antigen specific immune response and promoting long term graft survival [59]. This mechanism is disrupted when lymph vessels and the vasculature invade the cornea, such as during LSCD. Several conditions which eliminate corneal allograft immune privilege do not adversely affect the induction and expression of ACAID, and there is evidence that regulatory T cells are generated through a glucocorticoid-induced TNF receptor family-related protein ligand (GITRL)-dependent process within the corneal allograft [60]. Antibody blocking of the GITRL process results in 100% corneal allograft rejection, yet does not prevent the induction of ACAID [60]. T-regs induced by corneal allografts are CD4⁺CD25⁺Foxp3⁺ cells capable of suppressing donor-specific T cell activation within the corneal allograft [61, 62]. The long-term survival of corneal

allografts and the generation of T-regs by orthotopic corneal allografts also requires the presence of IL-17, however it is not needed for the induction and expression of ACAID [62].

The non-specific innate immune responses of the ocular surface are a vital first line of defence against toxins and infections, for example, the pre-corneal tear film which contains lactoferrin, mucin, and lysozyme which have antimicrobial properties, plus immunoglobulin-A [63]. Inflammatory cytokines such as interleukin (IL) 1 α , IL-6, IL-8, and tumour necrosis factor (TNF)- α are further crucial components of the ocular innate immune system, as well as the ability of cells to recognise pathogen associated molecular patterns is through the expression of several Toll-like receptors (TLRs) [64]. IL-1 β is a proinflammatory cytokine which carries out a vital function in acute and chronic inflammation, but also plays an important role in ocular wound healing. Wounding can initially induce IL-1 β expression by endogenous danger signals or alarmins released from injured cells that can stimulate Toll-like receptors to induce IL-1 β synthesis, as well as epidermal growth factor receptor activation [65]. IL-1 β induces FGF-2 production, which in turn is capable of promoting angiogenesis by inducing VEGF expression in endothelial cells[66].

Chemokines are secreted proteins with chemotactic properties for cells which mediate acute and chronic inflammation in the body and can be divided into two main classes. CXC-chemokines are generally potent chemoattractants for neutrophils but not monocytes, whereas CC-chemokines have little effect on neutrophils but exert their effect on monocytes and lymphocytes. Chemokine synthesis is induced by proinflammatory mediators such as IL-1 and TNF α , both of which are present in corneal inflammation [67]. Chemokines also have additional functions which contribute to inflammation and tissue damage such as enhancing T cell activation, regulating T helper cell polarisation, and stimulating macrophage function [68]

1.6 Corneal allograft rejection

Current research into the role of the immune response in LESC allograft rejection is limited. While allogeneic keratoplasty is usually a highly successful procedure, studies into the mechanisms involved in full thickness central corneal rejection may provide valuable insights into the mechanisms involved in the unique immune environment of the compromised corneal epithelium.

The complex mechanisms of immunity which normally serve to protect the body, can pose a significant barrier to successful transplantation. In cases where the grafted tissue is generated from the patient's own cells, termed an autograft, such as skin grafts then rejection by the immune system is not usually an issue. In cases where the graft is from an individual who is not genetically identical, termed an allograft, which is the most common type of transplant then the immune system can identify the graft cells as foreign and trigger a response designed to destroy the donor tissue or organ. To reduce the frequency and severity of this reaction and minimise the possibility of rejection, donor and recipient are often carefully selected for immune compatibility. The degree of mismatch between the MHC complexes, also known as human leukocyte antigens (HLA) in humans, are a key indicator determining the risk of rejection, with several subtypes traditionally used including HLA-A, -B, and DR [69, 70]. HLA-DR mismatch is most significant in the first six months following transplantation, followed by the effect of HLA-B in the first two years, and HLA-A mismatches having a negative effect on long term graft survival [71]. There are also several non-HLA antigens implicated in graft rejection: for example the ABO blood group antigens which can result in hyperacute rejection of vascularised grafts like the kidney or heart; or the minor histocompatibility antigens (MiHA) which are known to play an important role in graft-vs-host disease in patients who receive HLA matched cells [48, 72].

Allorecognition occurs through one of three known pathways. During the direct recognition pathway recipient T cells recognise intact donor allogeneic HLAs, typically presented by donor derived 'passenger' dendritic cells. This triggers a rapid

immune response leading to graft loss unless immunosuppression is used immediately following transplantation [73]. Conversely in the indirect pathway donor HLA peptides are presented by recipient APCs for T cell recognition in the context of MHC class II.

In vivo data has shown that in the absence of prior exposure to alloantigen, 1-10% of memory T cells are able to react to intact allogeneic MHC molecules through the direct allorecognition pathway [74]. In humans, transplant recipients can be sensitised from exposure to alloantigens from previous transplants, pregnancy, and blood transfusion. These memory T cells can also be generated through homeostatic proliferation in a lymphopenic environment, including potentially alloreactive and pathogenic T cells. Existing studies have established the relationship between CD8⁺ and CD4⁺ memory T cell subsets and allograft rejection, detailing the distinct mechanisms involved [75]. Memory CD4⁺ T cells not only become effector cells upon reactivation, but also provide help for the robust activation of donor reactive effector CD8⁺ T cells. Limiting the migration of these cells into recipient graft tissue or depleting cell populations prior to transplant is able to significantly extend allograft survival. Neutralising chemokines or chemokine receptors such as CCR5 or CXCR3 in an attempt to prevent the entry of memory T cells into the graft tissue has not yet proven to be effective, likely due to the redundancy of the chemokine/receptor network with chemokines binding to multiple receptors and vice versa [76].

The idea that cytotoxic CD8⁺ T lymphocytes are able to mediate corneal allograft rejection is well established in the literature [77]. Corneal allografts are devoid of APCs expressing MHC Class II, and it has been shown that in mice transplanted with allogeneic full thickness corneal grafts around 60% of the corneas were rejected in a process mediated predominantly by two T cell subsets. CD4⁺ T cells recognising alloantigens indirectly and releasing IL-2, and CD8⁺ T cells directly recognising donor MHC to produce IFN- γ were both involved in the process, however direct activation of CD8⁺ T cells was not required for graft rejection [78].

CD8⁺ CTL *in vitro* kill allogeneic cells corneal cells and are found in rejected corneal allografts, however, in some rodent studies, CD8⁺ T cell activity is not elicited by corneal allografts. Rejection is observed in CD8-deficient mice and wild-type mice treated with anti-CD8 antibody, and orthotopic corneal allografts irregularly elicit the generation of donor-specific CTL [79-82]. In high-risk hosts, i.e those with pre-vascularised graft beds, corneal allografts induce the generation of donor-specific CD8⁺ T cells to mediate rapid corneal allograft rejection when adoptively transferred to severe combined immune deficient (SCID) hosts [83]. Furthermore, corneal allografts in the same high-risk hosts also promote the generation of a CD4⁻/CD8⁻ double negative T cell population with delayed-type hypersensitivity (DTH) responses to donor alloantigens *in vivo*, as well as mediating donor corneal endothelial cells apoptosis *in vitro*. Approximately 100% corneal allograft rejection can be observed when adoptively transferred these T cells to SCID mice. Any rejection involving CD4⁻/CD8⁻ T cells is significantly faster onset and duration than that produced by adoptively transferred CD4⁻/CD8⁺ T cells from the same high-risk lymphocyte donors [83]. This implies that while CD8⁺ T cells are not essential for corneal allograft rejection, they are capable of mediating corneal allograft rejection if CD4⁺ T cells have been ruled out as potential effector cells.

Research indicates that although CD4⁺ T cells are crucially involved in corneal allograft rejection, effector T cells can be produced despite the absence of CD4⁺ T cell help [79, 84, 85]. Depletion of CD4⁺ T cells with either antibody or by gene deletion results in a significant decline in corneal graft rejection in *in vivo* animal models, and there is a strong correlation between long-term corneal allograft survival and the downregulation of CD4⁺ T cell-dependent DTH response to the donor histocompatibility antigens [85]. The variety of factors involved in a normal DTH response, such as IFN- γ , nitric oxide, superoxide radicals, and tumour necrosis factor- α (TNF- α), will each inflict extensive damage on corneal allograft tissue. CD4⁺ T cells normally function as helper cells in activating the CD8⁺ T cytotoxic response and generation of alloantibodies, however previous studies have shown that in CD8 knockout and B-cell deficient mouse models of corneal allograft transplantation,

rejection of the graft is not impaired implying they are also able to act as effector cells [81, 86, 87].

Found in almost all tissues, macrophages are a diverse and highly functional cell type with roles in antigen presentation, tissue repair and immunity, as well as homeostasis and development [88]. Normally present in the conjunctiva, it has also been reported that CD45+/CD11b+ macrophage and monocyte cells are detected in the central corneal stroma of both mice and humans [89, 90]. In addition to their role as APCs macrophages are also able to act as end-stage effector cells in the rejection of skin allografts [91]. The depletion of periocular macrophages prevents the rejection of corneal allografts in *in vivo* models, while alone, they are incapable of producing complete rejection [81, 92]. The depletion of macrophages in normal mice prevents rejection, however depletion of macrophages once the CD4+ T cell population has been sensitised is not able to stop corneal allograft rejection, indicating that macrophages contribute to the induction but not ongoing process of rejection [81]. Further results imply that both macrophages and tissue resident Langerhan cells, the two ocular APC populations, are needed for the induction of CD4+ T cell-dependent corneal allograft rejection. Elimination of either population prevents the induction of alloimmune response and promotes long-term graft survival.

Neutrophils are the most abundant immune cell population in human blood, accounting for 50-70% of all circulating leukocytes, and function as an initial defence response to a range of pathogens [93]. Generated from myeloid progenitors at a rate of 10^{11} cells per day in homeostasis, neutrophils are terminally differentiated and fairly short lived, with 55-60% of bone marrow dedicated to their production however are able to prolong their lifespan by sevenfold once activated [94, 95]. Proliferation, differentiation, and mobilisation are predominantly regulated by granulocyte colony stimulating factor (G-CSF). While it was once thought that neutrophils were only present during the acute inflammatory response it is now known that they are able to communicate with cells of the adaptive immune response such as dendritic cells and macrophages, through soluble mediators or

direct cell-cell contact [93]. During infection or detection tissue stress, neutrophils rapidly promote phagocytosis and intracellular degradation, release of microbicidal granules, release of oxidative bursts, and the formation of neutrophil extracellular traps (NETs) [96].

Neutrophils are one of the first circulating leukocytes to infiltrate transplanted organs and are a well-established marker of transplant injury, however most work on neutrophils in transplanted organs has focused on their destructive role during ischemic reperfusion injury (IRI). Advances in our understanding of the underlying mechanisms of inflammation have revealed that both neutrophil infiltration and activation are assisted by the release of damage-associated molecular patterns (DAMPs) from necrotic cells and the ECM. Accordingly, DAMPs stimulate pattern recognition receptors (PRRs) on macrophages, which induces the expression of inflammatory chemokines and cytokines including CXCL8 and IL-1 β , which play a key role in neutrophil recruitment by activating vascular endothelium [97]. Neutrophils also express PRRs which induce the generation of reactive oxygen species (ROS) and hydrolytic enzymes that increase graft damage. Similar to professional APCs, neutrophils have the capacity to deliver antigen to lymph nodes and induce the differentiation of T cells via the expression of MHC and costimulatory molecules[98]. Neutrophil depletion experiments have revealed the importance of neutrophils in promoting alloimmune responses, where neutrophil depletion in a mouse model of skin transplant slowed acute rejection by moderating the recruitment of alloreactive memory CD8⁺ T cells[99].

Natural killer cells are crucial components of the innate immune system which do not require pre-stimulation to carry out their effector function. Derived from haematopoietic stem cells of the bone marrow, they represent 10% of the total peripheral blood mononuclear cell population and are also found in the spleen, liver, lung, lymph nodes, thymus, and peritoneal cavity [100]. NK cells are large, granular, and phenotypically defined as being CD56⁺ CD3⁻. Most circulating NK cells are in resting state but cytokine activation causes them to infiltrate into pathogen infected tissues or those with malignant cells [101]. They also play an important

immunoregulatory role by secreting cytokines such as IFN- γ in response to interaction of cell-surface receptors with their ligand. CD56^{dim} subset of NK cells comprise 90% of the cell population and are mostly found in peripheral blood and exhibit high cytotoxic activity. The remaining 10% are of the CD56^{bright} subset which is mostly involved in cytokine production [100].

Cells lining the internal corneal and retinal surfaces do not express MHC class I molecules, making them vulnerable to NK cell mediated lysis and so in a healthy eye their presence is limited in the eye by the mechanisms of immune privilege [102]. However, when this is compromised such as during injury or transplant failure, NK cells have also been detected in the corneal stroma and in the aqueous humour of hosts with rejecting corneal allografts. While they do not normally display antigen specificity, NK cells express killer inhibitory receptors (KIR) capable of recognising syngeneic MHC class I antigens which once activated, NK cytolytic machinery is silenced, however allogeneic MHC class I molecules fail to engage and activate the KIR on NK cells and so allogeneic cells within the allograft are vulnerable to NK cell-mediated cytotoxicity. (66, 69, 91).

1.7 Aims

We hypothesise that a combination of intrinsic (LESC graft related) and extrinsic (recipient microenvironment and immunological) factors determine the success of LES C transplant engraftment and subsequent regeneration of the ocular surface.

The primary aims of this project are threefold:

- (i) Establish a mouse model of LSCD. Current *in vitro* and animal models of LSCD and LES C transplantation are limited, so we aim to develop a novel method of inducing a clinical LSCD phenotype which can be reversed through the transplantation of allogeneic donor LES C. This will allow us to investigate the factors important for successful engraftment as well as subsequent rejection or failure.
- (ii) Investigate the role of the innate and adaptive immune response to allogeneic LES C grafts. We will investigate a selection of immune cell types known to be involved in the immune response to allograft transplantation, through the adoptive transfer of cells into immunodeficient recipients. Furthermore we will develop a humanised mouse model to determine whether the factors identified using the mouse model are also applicable to human LES C transplants.
- (iii) Identify the key variables which determine LES C transplant success. Using a novel mouse model of LSCD, we aim to examine how the composition of stem cell grafts, the absolute LES C number, and their phenotype can influence the engraftment and survival of transplants and their ability to reverse LSCD. This will require the development of methods for the isolation, enrichment, and expansion of LES Cs.

CHAPTER 2. MATERIALS AND METHODS

2.1 Human limbal epithelial cell culture

2.1.1 Human corneal tissue

Human cadaver donor corneal tissue was obtained from Moorfields Lions Eye Bank, London (licensed by the UK Human Tissue Authority). Ethical permission for this study was obtained from the Research Ethics Committee (reference no: 15/SW/0104), and all tissue was handled in compliance with the Declaration of Helsinki. Corneas were stored in organ culture medium at room temperature post-mortem. The mean donor age was 69 years \pm 11 years. All human cells were cultured in corneal SM medium[103] containing Dulbecco's modified Eagle's medium-F12 plus Glutamax (DMEM) and MCDB-201 medium (3:2 dilution, Sigma Aldrich), 2% FBS, human epidermal growth factor (10ng/mL, Sigma Aldrich), human platelet derived growth factor (2ng/mL, Sigma Aldrich), insulin-selenium-transferrin (1X solution, Gibco), ascorbic acid-2 phosphate (120 μ M, Sigma Aldrich), dexamethasone (0.01 μ M, Sigma Aldrich), Penicillin/ Streptomycin (Pen/Strep) (1:100, Gibco), Gentamicin/ Amphotericin B (Gent/Amp) (50 μ g/mL, Gibco), cholera toxin (100ng/mL, Sigma Aldrich), albuMAX-I (1mg/mL, ThermoFisher). Corneas were washed twice in PBS with Pen/Strep and excess conjunctiva, iris, central cornea was removed before a thin layer of superficial limbus dissected from the rim using a crescent bladed scalpel and vannas scissors, before being cut into 2mm segments with a scalpel.

2.1.2 Collagenase digest

Limbal segments were incubated for 16 hours at 37°C, 5% CO₂, in 0.5mg/mL collagenase type-L (Sigma-Aldrich) diluted in DMEM containing Pen/Strep, Gent/Amp, and DNase (1:100), before being dissociated by pipetting.

2.1.3 Alternative collagenase digest

Limbal segments were incubated for 8 hours at 37°C, 5% CO₂, in 1mg/mL collagenase type-L, with regular vigorous pipetting.

2.1.4 Dispase digest

Limbal segments were incubated for 1.5 hours at 37°C, 5% CO₂ in 1mL of Hanks Balanced Salt Solution (HBSS, Gibco) containing 5mg/mL Dispase II (neutral protease, grade II, Roche) and 1:100 DNase (Sigma Aldrich). Epithelial cells were scraped off and further digested with 0.05% trypsin-EDTA (Gibco) for 20 minutes at 37°C, 5% CO₂.

2.1.5 Trypsin digest

Limbal segments were cut into 1x1mm pieces and incubated in a 50mL falcon tube in 4mL 0.05% trypsin-EDTA (Gibco) at 37°C for a total of 80 minutes. The solution was mixed by pipetting every 10 minutes, and the trypsin collected and replaced with fresh solution every 20 minutes. The collected trypsin containing cells was inactivated immediately with an equal volume of defined trypsin inhibitor (DTI) (Gibco), centrifuged at 528xg for 5 minutes, and resuspended in SM medium. This was repeated 4 times during the 80 minute incubation, before all cells were collected, counted, and seeded for subculture.

2.1.6 Explant culture

Limbal segments were placed stromal side facing down onto a dry 10cm or 6cm tissue culture dish and kept at 37°C, 5% CO₂ for 15 minutes. SM medium was added slowly to be sure explants had adhered to the dish before incubation until outgrowth was observed, after which, medium was changed every 3 days. Once sufficient outgrowth was achieved, cells were washed in PBS, incubated in 0.05% trypsin-EDTA for 2 minutes, and then cell scraped around the explant to harvest the cells without dislodging the tissue. Trypsin was inactivated with DTI and fresh SM medium added to the explants to allow further growth.

2.1.7 Culture conditions

Feeder layers of 3T3 cells, growth arrested with 4 μ g/mL mitomycin C (Sigma-Aldrich) for 3 hours at 37°C. Feeder cells were seeded at a density of 24,000/cm² into 6-well plates and rested in DMEM + 10% FBS + Pen/Strep (1:100) for 24 hours at 37°C, 5% CO₂. Freshly digested human corneal cells were seeded onto feeder layers in SM medium at a density of 15,000/cm² with medium changes every third day until confluency. At this point, cells were washed with PBS, any remaining 3T3 cells removed through vigorous pipetting with 10X EDTA (Sigma-Aldrich), and incubated at 37°C, 5% CO₂ in 0.05% trypsin-EDTA until cells detached. Trypsin was inactivated with equal volume of DTI and cells were reseeded on fresh feeder layers at a density of 6,000/cm² for further culture.

2.1.8 GFP transduction

Preparation of virus: The lentiviral vector was generated by co-transfection of human kidney derived 293T cells with three plasmids: p8.91, pMSG, and pDUAL-GFP under the CMV-EF1 α hybrid (CEF) promoter. Lentiviral titres were determined by infection of 293T cells with concentrated viral supernatant in the presence of 8 μ g/mL polybrene for 24 hours. GFP fluorescent cells were identified by flow cytometry. Virus titre = 9.92x10⁷ TU/mL.

Transduction of primary human cells: Primary human corneal epithelial cells (passage 1) were seeded at a density of 6,000/cm² onto a feeder layer of 26,000/cm² growth arrested 3T3 cells in SM medium and left to adhere for at least 4 hours. Concentrated lentiviral stock was added to cell cultures at molarity of infections of 1, 2, 5, 10, and 20, along with 8 μ g/mL polybrene. After 24 hours cultures received fresh SM medium and were further cultured for 4 days before harvesting and analysing GFP expression by flow cytometry.

2.2 Enrichment strategies

2.2.1 Percoll

A 100% stock Percoll solution was prepared by mixing neat Percoll (Santa Cruz Biotechnology) with 10X PBS at a ratio of 10:1. This was then used to create 80% and 40% fractions by diluting with 1X PBS. 2mL of each of the fractions were carefully layered on top of each other in a 15mL falcon tube with the densest 80% fraction at the bottom. Digested human limbal cells suspended in 2mL SM medium were layered on top before centrifugation at room temperature, 300xg, for 20 minutes, with acceleration and braking set to 0. The cells at the interface of each fraction were collected and washed three times in PBS, counted, and processed for analysis by CFE assay, flow cytometry, or stored in RNAlater (Ambion) for qPCR.

2.2.2 MACS positive selection

Digested human limbal epithelial cells were washed in PBS+1%FBS+2mM EDTA (FACS buffer) and incubated sequentially with unconjugated polyclonal rabbit primary antibody for ABCB5 (Gentex), PE-conjugated goat anti-rabbit secondary antibody (Mitenyi Biotec), each for 30 minutes, and anti-PE microbeads (Mitenyi Biotec) for 15 minutes at 4°C with washing and centrifugation between each incubation. LS columns (Mitenyi Biotec) were prepared by placing in a QuadroMACS separator and rinsing with 3mL MACS buffer. Cell suspension was passed through the column, the effluent discarded, and the ABCB5+ cells bound in the column flushed out with MACS buffer, collected, counted, and processed for analysis with the staining panel described below, excluding further ABCB5 antibody.

2.2.3 MACS depletion

Dead and apoptotic cells were removed from the limbal digests with the dead cell removal kit and LS columns (Mitenyi Biotec), and then incubated in unconjugated EpCAM-IgG1 monoclonal mouse antibody (ThermoFisher), unconjugated CD90-IgG1 monoclonal mouse antibody (ThermoFisher), and APC conjugated CD105-IgG1

monoclonal mouse antibody (EBioscience) for 30 minutes at 4°C. Cells were washed and further incubated in anti-IgG1 microbeads (Mitenyi Biotec) for 15 minutes at 4°C, before passing through pre-prepared LD columns in a QuadroMACS separator. The eluted solution containing the enriched cell population was collected, counted, and processed for analysis.

2.2.4 Cell sorting

Human limbal cells were incubated in PE-conjugated CD200-IgG1 monoclonal mouse antibody (BioLegend) for 30 minutes at 4°C, before washing and resuspension in FACS buffer. DAPI was added as a live/dead stain and cells incubated for 10 minutes at 4°C before being sorted on a BD FACSAria and gated on CD200^{high}, FSC^{low}. Enriched CD200+ populations were processed for analysis.

2.2.5 Flow Cytometry

Cells were incubated in APC-conjugated anti-PAX6 (496, NovusBio), and unconjugated anti-ABCB5 (polyclonal rabbit, GeneTex) with an AF555 conjugated goat anti-rabbit secondary antibody (polyclonal rabbit, BD) and LIVE/DEAD Fixable Aqua Dead Cell Stain Kit (ThermoFisher). Analysis was performed on an LSRFortessa (BD) and data was gated, compensated, and displayed on FlowJo software V10 (Tree Star, San Carlos, CA).

2.2.6 Colony Forming Efficiency (CFE) Assay

1500 human limbal cells were seeded in a 6-well plate on growth arrested feeder layer of 3T3 cells at a density of 4.8×10^4 cell/cm² in SM medium. Medium was changed every other day, and cells cultured for 7-12 days. When colonies reached a diameter of 2mm, wells were washed with PBS and fixed with cold methanol at 4°C for 30 minutes before staining with 1% Toluidine Blue for 30 minutes at 37°C. Colonies were identified as holoclones, meroclones, or paraclones, imaged, and counted to calculate CFE:

$$CFE (\%) = \frac{\text{No. of holoclone colonies} > 2\text{mm}}{\text{No. of cells seeded}} \times 100$$

2.2.7 RNA isolation and qPCR

RNA was isolated from cells using the PicoPure™ RNA Isolation Kit (ThermoFisher). Quantitative real-time RT-PCR was performed on the CFX96 Real Time System Thermal Cycler (BioRad) using a custom configured PrimePCR Multiplex Immunoassay System (BioRad) with the following PrimePCR probes: ABCB5 (ID: qHsaCIP0031906), ABCG2 (ID:qHsaCEP0058168), CD105 (ID:qHsaCIP0027737), HPRT1 (ID:qHsaCIP0030549), K12 (ID:qHsaCEP0055161), K14 (ID:qHsaCEP0055128), Lgr5 (ID:qHsaCEP0035443), PAX6 (ID:qHsaCIP0028341). The PCR conditions were as follows: 1 activation cycle at 95°C, 2 minutes; 40 denaturation cycles at 95°C, 5 seconds; 40 anneal/extension cycles at 60°C, 30 seconds; 1 melt curve cycle at 65-95°C (0.5°C increments) at 5 seconds/step. Expression results were based on cycle threshold (Ct) values and calculated as relative fold change between the target gene and HPRT reference gene.

2.2.8 Multiplex cytokine & chemokine profiling

Experiment carried out by Dr. Pervinder Sagoo.

Analysis of supernatants from primary human limbal tissue derived stromal or epithelial cells was performed using Bio-Plex Pro™ Human Chemokine Panel 40-Plex (Bio-Rad Laboratories) according to the manufacturer's instructions. The samples were diluted in lysis buffer and the sample diluent of the kit. Data was measured and analysed using the Bioplex 3D system and the Bioplex Manager software according to manufacturer's instructions. All samples were measured in duplicate. We excluded findings where the concentration was above the manufacture-defined reliable range from the analysis. Statistical significance calculated by two-way ANOVA (P<0.05, **P<0.01).

2.3 Mouse model of LSCD and LESC transplantation

2.3.1 Animals:

In all experiments non-obese diabetic (NOD)-scid-IL2r^{null} (NSG) mice were used as recipients, BALB/c-GFP (CByJ.B6-Tg(UBC-GFP)30Scha/J) mice were used as transplantation donors, and 2C-TCR Tg x Rag1 KO mice and CD2-dsRed mice were used as T cell donors. All mice were bred in our animal facility under specific pathogen-free conditions and littermates were randomly assigned to experimental treatment groups. All donors were killed by a rising concentration of CO₂ and confirmed by cervical dislocation.

2.3.2 Epithelial sheet preparation

Full thickness corneas were dissected from the enucleated whole eyes of GFP transgenic donor mice and incubated in a 24-well plate in 1mL of Hanks Balanced Salt Solution (HBSS, Gibco) containing 50mg/mL Dispase II (neutral protease, grade II, Roche), 50μM Y-27632 ROCK inhibitor, and 1:100 DNase (Sigma Aldrich) for 10 minutes at 37°C on a plate shaker at 350rpm. Corneas with loosened epithelial sheets were gently washed with PBS before transplantation.

2.3.3 LESC fibrin gel preparation

Thin fibrin gels were prepared with 300μL fibrinogen (10mg/mL) combined with 300μL thrombin (10U/mL) in a 12 well plate before being set at room temperature for at least 1 hour before plating with irradiated 3T3 fibroblasts. Human corneas were dissected and digested by standard collagenase protocol (Method 2.1.2) prior to seeding on fibrin gels and culture.

2.3.4 LSCD and LESC transplantation

Mice were anaesthetised prior to surgery with inhalation of isoflurane, subcutaneous injection of 0.02mL of 50mg/mL carprofen, and topical administration of tetracaine. LSCD was induced in the left eye only by 2 minute soak of the cornea in 20% EtOH followed by extensive PBS washing and gentle debridement of the loosened epithelium with a small surgical sponge. The eye surface was coated with neat FBS before a minimum of 2 pre-prepared GFP+ epithelial sheets were placed stromal side down onto the recipient cornea and air dried briefly. Mouse contact lenses were pre-prepared by fixing whole enucleated NSG eyes in 4% PFA for 30 minutes, followed by dissection of the full thickness cornea. This lens was then placed over the graft during surgery, before the eyelid was closed and secured with a single suture with 8-0 Ethilon. Sutures were removed after 4 days and eyes were imaged to detect evidence of engrafted cells using a Leica dissecting microscope equipped with fluorescence filters.

2.3.5 Intravital multiphoton imaging

Experiment carried out by Dr. Pervinder Sagoo.

Two-photon imaging of mouse corneas were performed using an upright microscope (DM6000B, Leica Microsystems) with a 20X/0.95 NA water-dipping objective (Olympus). Excitation was provided by a Chameleon Ultra Ti:Sapphire (Coherent) tuned to 950 nm. The following filter sets were used for imaging second harmonics generation (SHG)/ GFP/ PE, and Hoechst/ GFP: 483/32 BP, 495 LP, 520/35 BP, 562 LP, 607/20 B; 483/32 BP, 495 LP, 520/35 BP. Datasets were processed and analysed using Imaris (Bitplane) and Fiji softwares.

2.3.6 2C-TCR graft rejection

Cells harvested from the spleens and lymph nodes of 2C-TCR donor mice were screened by flow cytometry for T cells, before i.v. tail vein injection of 1.5×10^6 CD8 T cells in 150 μ L per mouse along with 0.5% of residual CD4/CD19+ cells. Mouse body weights were recorded to monitor for signs of graft-vs-host disease. Grafts were

serially imaged daily over the course of 13 days before mice were killed and corneas harvested, dissected, and digested in PBS containing 1:100 Pen/Strep, 1:200 DNase, and 4.5mg/mL collagenase-D for 1 hour at 37°C, 5% CO₂. Cells were washed in PBS containing 1% FBS, and 2mM EDTA and stained for flow cytometry with the following antibodies: AF700 conjugated anti-CD8 (53-6.7, Ebioscience), AF647 conjugated anti-Ki67 (B56, BD), BV711 conjugated anti-CD3 (145-2C11, BD), BV605 conjugated anti-CD69 (H1.2F3, BD), BV421 conjugated anti-EpCAM (G8.8, Biolegend), BUV737 conjugated anti-CD62L (MEL14, BD), PeCy7 conjugated anti-CD11b (M1/70, Ebioscience), PE-Dazzle 594 conjugated anti-CD45.1 (A20, Biolegend), PE conjugated anti-CD44 (IM7, Biolegend), and DAPI. Analysis was performed on an LSRFortessa (BD) and data gated, compensated, and displayed on FlowJo software V10 (Tree Star, San Carlos, CA).

2.3.7 dsRed T cell graft rejection

Cells harvested from the spleens and lymph nodes of B6-dsRed mice were mashed through a 70µm cell strainer in PBS with 1% FBS, and 2mM EDTA, before a 5 minute incubation at room temperature in ACK lysing buffer (Gibco). CD8 T cells were selected using the Dynabeads Untouched Mouse CD8 Cells Kit (ThermoFisher), resuspended in T cell medium (TCM) containing RPMI (Gibco), 10% FBS, 1:100 beta-2-mercaptoethanol, 1:100 Pen/Strep, and 5µL/mL HEPES buffer (Gibco). Cells were cultured for 4 days *in vitro* with BALB/c splenocytes, irradiated at 20Gy at a ratio of 1:1 in 6-well plates to expand BALB/c alloreactive B6-dsRed CD8 T cells. On day 4 all cultures were harvested, ficoll separated, and placed back in culture with 30U/mL IL-2 (Cambridge Bioscience) until day 8. Cells were harvested from culture and adoptively transferred to recipient NSG mice by i.v tail vein injection of 2x10⁶ CD8 T cells per mouse, along with 0.5x10⁶ freshly isolated T- cell depleted B6 splenocytes. Mouse body weights were recorded to monitor for signs of graft-vs-host disease. Grafts were serially imaged every 2-3 days over the course of rejection until graft size had been reduced by approximately 50%, at which point mice were killed, corneas dissected, and digested in PBS containing 1:100 Pen/Strep, 1:200 DNase, and 4.5mg/mL collagenase-D for 2 hours at 37°C, 5% CO₂. Cells were washed in PBS

containing 1% FBS, and 2mM EDTA and stained for flow cytometry with the following antibodies: PerCP-Cy5.5 conjugated anti-CD11b (M1/70, Biolegend), APC-eFluor780 conjugated anti-Ly6C (HK1.4, Ebioscience), AF647 conjugated anti-CD44 (IM7, Biolegend), BV711 conjugated anti-CD3 (145-2C11, BD), BV605 conjugated anti-CD69 (H1.2F3, BD), BUV737 conjugated anti-CD62L (MEL14, BD), BUV 395 conjugated anti-CD8 (53-6.7, BD), LIVE/DEAD Fixable Aqua Dead Cell Stain Kit (ThermoFisher). Analysis was performed on an LSRFortessa (BD) and data gated, compensated, and displayed on FlowJo software V10 (Tree Star, San Carlos, CA).

2.3.8 CFP T cell graft rejection

Cells harvested from the spleens and lymph nodes of B6-CFP mice were mashed through a 70 μ m cell strainer in PBS with 1% FBS, and 2mM EDTA, before a 5 minute incubation at room temperature in ACK lysing buffer (Gibco). CD4 T cells were selected using the Dynabeads Untouched Mouse CD4 Cells Kit (ThermoFisher), resuspended in T cell medium (TCM) containing RPMI (Gibco), 10% FBS, 1:100 beta-2-mercaptoethanol, 1:100 Pen/Strep, and 5 μ L/mL HEPES buffer (Gibco). Cells were cultured for 4 days *in vitro* with BALB/c splenocytes, irradiated at 20Gy at a ratio of 1:1 in 6-well plates to expand BALB/c alloreactive B6-CFP CD4 T cells. On day 4 all cultures were harvested, ficoll separated, and placed back in culture with 30U/mL IL-2 (Cambridge Bioscience) until day 8. Cells were harvested from culture and adoptively transferred to recipient NSG mice by i.v tail vein injection of 2x10⁶ CD4 T cells per mouse, along with 0.5x10⁶ freshly isolated T- cell depleted B6 splenocytes. Mouse body weights were recorded to monitor for signs of graft-vs-host disease. Grafts were serially imaged every 2-3 days to detect presence of T cells.

2.3.9 BMDC T cell preparation:

Bone marrow (BM) was harvested from tibias and femurs of BALB/c donor mice gender matched with proposed recipients, and collected into 70% EtOH for 1 minute before flushing out BM with a syringe and needle, passed through a 40 μ m cell strainer, and centrifuged at 1500rpm for 10 minutes. Cell pellet was resuspended in 1mL ACK lysis buffer for 1 minute, diluted in RPMI, and recentrifuged. BM cells were

resuspended in T cell medium containing RPMI (Gibco), 10% FBS, 1:100 beta-2-mercaptoethanol, 1:100 Pen/Strep, and 5 μ L/mL HEPES buffer (Gibco), and plated in a flat bottom 24-well plate at a density of 2.5x10⁶ cells per well in 1mL TCM + 20ng/mL GM-CSF. Cells were incubated for 6 days at 37°C, 5% CO₂, and received fresh TCM+GM-CSF every other day. On day 6, 1 μ g/mL LPS was added to fresh medium to mature the BMDC overnight before harvesting on day 7. BMDCs were washed in PBS containing 1% FBS, and 2mM EDTA and stained for flow cytometry with the following antibodies: APC conjugated anti-CD86, BV650 conjugated anti-IA/E, eF450 conjugated anti-CD11c, PeCy7 conjugated anti-CD11b, PeCy5 conjugated anti-CD80, PE conjugated anti-H-2Kd, LIVE/DEAD Fixable Aqua Dead Cell Stain Kit (ThermoFisher). Analysis was performed on an LSRFortessa (BD) and data gated, compensated, and displayed on FlowJo software V10 (Tree Star, San Carlos, CA). T cells were isolated from dsRed donor splenocytes using the Dynabeads Untouched Mouse CD8 Cells Kit (ThermoFisher) as described above. T cells were seeded with mature BMDC in culture at a ratio of 1:10 BMDC (stimulator) : T cell (responder), with 5x10⁶ per well in a 6 well plate. Cells were incubated for 4 days before resuspension in fresh TCM+ 10IU/mL IL-2 (Peprotech) in new 24 well plates (leaving BMDC adhered to original 6 well plates. T cells were incubated for 48hours in IL-2 before collection and dilution ready for i.v adoptive transfer. T cells were harvested from culture, counted, and adoptively transferred to recipient NSG mice by i.v tail vein injection of 2x10⁶ T cells per mouse, along with 0.5x10⁶ freshly isolated T- cell depleted B6 splenocytes. Mouse body weights were recorded to monitor for signs of graft-vs-host disease. Grafts were serially imaged every 2-3 days over the course of rejection at which point mice were killed, corneas dissected, and digested in PBS containing 1:100 Pen/Strep, 1:200 DNase, and 4.5mg/mL collagenase-D for 2 hours at 37°C, 5% CO₂. Cells were washed in PBS containing 1% FBS, and 2mM EDTA and stained for flow cytometry with the following antibodies: PerCP-Cy5.5 conjugated anti-CD4, AF700 conjugated anti-CD8, AF647 conjugated anti-CD44 (IM7, Biolegend), BV650 conjugated anti-IA/E, BV605 conjugated anti-CD69 (H1.2F3, BD), BUV737 conjugated anti-CD62L (MEL14, BD), PE-Cy5 conjugated anti-CD3, PE conjugated anti-EpCAM, and LIVE/DEAD Fixable Aqua Dead Cell Stain Kit (ThermoFisher). Analysis was

performed on an LSRFortessa (BD) and data gated, compensated, and displayed on FlowJo software V10 (Tree Star, San Carlos, CA).

CHAPTER 3. ESTABLISHING A MOUSE MODEL OF LSCD AND LESC TRANSPLANTATION

While corneal alkali burns are reported as the most common LSCD cause, there are significant limitations to the methods, models, and effectiveness reported in the literature [23]. Wide variability in factors such as the animal model used, the cause of injury, classification and severity of LSCD, treatment protocols, and the lack of necessary detail in methods, all contribute to the lack of consistency and problems recreating published results.

The most common animal used is the rabbit [104-106], as their eye is closest in size and structure to the human eye, although mice are also becoming more commonly used in corneal studies [107-109]. Differences in the structure of the mouse cornea compared to human must be considered, for example the lack of Palisades of Vogt at the limbus and a thinner central cornea, however the wide availability of fluorescent reporter and knock out strains make them useful as a tool to study immunological mechanisms. Using mice over rabbits or other larger animal models also follows the principles of the 3R's to reduce the numbers and harm done to animals in research.

Another issue with published models is the inconsistency in the induction of LSCD, with methods ranging from mechanical debriding the epithelium with Algerbrush or scalpel, to chemical injury with heptanol, sodium hydroxide, or ethanol. In a review of corneal alkali burns in animal models, Kethiri *et al.* (2019) demonstrated that only 50% of the recipients were developing total LSCD [110].

This chapter describes the development of a reliable and reproducible mouse model which recapitulates the classic clinical disease phenotype of LSCD, as well as establishing a protocol for the transplantation of donor derived corneal epithelial cells containing LESC to reverse the underlying LSCD phenotype.

3.1 Experimental chemical injury to the mouse cornea recapitulates clinical features of LSCD

Ocular surface chemical burns and injuries account for the majority of causes of clinical LSCD and resulting indication for therapeutic limbal stem cell transplantation [23]. We have developed an experimental model of chemical injury to induce LSCD in mice in order to simulate and understand the pathological process seen in human patients. Briefly exposing the surface of the mouse eye to a 20% solution of ethanol for two minutes, damaged and loosened surface corneal epithelium from the central corneal and limbal regions could then be carefully debrided using a small surgical sponge as illustrated in Figure 3.1.

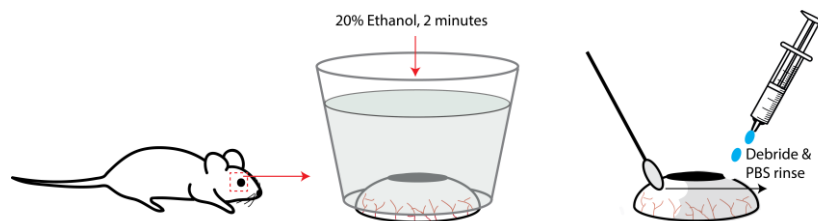


Figure 3.1 Schematic diagram illustrating the surgical protocol for the induction of LSCD in the mouse cornea.

During this procedure all mice received anaesthesia and analgesia, and only a single eye was operated on to reduce severity. Using this method, the corneal epithelial layer was completely removed without any abrasive or mechanical injury to the eye or damage to the underlying stromal or endothelial corneal layers as determined by immunofluorescent imaging, shown in Figure 3.2. Chemical injury induced macroscopic changes in corneal morphology indicative of LSCD including development of corneal haze (loss of transparency) and corneal barrier dysfunction were detectable from day 3 post-injury, which later developed into persistent epithelial defects, fibrovascular pannus formation across the limbus, and superficial neovascularisation of the central cornea (Figure 3.3).

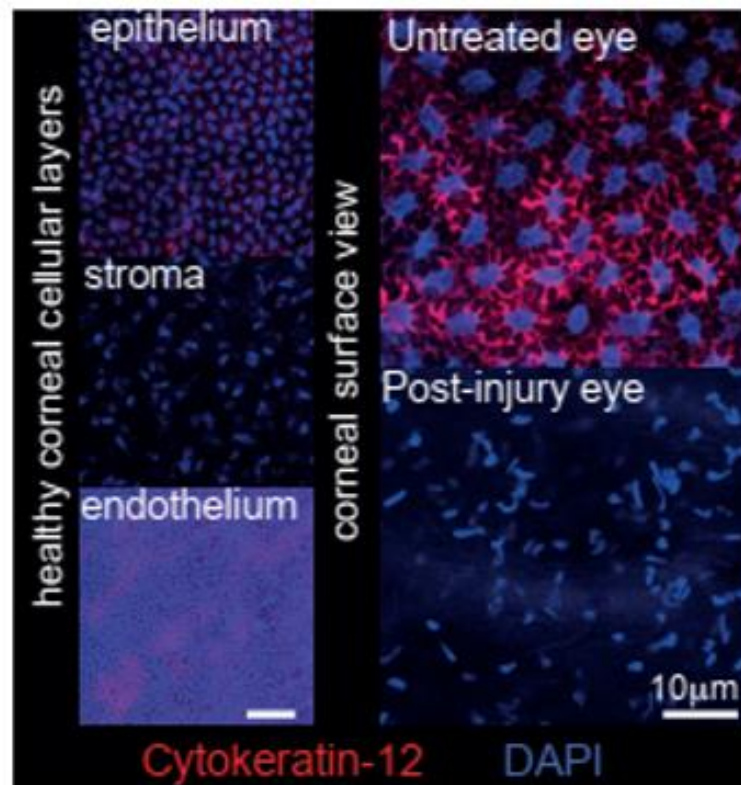


Figure 3.2 Immunofluorescent imaging of murine corneal layers following induction of LSCD. The loss of normal corneal epithelial cells is visualised through cell nuclear staining with DAPI (blue stain) and the loss of K12 expressing differentiated corneal epithelial cells.

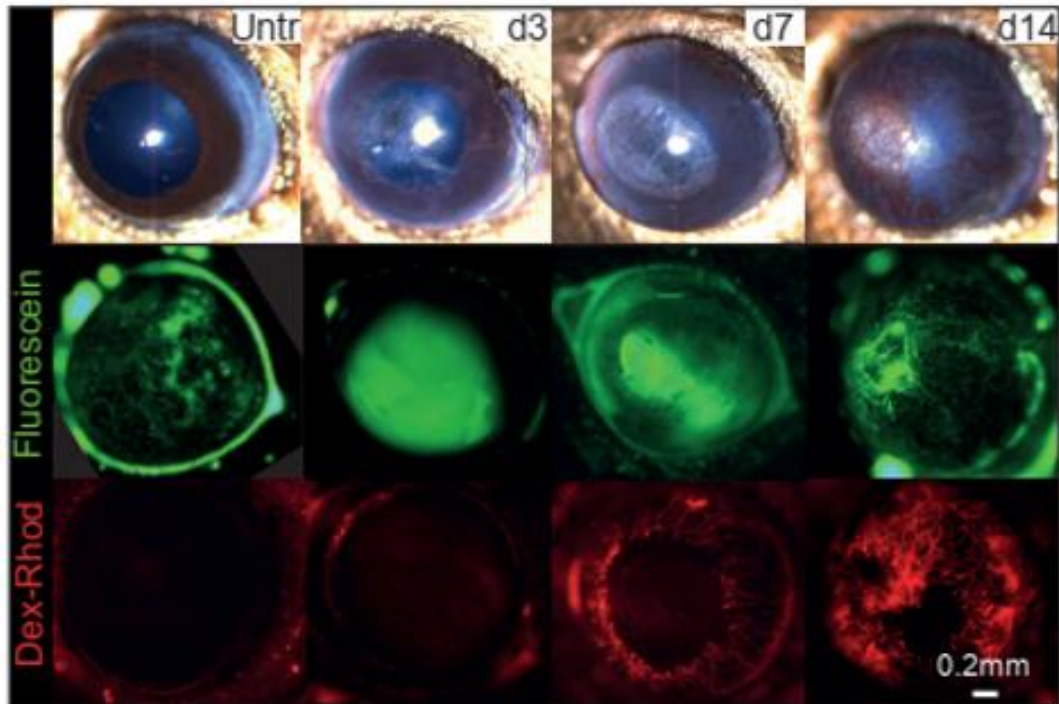


Figure 3.3 *In vivo* imaging of LSCD progression in the murine cornea following chemical injury. Chemical burn injury of the cornea followed by debridement removes corneal surface epithelium, identified by the development of corneal macroscopic features of LSCD. These include loss of corneal clarity (top panel), corneal barrier dysfunction identified by fluorescein stain uptake (middle panel), and neovascularisation detected by intravascular injection of Dextran-Rhodamine (Dex-Rhod) (lower panel). Images show days 3-14 post-injury compared to untreated control, and are representative of at least 4 independent experiments.

These features also correlated with significant corneal oedema as detected by spectral optical coherence tomography carried out by Dr. Pervinder Sagoo (Figure 3.4), beginning within one day of initial injury and progressively increasing between 7-28 days. Loss of limbal epithelial cell progenitors leads to long-term loss of differentiated epithelium (K12+ cells) and the presence of abnormal conjunctival epithelium (K19+ cells) and goblet cell derived mucins (Mucin-5AC+ cells) [111]. The presence of these changes to cellular composition, induced by chemical injury, was confirmed by RT-PCR analysis of corneal tissues both pre- and post-injury as shown in Figure 3.5.

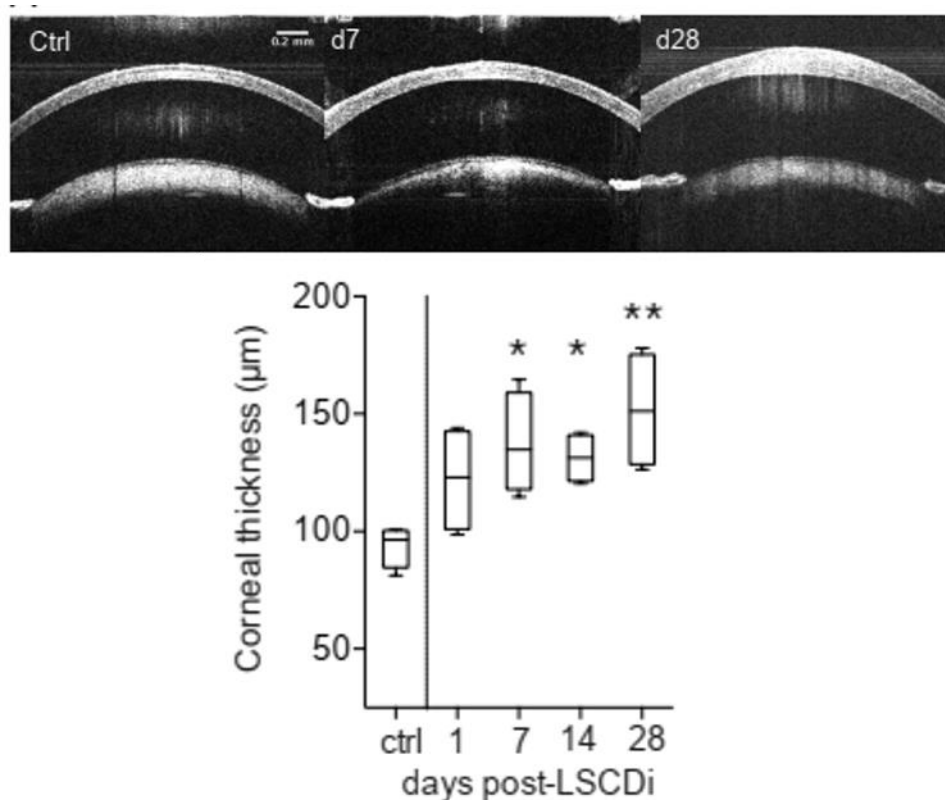


Figure 3.4 Analysis of corneal topography following LSCD corneal injury, by spectral optical coherence tomography. Corneal thickness was measured and plotted from spectral optical coherence tomography images, which demonstrate an increase in corneal thickness between day 1 – 28 following corneal injury relative to an untreated control.

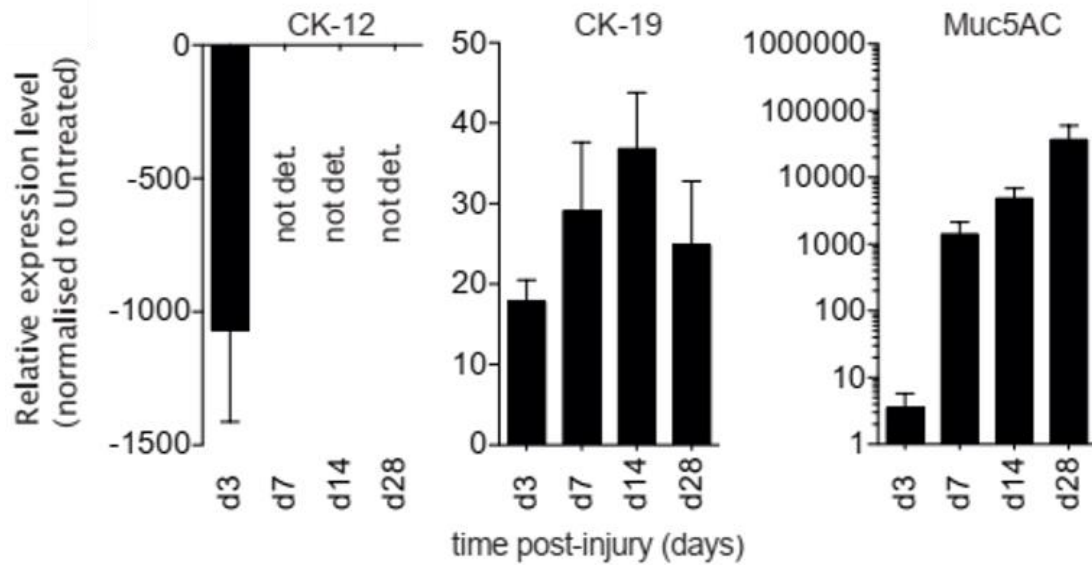


Figure 3.5 Quantitative PCR analysis of the murine cornea following induction and development of LSCD. Chemical injury to the murine cornea resulted in the loss of corneal epithelium and the invasion of conjunctival epithelium as part of the LSCD phenotype. Gene expression data shows the loss of K12, and increase in expression of Cytokeratin-19 and Mucin 5A between days 3-28 post injury.

Corneal conjunctivalisation and infiltration of goblet cells into central corneal regions were detected by histological analysis of corneas following injury. Figure 3.6 demonstrates a clear loss of differentiated epithelial cells corresponding with the appearance of conjunctival epithelium and goblet cells, in contrast to the healthy intact epithelium of the untreated control (top row) [112]. Also the thickness of the injured cornea relative to the untreated control is increased in these IHC images, further confirming the presence of corneal oedema. Incomplete loss of LESC following LSCD induction would result in the eventual re-epithelialisation of the corneal surface, as described in several other studies using alternative experimental models of epithelial injury [113, 114]. Corneal haze, vascularisation, and epithelial integrity were also imaged regularly and assessed in a double-blind manner, graded, with the results summarised in Figure 3.7 [35]. Combined, this data confirms that an irreversible form of experimental LSCD can be established in a mouse model which consistently and accurately recapitulates features of the clinical disease.

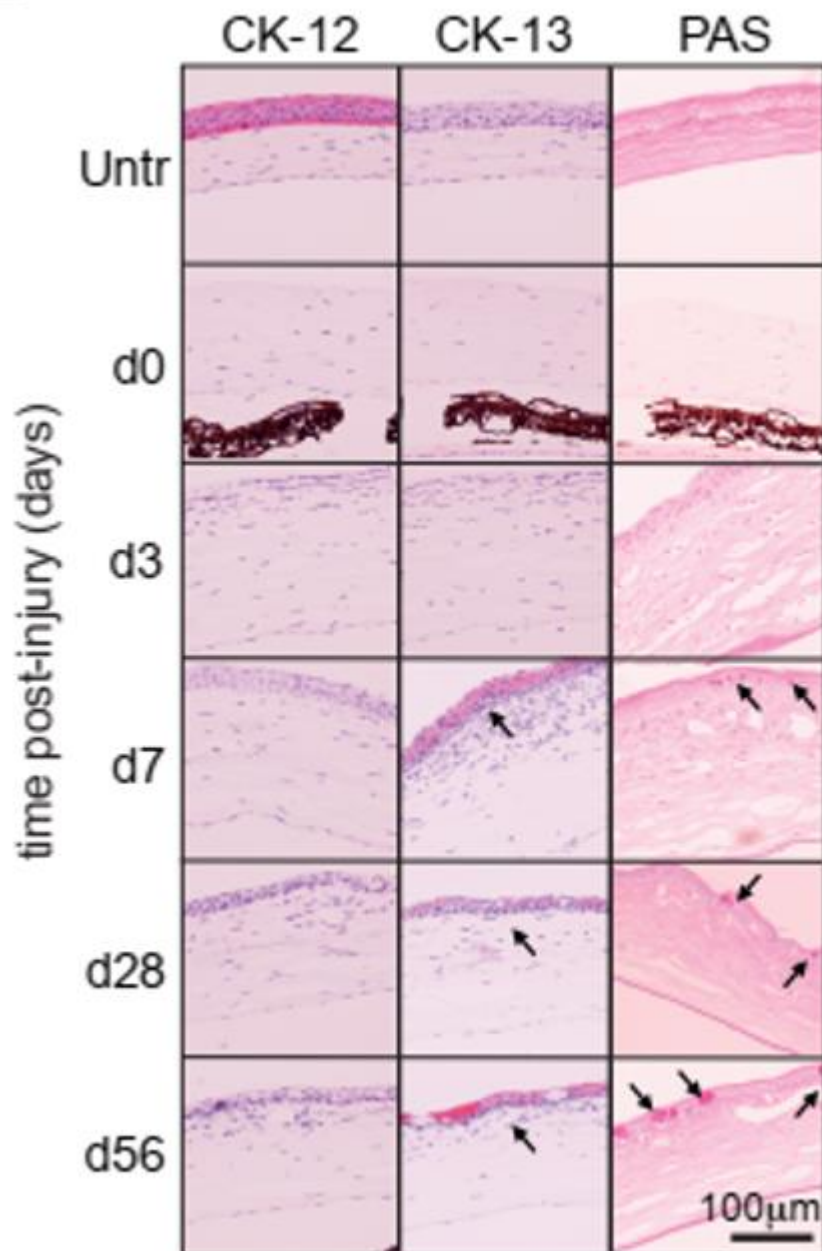


Figure 3.6 Immunohistochemical imaging of the murine cornea following induction and development of LSCD. Immunohistochemical staining of corneas following LSCD injury showed a loss of K12 expression and the arrival of K13 expressing conjunctival epithelial cells and Periodic Acid Schiff (PAS) positive stained goblet cells into the central cornea as indicated by arrows. Images shown are representative of at least 4 independent experiments.

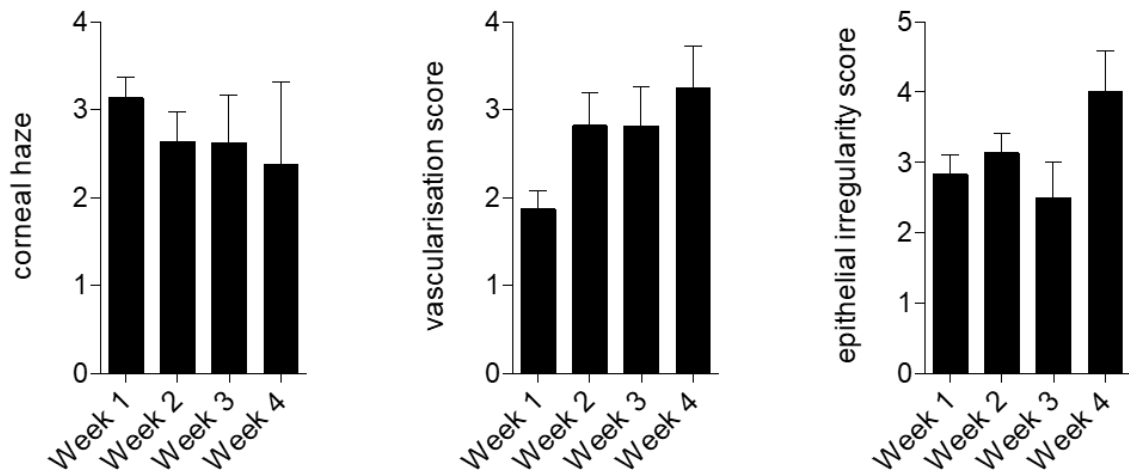


Figure 3.7 Visual assessment and scoring of the progression of LSCD. Visual scoring of the severity of several features of LSCD, corneal haze, vascularisation, and epithelial integrity on a scale of 1-5, where 1=least severe and 5=most severe. All images were assessed by three double blinded individuals.

3.2 The corneal response to chemical injury is an acute inflammatory episode characterized by a stromal & epithelial wound healing response.

Corneal inflammation results in the loss of several factors required for ocular immune privilege which can significantly influence the outcome of full thickness corneal transplantation [115, 116]. As the condition of the LSCD graft bed is also likely to influence the success of LESC transplant outcome we therefore next examined changes in chemokine, cytokine, and cellular components of the acute and chronic immune response to LSCD. FACS analysis of a single cell suspension from the LSCD mouse cornea following injury (Figure 3.8) demonstrated a biphasic pattern of innate immune cell infiltration with peaks at days 3 and 14 post-injury. This observation was clear for neutrophils; identified by positive staining for Ly6G and CD11b, as well as for macrophages and monocytes; identified by positive staining for Ly6C and F4/80. Few dendritic cells, identified by CD11c and MHC class II, are present in the cornea in the early stages of LSCD.

Flow cytometry performed at 3 weeks following injury determined the cell number of CD45+, CD3+ CD8+ cells, macrophages, monocytes, and neutrophils using cell counting beads. This data showed a significant difference between LSCD and an untreated control for the number of CD45+ cells and the number of macrophages present in the cornea at this time point (Figure 3.9) with an increase in CD45+ and macrophages in response to LSCD induction. The presence of MHC class I and II expressing cells in LSCD corneas compared to controls was evaluated at the 3 week post injury time point (Figure 3.10). It was observed that the expression of class I was significantly higher in the LSCD cornea than the healthy control implying a greater number of nucleated cells present. The gMFI for MHC class II expression was not significantly different in this case. Data from other time points during this experiment was limited due to issues with very low cell numbers obtained from the cornea for flow cytometry.

Establishing A Mouse Model of LSCD and LESC Transplantation

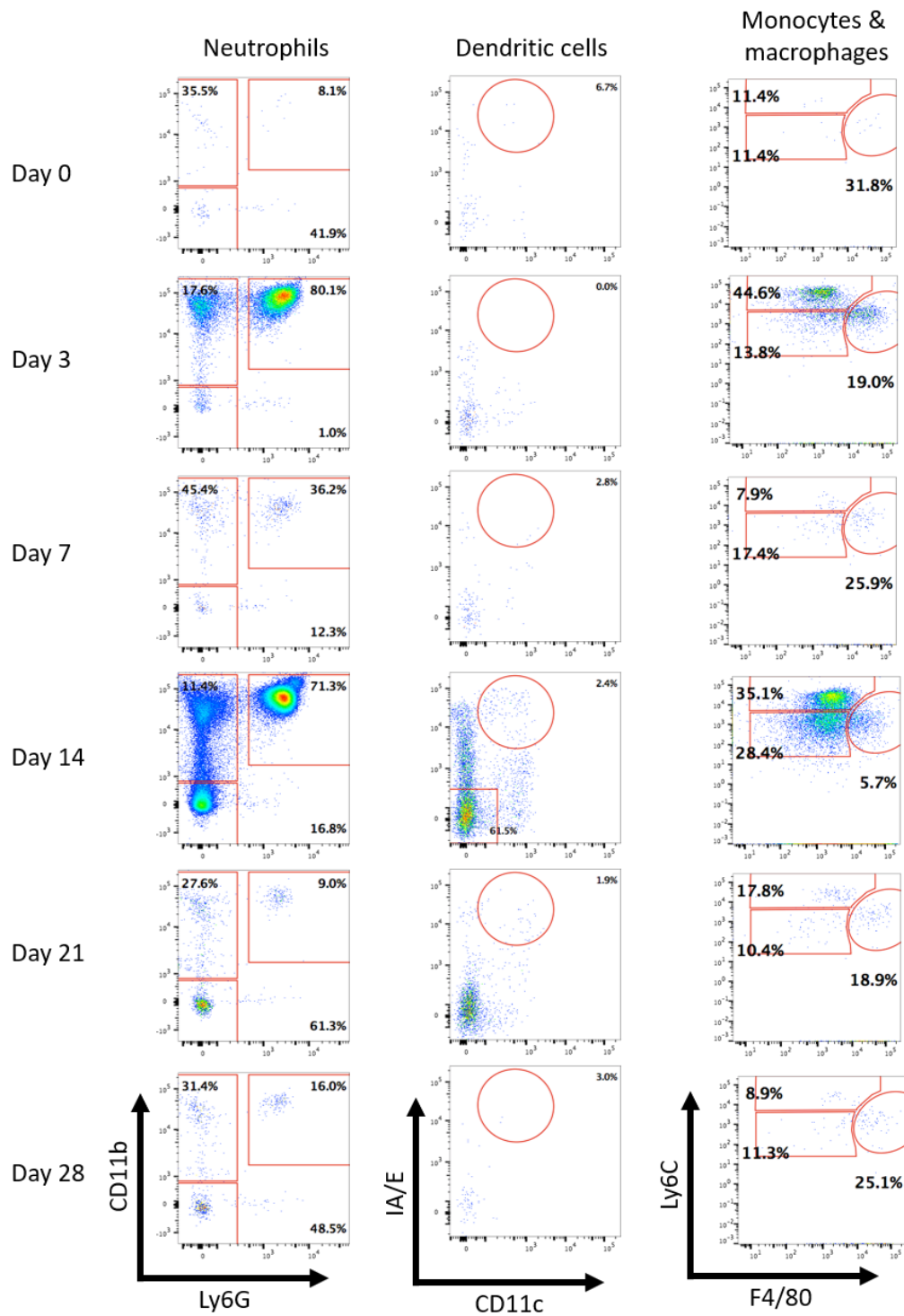


Figure 3.8 FACS plots showing the infiltration of immune cells into the LSCD mouse cornea following injury. Corneas of LSCD B6 mice at each time point were digested into a single cell suspension and analysed by FACS for the presence of neutrophils, dendritic cells, and monocytes & macrophages. The representative plots above show a clear infiltration at days 3 and 14 post injury for neutrophils and macrophages & monocytes, but very few dendritic cells. N=4 for each time point.

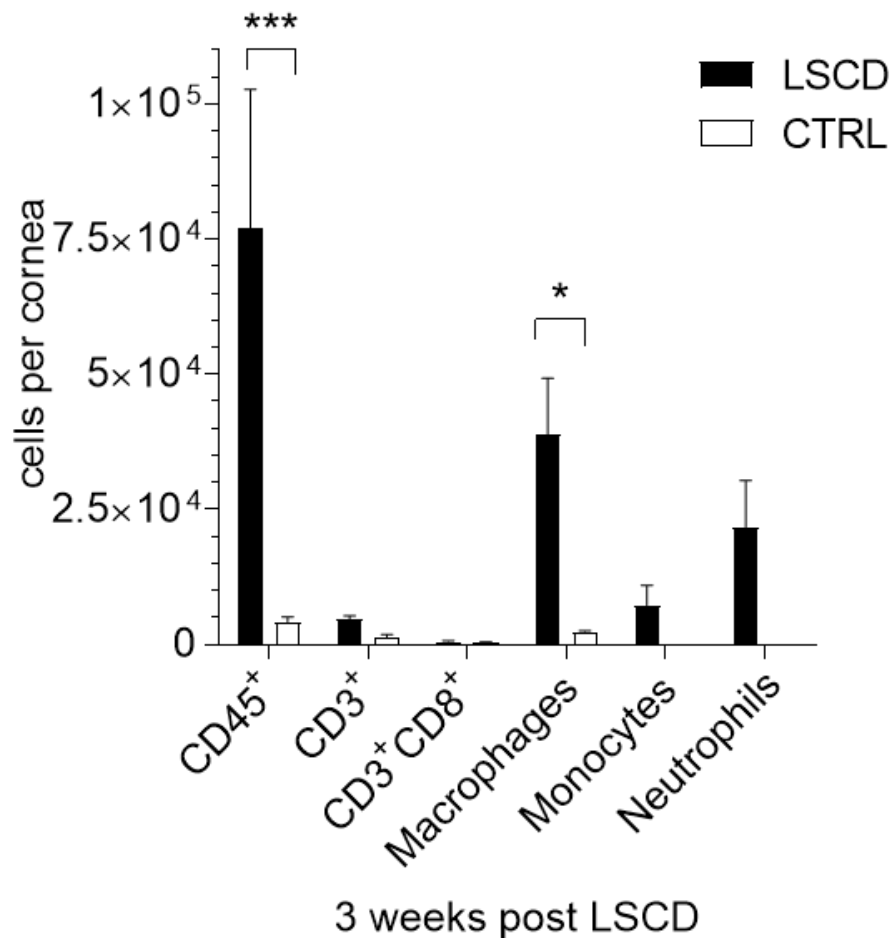


Figure 3.9 Summary of FACS data showing the infiltration of immune cells into the mouse cornea 3 weeks post LSCD. Corneas of LSCD B6 mice 3 weeks following injury were digested into a single cell suspension and analysed by FACS for the presence of CD3⁺ cells, CD8 T cells, neutrophils, monocytes & macrophages. This figure shows the absolute number of cells per cornea, assessed by counting beads, in comparison between an LSCD cornea and an untreated control. Data shown is representative of mean \pm S.E.M plotted for each mouse. N=4 animals per group, * $P < 0.05$, ** $P < 0.01$, *** $P < 0.001$ compared to untreated mice, two-way analysis of variance (ANOVA).

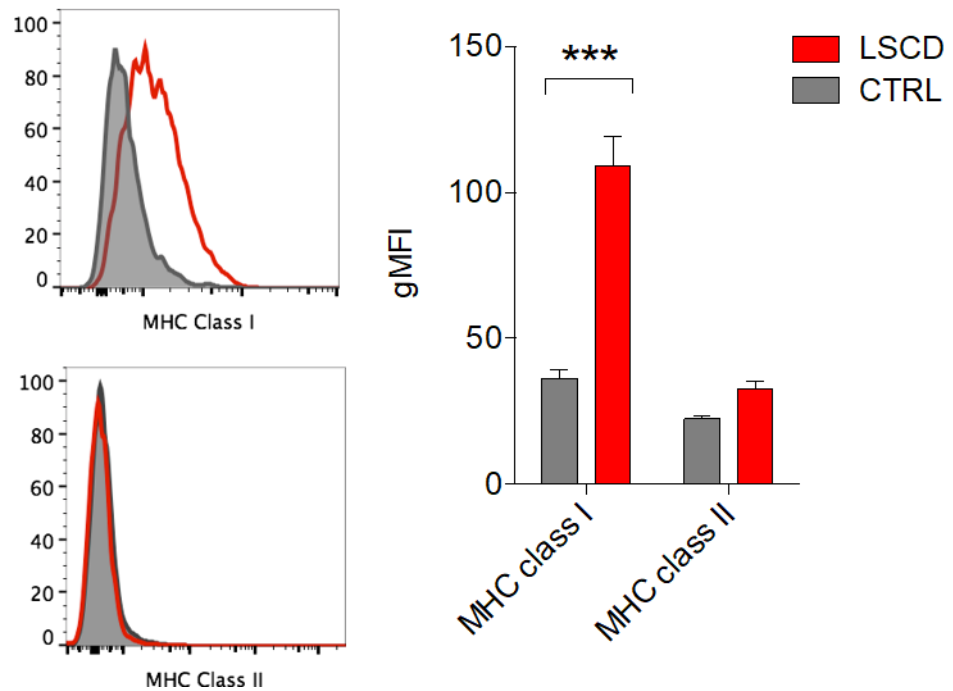


Figure 3.10 Summary of FACS data showing the detection of MHC class I and II the mouse cornea 3 weeks post LSCD. Corneas of LSCD B6 mice 3 weeks following injury were digested into a single cell suspension and analysed by FACS for the mean fluorescence intensity of MHC class I and II, in comparison between an LSCD cornea and an untreated control. Data shown is representative of mean \pm S.E.M plotted for each mouse. N=4 animals per group, * $P < 0.05$, ** $P < 0.01$, *** $P < 0.001$ compared to untreated mice, two-way analysis of variance (ANOVA).

Further investigation into the LSCD corneal tissue by gene expression analysis using a targeted cornea inflammatory gene panel, in Figure 3.11, demonstrated an acute chemokine and proinflammatory cytokine response to chemical injury. Most notably, a rapid and significant increase in CXCL1 and the proinflammatory cytokine IL-1 β was detected within several hours after corneal injury. Elevated expression of the inflammatory cytokines IFN γ and TNF α were also detectable from 1-3 days following injury. The biphasic pattern of upregulation of IFN γ expression at days 3 and 14 was indicative of tissue infiltrating myeloid cells recruited to the cornea after 3 days and approximately 2 weeks after injury, as seen in Figure 3.8. Significant increases in expression of several other chemokines and cytokines were also detected at day 3 post-injury (mean fold expression \pm S.E.M, α -Enolase 6.7 \pm 1.4, Insulin growth factor 43 \pm 16.4, IL-10 7.4 \pm 2.8), whereas others were either not significantly differentially regulated (TATA box binding protein 2.8 \pm 1.5, Calreticulin 2.8 \pm 0.9), or remained undetected (IL-4). Several angiogenic and lymphangiogenic factors are reported as acute stromal cell stress and epithelial wound healing responses, including vascular endothelial growth factor (VEGF) -A and -C, vascular endothelial growth factor receptor 2 (VEGF-R2), and fibroblast growth factor-2 (FGF-2), all of which were significantly upregulated early post-injury (Figure 3.11) [117-119].

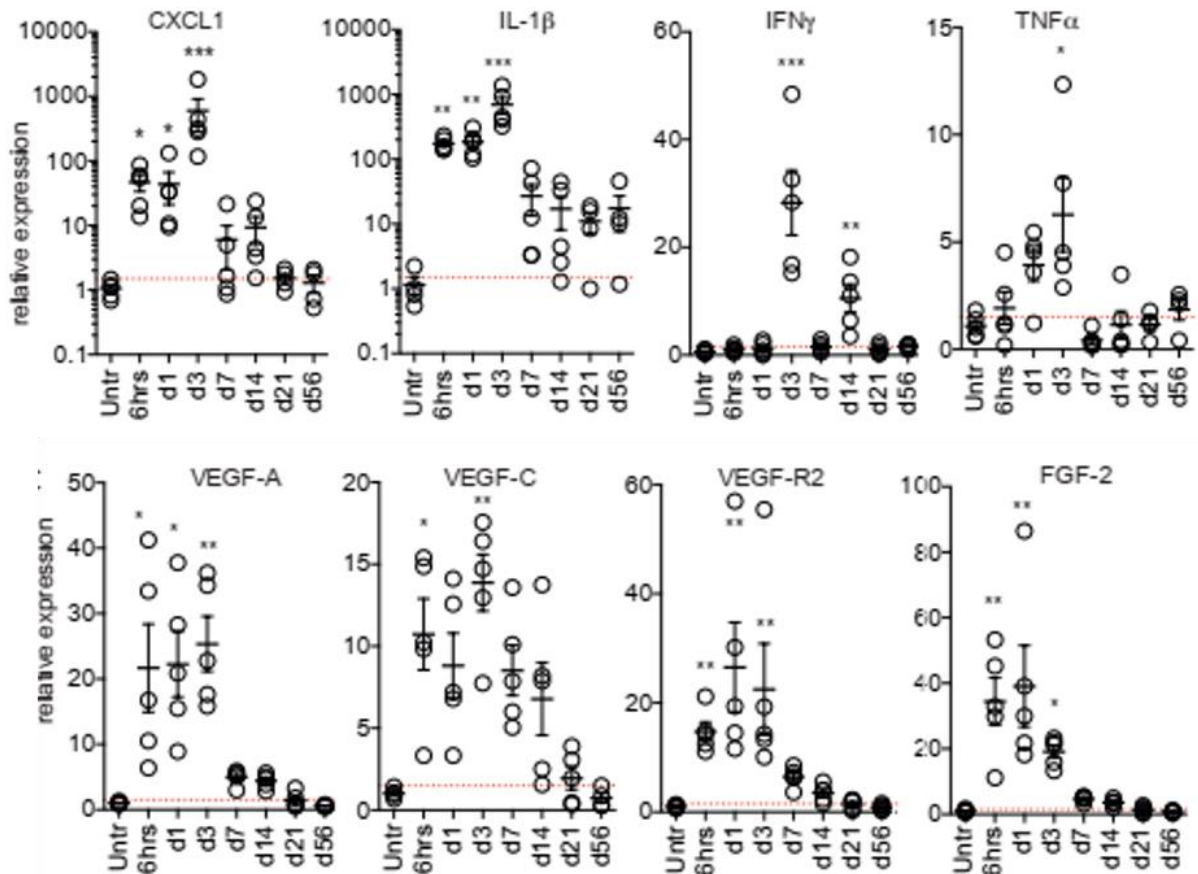


Figure 3.11 Gene expression of key inflammatory mediators and angiogenic factors expressed in response to LSCD induction. Quantitative RT-PCR analysis of change in gene expression in corneal tissue following LSCD shown as fold change in gene expression 6 hours, or 1-56 days after LSCD induction, relative to untreated corneas. Red lines indicate 2-fold increase in expression. Data shown is representative of 2 independent experiments, with mean \pm S.E.M plotted for each mouse. N=5 animals per group, * $P < 0.05$, ** $P < 0.01$, *** $P < 0.001$ compared to untreated mice, one-way analysis of variance (ANOVA).

Analysis of whole corneal tissues was also performed by ELISA to detect key proinflammatory mediators following LSCD induction (Figure 3.12), which similarly demonstrated a rapid and significant increase in the expression of CXCL1, IL-1 β , IFN γ , and TNF α . While these factors returned to near baseline levels in later stages post-injury, mildly elevated levels of IL-1 β persisted, suggesting the presence of continued low-grade corneal inflammation. In addition to corneal resident myeloid derived APCs, production of these proinflammatory factors immediately following injury would also likely be derived from stromal and residual epithelial compartments [120-122].

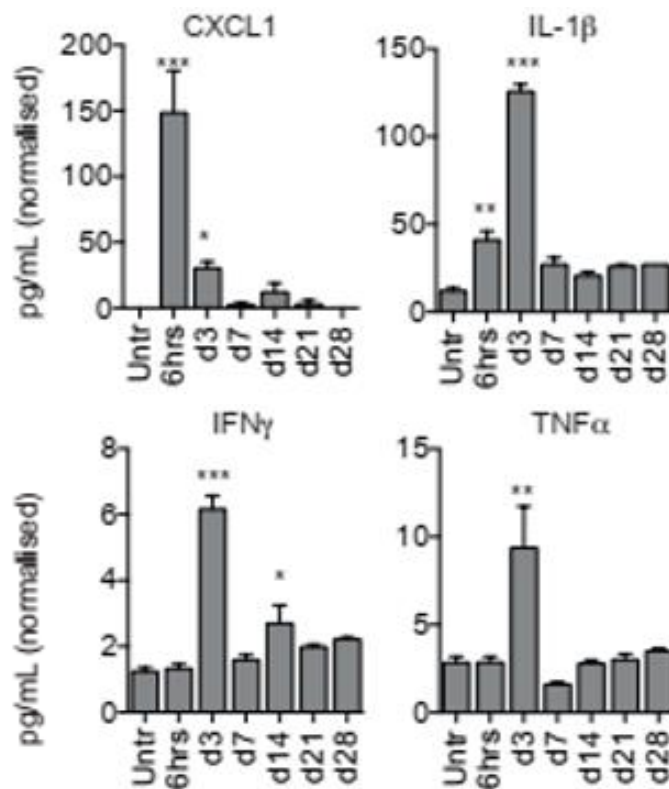


Figure 3.12 Murine corneal chemokine and cytokine expression levels in response to LSCD induction. Detection of chemokine and cytokine levels in whole murine corneal tissue by ELISA 6 hours, or 1-56 days after LSCD induction, relative to untreated corneas. Data shown is representative of 2 independent experiments, with mean \pm S.E.M plotted for each mouse. N=5 animals per group, * $P < 0.05$, ** $P < 0.01$, *** $P < 0.001$ compared to untreated mice, one-way analysis of variance (ANOVA).

To explore this further, we examined the capacity of enriched murine corneal stromal and epithelial subsets to produce other factors capable of remodelling the corneal microenvironment. Primary corneal cell subsets were cultured in the presence of single proinflammatory cytokines IL-1 β , TNF α , IFN γ , or a combination of all three, which have previously been found to be elevated in LSCD corneas. These stromal and epithelial cell subset supernatants were then screened by ELISA for the induction of chemokine protein production (Figure 3.13). Corneal stromal cells secreted high concentrations of CXCL1 and CXCL2 in response to IL-1 β , and high concentrations of CCL5 and CCL7 in response to IFN γ . A further increase was detected in levels of CCL5 when cells were treated with a combination of all three cytokines (CytM). The epithelial response to the same cytokines was more restricted, with only levels of CCL5 significantly increased in response to IL-1 β , IFN γ , or CytM. This data together suggests that activated corneal stromal cells are important for generating the inflammatory environment of the LSCD graft bed. Combined, the proinflammatory cytokine and chemokine responses was detected post-injury would serve to dramatically alter the corneal microenvironment by inducing neovascularisation, as well as recruiting neutrophils, macrophages, and other myeloid subsets. Inhibition of any of these key parameters or processes may therefore serve to minimise the inflammation seen following LSCD injury.

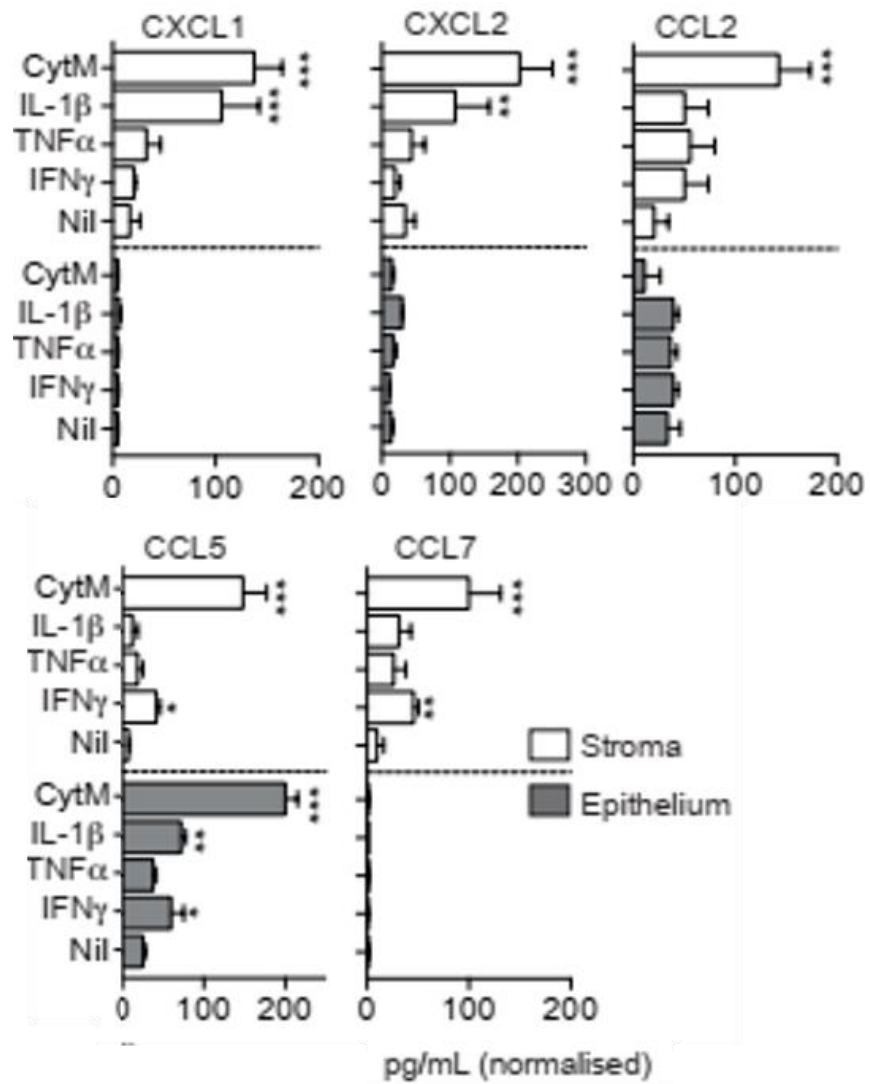


Figure 3.13 Murine corneal chemokine and cytokine levels expressed by cultured primary murine corneal epithelial and stromal cells. Supernatants from enriched cultured primary mouse stromal and epithelial cells were screened for chemokine production by ELISA following 24 hours *in vitro* with proinflammatory cytokines IL-1β, TNFα, IFNγ, or a combination of all three (CytM). * $P < 0.05$, ** $P < 0.01$, *** $P < 0.001$, one-way ANOVA, compared to no stimulation (Nil).

3.3 Development and optimisation of a protocol for LESC transplantation.

With the model of LSCD well established, we next developed an experimental model of limbal epithelial stem cell transplantation. Our novel model, utilising GFP expressing donor cells, allows the *in vivo* long-term tracking of LESC engraftment and outgrowth and was achieved by transplantation of murine corneal and limbal derived epithelial sheets onto the recipient's LSCD induced cornea. Immunodeficient NSG mice were used as recipients in all transplant experiments, for two main reasons: (i) firstly, during protocol optimisation, transplantation into a recipient with minimal immune function would be expected to optimise the success of the grafting procedure and subsequent engraftment. This would therefore allow us to identify whether graft failures were due to technical issues rather than any immune involvement. (ii) secondly, transplantation of donor LESC requires time for engraftment, and for differentiated epithelial progeny to repopulate the recipient cornea. While in the clinical setting the use of systemic immunosuppressive therapy prevents graft rejection, here we have opted to use an immunodeficient strain as recipients instead. As LESC donors, transgenic mouse strains which ubiquitously express GFP as a fluorescence reporter were used to allow transplanted cells to be observed and serially tracked *in vivo* by fluorescence stereomicroscopy.

Establishing A Mouse Model of LSCD and LESC Transplantation

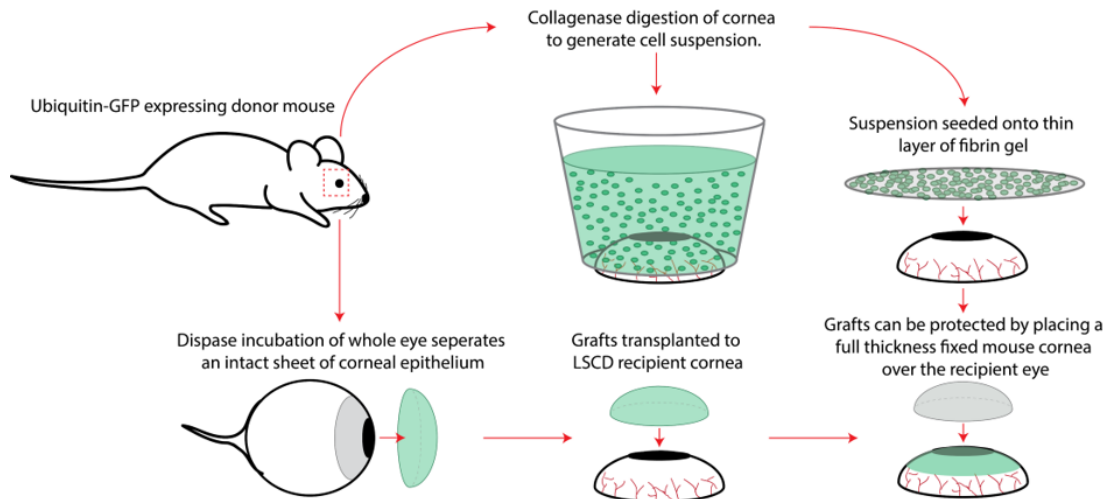


Figure 3.14 Illustration detailing the development process to establish and optimise a mouse model of LESC transplantation.

Developing a successful experimental protocol for transplantation of donor-derived limbal epithelial cells to the recipient cornea proved to be a significant challenge, with some of the unsuccessful protocols attempted and their outcomes summarised in Figure 3.15. The suspension method, where donor mouse corneas were enzymatically digested into a single cell suspension using either dispase or collagenase, and then added into round plastic tubing placed directly over the exposed corneal surface, allowed the greatest numbers of cells to be transferred to the eye, however cells suspended in fluid did not adhere to the surface of the eye [123]. In contrast, these donor corneal cell suspensions were able to readily adhere to a thin layer of fibrin gel in *in vitro* culture which could then be used as a carrier membrane to transfer the attached cells to the cornea. However, we were unable to produce a gel thin enough to flex and cover the convex surface of the eye successfully while also remaining thick enough to avoid disintegration during cell culture, despite this protocol being previously described [17]. The most effective method initially attempted was to transfer intact corneal epithelial cell sheets derived from incubating an enucleated donor eye in dispase solution, which disrupts the basement membrane and loosens an intact sheet of epithelium from the stroma [124, 125]. Optimising the duration of tissue digestion to release the corneal epithelium proved

to be crucial in producing an intact and viable cell sheet, which could be separated within 10 minutes of dispase treatment. Using this intact sheet method, long-term limbal epithelial cell engraftment could be detected within the recipient cornea (Figure 3.16), although this was still extremely limited.

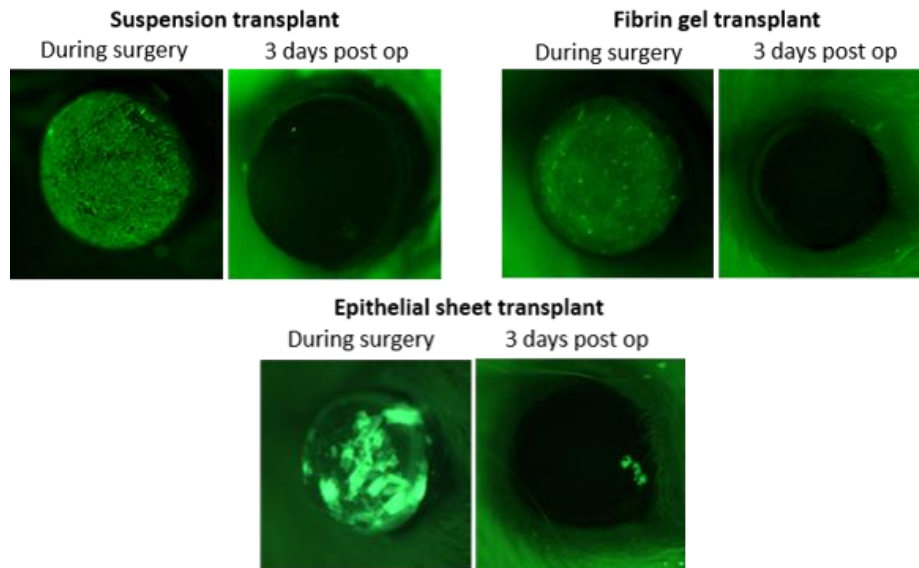


Figure 3.15 Representative images contrasting several unsuccessful transplant methods in the mouse cornea. These images of GFP+ mouse epithelial cell transplant serve as examples as to the typical outcomes and failures resulting from three methods of transplant: cell suspension, cells confluent on a thin fibrin gel, and whole epithelial sheet. Images show GFP expressing cells at day 0 during transplant and their absence or minimal presence at day 3 after suture removal.

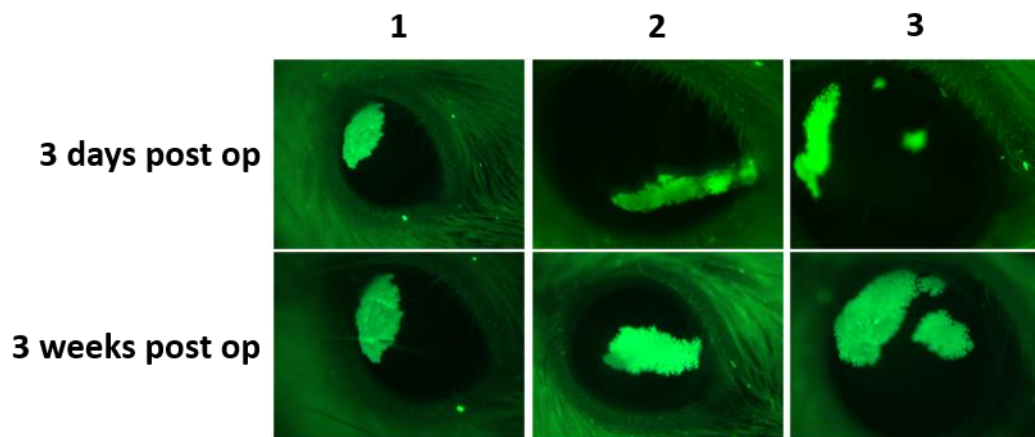


Figure 3.16 Representative images of inefficient intact epithelial sheet transplant method in the mouse cornea. These images of three representative GFP+ mouse epithelial cell transplant serve as examples of successful but inefficient and slow growing grafts. Images show GFP expressing cells at day 3 post transplant and their limited growth by week 3.

To further improve donor cell engraftment, we investigated strategies to improve the integrity of donor cell sheets and better preserve epithelial cells during digestion. Y-27632, a Rho-associated protein kinase (ROCK) inhibitor, has been shown to accelerate limbal epithelial proliferation *ex vivo*, improve wound closure rates in a rat model of corneal wounding, and reduce apoptosis of corneal endothelial cells [126, 127]. When included in the dispase digestion buffer we observed a marked improvement in the integrity of cell sheets and the ability to manipulate their shape and positioning during surgery without damaging it (not shown). However, addition of this reagent did not improve engraftment success rates.

As well as the transplant method and quality of donor cells, the condition of the graft bed is believed to be important to engraftment success. Whether it is growth arrested 3T3 cells *in vitro*, or the stromal cells of a healthy cornea, in order to adhere and expand, LSCs require the growth factors produced by such a feeder layer. We hypothesised that the chemical-injury used to induce LSCD may have created a hostile microenvironment into which we were transferring LESC, and this ultimately

compromised their subsequent engraftment, therefore we next sought to investigate methods to improve the condition of the recipient corneal graft bed. Sodium hyaluronate (Na-HA), a component of the extracellular matrix (ECM), has been widely used during ocular surgery, and is reported to effectively treat corneal erosion, alkali burns, and to accelerate epithelial wound healing [128-132]. Matrigel is a gelatinous protein mixture consisting of most of the components of the ECM, and has been used as such for culturing LSCs in vitro [133, 134]. Solutions of these components were used to coat the recipient cornea prior to transplantation in an attempt to provide a more favourable environment and promote engraftment, however no improvement in engraftment success was achieved.

It was observed that many of the transferred donor cells were lost from the corneal surface on closing and suturing the eyelid, and over the subsequent few days post-transplantation. To counter this issue we developed a protective mouse contact lens, formed of a formaldehyde fixed, full thickness, dissected mouse cornea, to place over the graft once the donor epithelial sheet was transferred to the eye. This physical barrier offered sufficient protection of the transferred cells during the initial days after transplantation and seemed to be key to success, resulting in improvements in the number of transferred cells engrafting.

3.4 Limbal epithelial stem cell transplantation prevents and reverts the LSCD phenotype.

Combining the protective contact lens with the short duration of dispase digestion, epithelial sheet production, and ROCK inhibitor treatment, the model began working reliably and consistently. This optimised protocol was then capable of reproducibly achieving complete expansion and coverage of the cornea within two weeks of transplant (Figure 3.18), in comparison to early versions of this mouse model in which the number of transplants resulting in successful engraftment was less than 5%. Of these early minor successes, the majority consisted of only single or small clusters of engrafted cells.

However, the individual engrafted cells were capable of regenerating the entire cornea of recipient NSG mice over the course of 6 months and were observed to gradually reverse LSCD and re-form a healthy, transparent, multi-layered corneal epithelium. Where transplanted cells did not engraft, LSCD continued to develop unchecked, with sustained inflammation, neovascularisation, and conjunctivalisation compared to healthy regenerated corneas (Figure 3.17). Technical improvements since these early experiments, outlined in section 3.3 above, significantly improved efficiency, achieving an engraftment success rate of 60-80% and consistently resulting in 40-80% coverage of the cornea by donor-derived cells by day 7 post-transplantation.

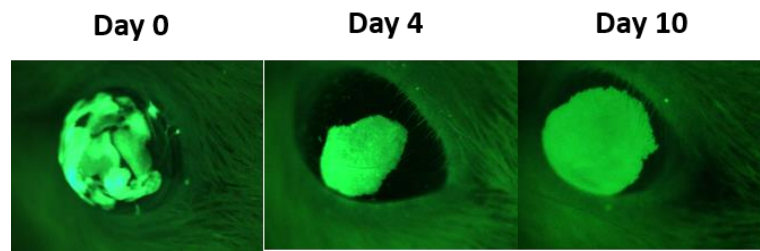


Figure 3.18 Short term *in vivo* imaging of transplanted LESC in an LSCD murine cornea using an optimised protocol. LSCD was induced in immunodeficient NSG, followed by transplant of GFP+ murine epithelial sheets containing LESC. Initial results using an optimised protocol consisted of a large patch of engrafted cells which rapidly expanded to cover the entire surface of the eye within 14 days.

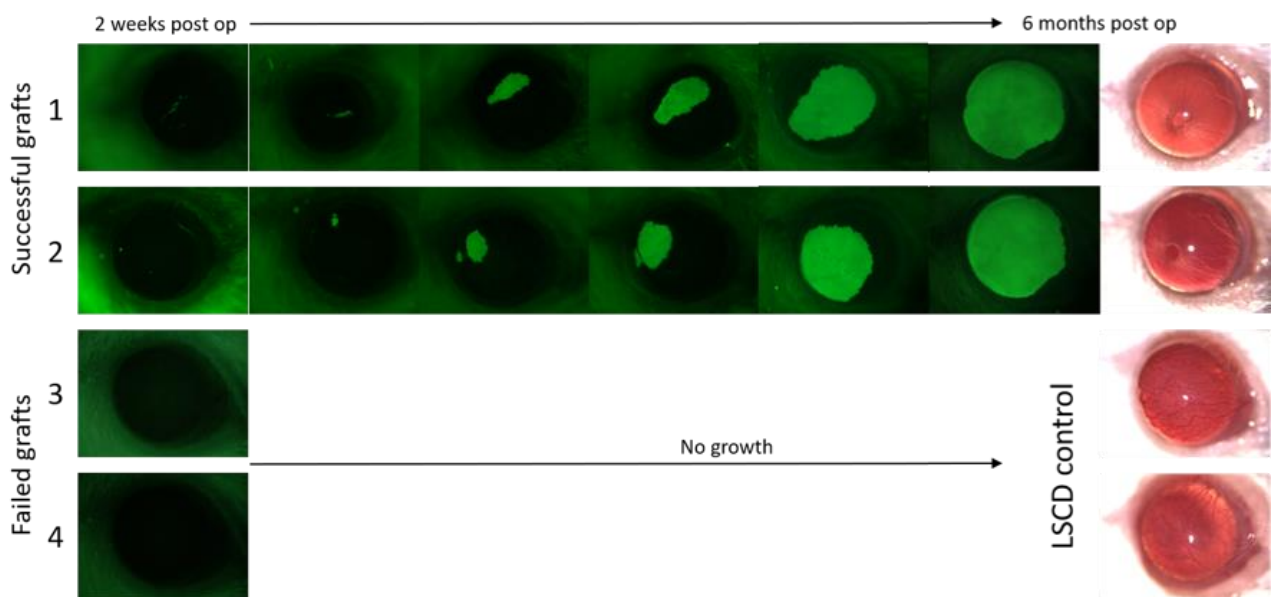


Figure 3.17 Long term *in vivo* imaging of individual transplanted LESC in an LSCD murine cornea. Serial imaging of two representative mice. LSCD was induced in immunodeficient NSG, followed by transplant of GFP+ murine epithelial sheets containing LESC. Initial engraftment consisted only of single cells which were observed to expand and cover the entire surface of the eye over the course of 6 months. Far right column shows a comparison between successful and failed grafts under white light, revealing the absence of an LSCD phenotype in the former, and severe LSCD in the latter.

With a working protocol established we were then able to extend the transplant model from immunodeficient NSG mice, to using fully immunocompetent B6 mice. In order to confirm complete re-epithelialisation of the cornea, we performed intravital multiphoton microscopy imaging of a syngeneic GFP+ mouse limbal epithelial graft from B6-GFP donor, fully engrafted onto a CFP+ recipient (B6-CFP) mouse eye. This imaging was performed with the assistance of Dr. Pervinder Sagoo. Images in Figure 3.19 show complete re-epithelialisation of the central cornea to the limbus, with an intact recipient-derived conjunctival region and a clear defined boundary between epithelium and stroma in the central cornea.

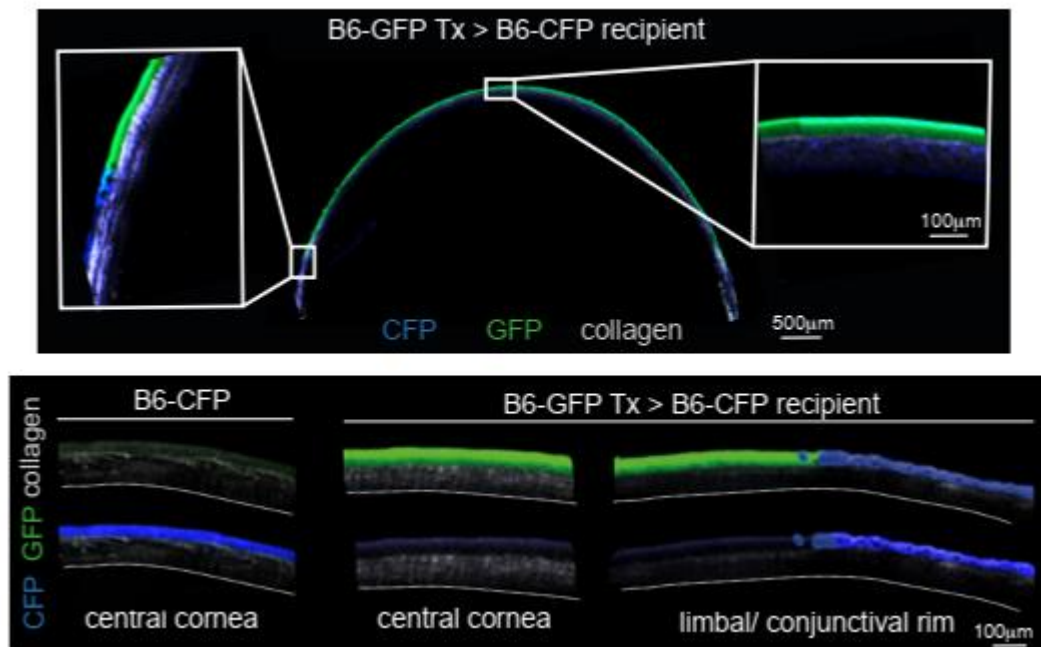


Figure 3.19 2-photon imaging of B6-CFP recipient with transplanted B6-GFP corneal epithelium. Intravital 2-photon imaging of a representative syngeneic mouse cornea with GFP expressing corneal epithelial cells successfully engrafted into a B6-CFP recipient. These images, 3 weeks post transplant, show full engraftment and complete regeneration of corneal epithelium after injury and transplant with donor cells, plus a distinct and defined border where the epithelium meets the conjunctiva and limbus. Images representative of 3 independent experiments.

Similar to data shown in Figure 3.5, quantitative PCR analysis was performed to compare the expression of K12, K19, and Muc5AC between an engrafted fully regenerated cornea 4 weeks post-transplant and an LSCD only mice, both relative to a healthy untreated control. Figure 3.20 demonstrates the reversal of the LSCD phenotype in the grafted recipients, with a return of CK-12 expressing cells to normal levels, and the complete loss of CK-19+ conjunctival cells, as well as a significant decrease in expression of Muc5AC conjunctival derived goblet cells.

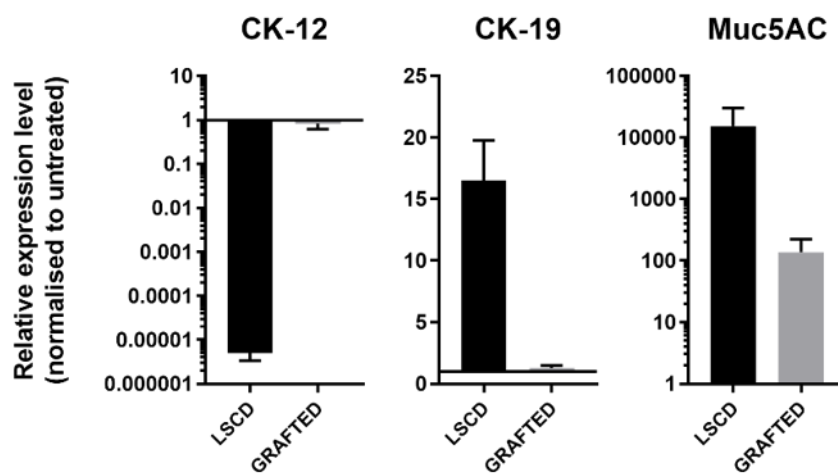


Figure 3.20 Quantitative PCR analysis of the murine cornea following induction of LSCD and reversal with transplanted donor murine corneal epithelial cells. Chemical injury to the murine cornea resulted in the loss of corneal epithelium and the invasion of conjunctival epithelium as part of the LSCD phenotype. Transplant of donor murine corneal epithelial sheets containing LESC is able to reverse this phenotype as demonstrated by qPCR. Gene expression data shows no expression the loss of K12 in LSCD only controls compared to grafted mice, and the lack of expression of Cytokeratin-19 in grafted mice compared to LSCD controls. Mucin 5A expression is detected in grafted mice, although at lower levels than LSCD controls. Data was collected at 4 weeks post transplant, and expression is relative to an untreated control. N=3.

3.5 Summary

In order to investigate LSCD it was necessary to develop a clinical animal model which accurately recapitulates the key clinical features of the disease. Evidence for this included *in vivo* imaging of neovascularisation and epithelial defects, and immunofluorescence histology showing the loss and gain of both epithelial and conjunctival cell types respectively, corroborated by qPCR gene expression analysis. Further investigation into the *in vivo* physiological response to LSCD demonstrated the cellular infiltration into the cornea, as well as the secretion of inflammatory mediators and angiogenic factors involved.

Development of the protocol for transplantation of donor LSCs was a lengthy and challenging process, with many of the strategies and modifications attempted having little or no effect. Despite this, the current established protocol works with high reproducibility and is capable of completely regenerating the recipient NSG mouse cornea with GFP expressing corneal epithelial cells. The use of fluorescently labelled donor epithelial cells has allowed the growth kinetics of these cells to be imaged once engrafted, even when originating from single or small clusters of cells localised to the central cornea. Multiphoton imaging of a regenerated cornea confirmed a full thickness epithelium which re-established a boundary at the epithelial-conjunctival junction, and qPCR gene expression analysis showed the reversal of the LSCD phenotype.

In summary, the development of an *in vivo* model of LSCD and LESC transplantation has allowed us to visualise and track the engraftment and growth kinetics of LESC as they regenerate the damaged mouse cornea. It also plays a key role in the next objective of this study; investigating the role inflammation and the immune response in LESC engraftment and transplant failure.

CHAPTER 4. DETERMINING THE ROLE OF THE INNATE AND ADAPTIVE IMMUNE RESPONSES IN LESC TRANSPLANT REJECTION

Despite the immune privileged status of the healthy human eye, these protective mechanisms can become compromised in patients with LSCD, resulting in significant inflammation and a response by the adaptive and innate immune response. Keratoplasty is one of the most commonly performed organ transplants, and allogeneic keratoplasty is usually a highly successful procedure with a 90% first year survival rate even without HLA matching [27]. However, this differs from procedures such as cultured limbal epithelial transplantation (CLET) which typically involve a highly inflamed, vascularised, and compromised graft bed or limbal niche. For patients receiving these allogeneic epithelial cell transplantations in the cornea there is a high risk of graft rejection by the host immune system, with 75% of allografts failing within 3 years, despite systemic immune suppression [35].

Currently publications investigating the role of the immune system are limited, and so the exact mechanism of action is not clear. One such question is whether the rejection involves the direct recognition of donor derived passenger APCs by recipient T cells, or indirect allorecognition of donor MHC presented by recipient APCs. It is established that donor derived macrophages do not survive *ex vivo* culture [33], however it is not clear how this affects the levels of MHC class I and II in allogeneic grafts, or how this affects the relative involvement of CD8+ and CD4+ T cells in the adaptive response. Understanding the precise cellular involvement during each stage of corneal epithelial allograft rejection would lead to improvements to clinical practice, and the potential development of treatments to block or dampen the immune response.

This chapter describes the investigation into the role of innate and adaptive immune responses in the rejection of transplanted epithelial cell sheets containing LESC, using our previously described mouse model of LSCD and transplantation.

4.1 Transplantation of allogeneic LESC into an immunocompetent mouse model of LESC results in graft rejection.

With the protocol for LESC transplantation well established in the immunodeficient NSG mouse model, we designed experiments to interrogate the mechanism of engraftment in a more clinically relevant immunocompetent model. Transplant of allogeneic GFP+ corneal epithelial sheets from a BALB/c-GFP donor into B6 recipients showed early signs of limbal epithelial allograft rejection, demonstrated by the characteristic epithelial rejection line or smoothing of the graft peripheral edge between days 7 and 28 (Figure 4.1). This was not observed in B6 recipients which received autologous B6-GFP grafts. Longer term imaging in the recipients of allogeneic grafts (Figure 4.2) showed the same edge smoothing, in addition to the loss of the GFP+ corneal graft on the cornea over the course of a month as it was rejected by the host.

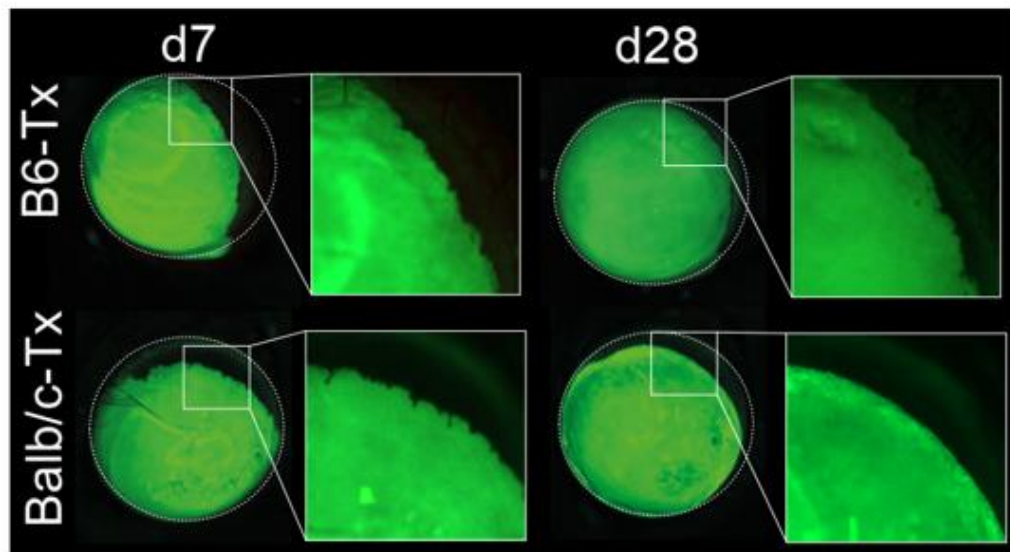


Figure 4.1 *In vivo* imaging of the onset of epithelial graft rejection in the mouse cornea. Representative images show the characteristic smoothing of the peripheral edge of a GFP+ limbal epithelial allograft. Top images show a syngeneic transplant of B6 donor into B6 recipient, bottom images show allogeneic BALB/c donor cells into B6 recipient, at both day 7 and day 28 post transplant. N=3.

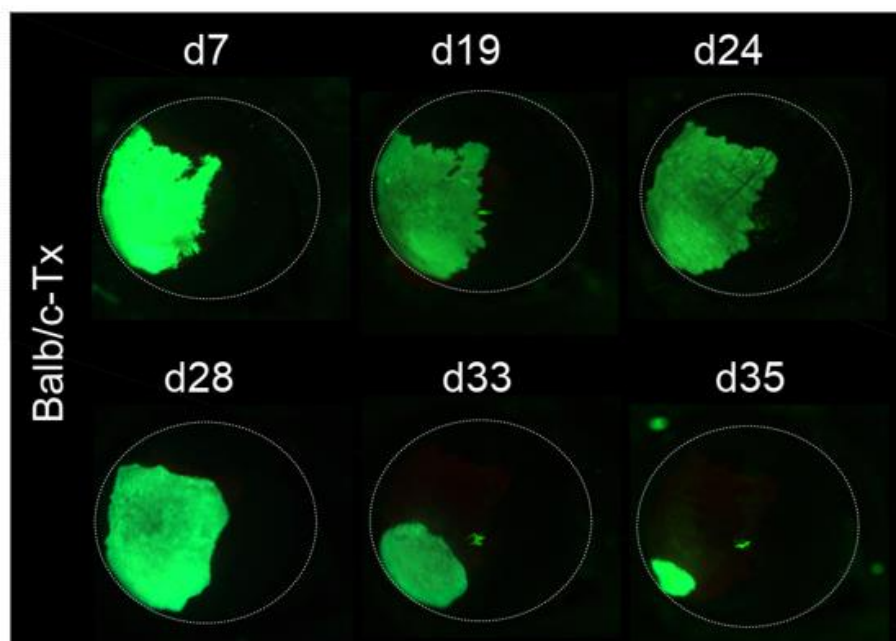


Figure 4.2 Long term *In vivo* imaging of epithelial allograft rejection in the mouse cornea. Representative images show the characteristic smoothing of the peripheral edge of a GFP+ limbal epithelial allograft, and shrinking of the graft over the course of 35 days post transplant. White dotted line marks the outer edge of the cornea. N=3.

Determining the Role of the Innate and Adaptive Immune Responses in LESC transplant rejection

Results from multiple transplant experiments, both autologous and allogeneic, are summarised in a Kaplan Meier survival plot (Figure 4.3), where mean allograft survival time was 46 days (\pm S.D 16 days) without additional immunosuppressive therapy.

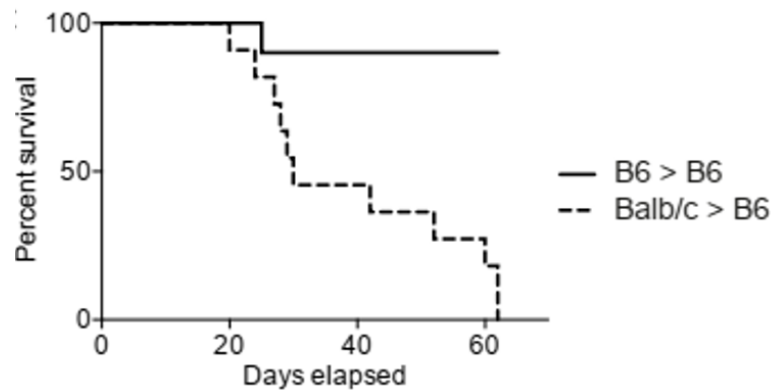


Figure 4.3 Kaplan Meier plot of limbal epithelial allograft survival in a mouse model. Kaplan Meier plot of autograft (B6 > B6 recipient, n=10) and allograft (BALB/c > B6 recipient, n=11) survival in a mouse model of limbal epithelial transplantation. Data pooled from 3 independent experiments.

Cellular infiltration within the transplanted cornea was assessed using flow cytometry in four experimental groups of B6 mice: BALB/c allograft recipients; B6 autograft recipients; LSCD only controls; and untreated healthy controls. FACS data showed the differences in the presence of T cells (CD3+), macrophages and monocytes (CD11b+, Ly6C+), NK cells (NK1.1+), and epithelial cells (EpCAM+) at day 28 post-transplant (Figure 4.4). Absolute cell numbers were quantified using counting beads during flow cytometry, allowing the generation of Figure 4.5. This data shows several significant differences between allogeneic BALB/c grafted recipients and the untreated healthy controls with respect to the number of all cell types present in the cornea at 28 days post-transplant. A significant difference was also observed between the untreated control and the B6 autograft recipient group with respect to the absolute number of neutrophils present at the time of analysis, with total cell numbers controlled using flow cytometry counting beads.

Determining the Role of the Innate and Adaptive Immune Responses in LESC transplant rejection

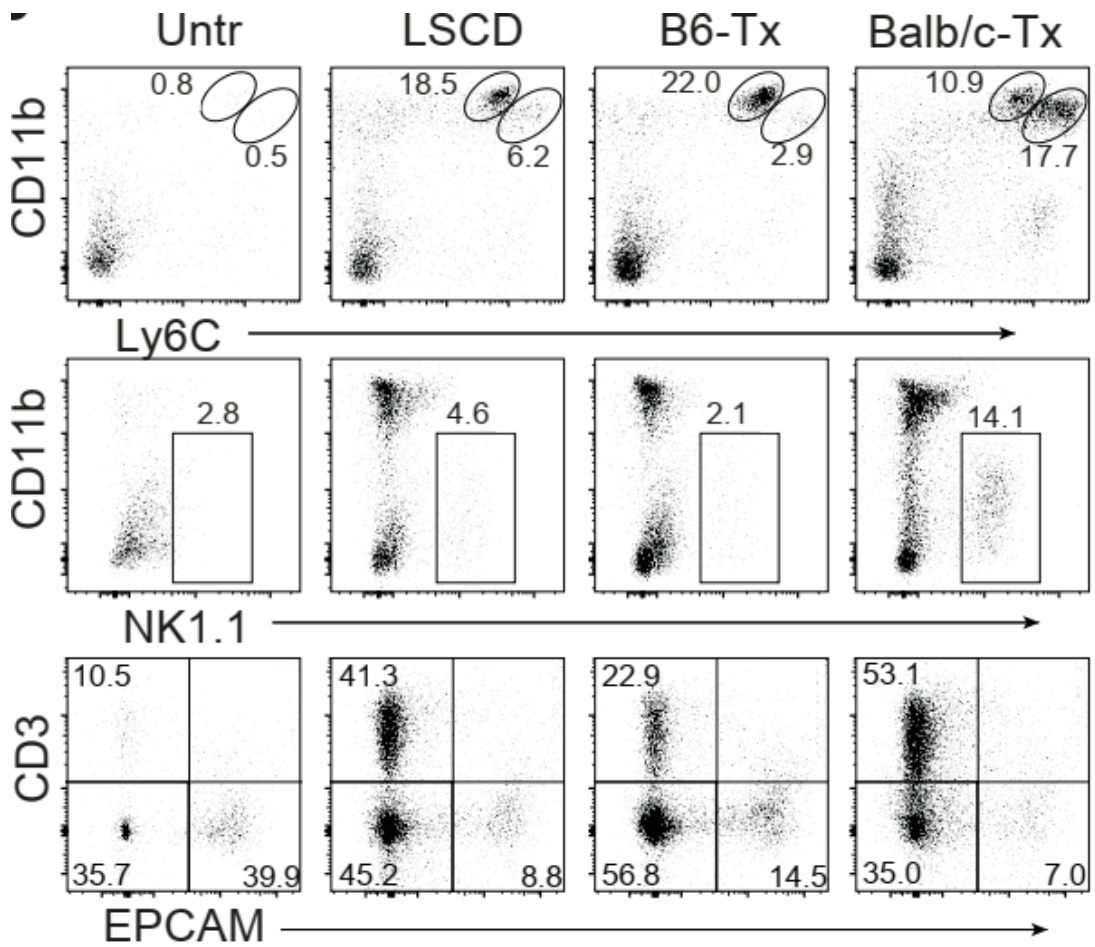


Figure 4.4 FACS plots of cellular infiltration into the mouse cornea during LESC graft rejection. Representative flow cytometry plots of digested corneal tissue 28 days after epithelial sheet transplantation, showing the infiltration of immune cell subsets into the cornea during graft rejection. N = 3 per treatment group.

Determining the Role of the Innate and Adaptive Immune Responses in LESC transplant rejection

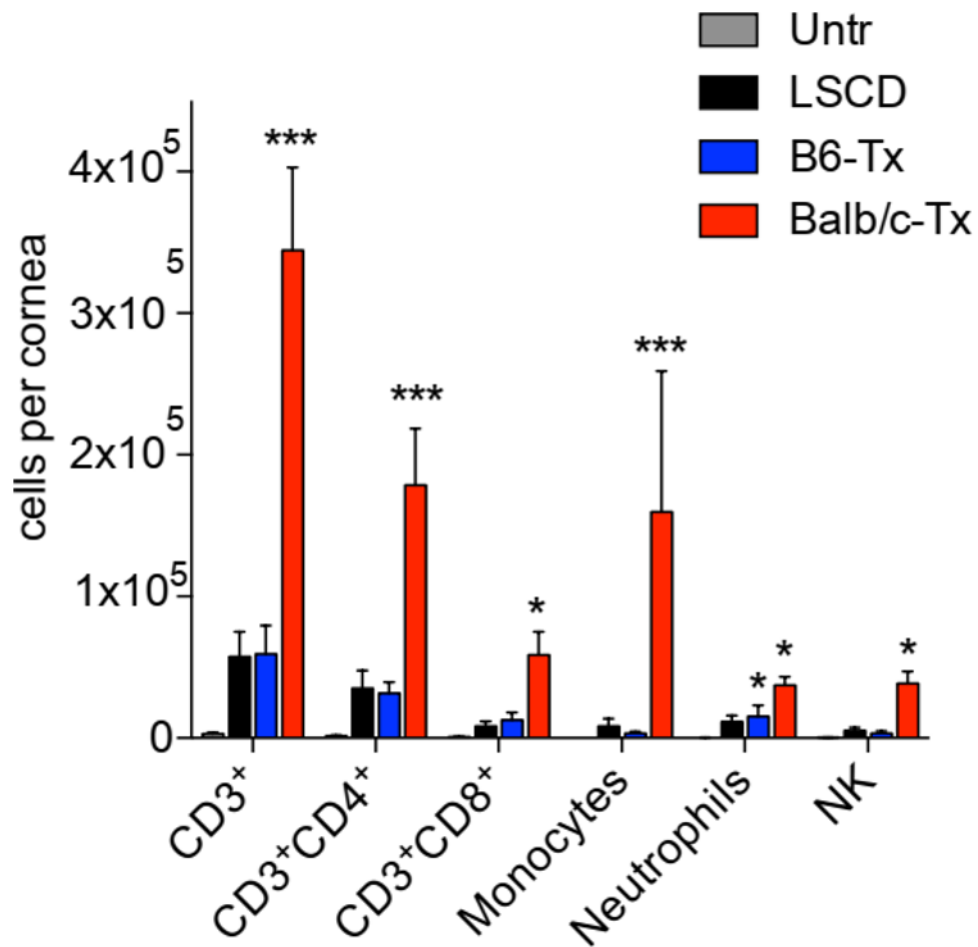


Figure 4.5 FACS summary data of cellular infiltration into the mouse cornea during LESC graft rejection. Summary plot of absolute numbers of lymphocyte and myeloid cell subsets detected in corneal tissue during onset of graft rejection (n=5-6 per group) **P* < 0.05, ***P* < 0.01, ****P* < 0.001, one-way ANOVA, compared to untreated mice.

Determining the Role of the Innate and Adaptive Immune Responses in LESC transplant rejection

Luminex analysis of cytokines and chemokines was performed on whole digested corneal tissue following either LSCD, autologous B6, or allogeneic BALB/c transplantation to determine any correlation between graft rejection and cytokine/chemokine concentrations in the LSCD cornea. Cytokines/chemokines investigated were known to be involved in corneal remodelling and microenvironment inflammation. Figure 4.6 and Figure 4.7 show the results displayed as a heatmap representing the fold change in expression for all cytokine and chemokines respectively, clustered by highest expression level. This data demonstrated that for both cytokines (Figure 4.6) and chemokines (Figure 4.7) there were significant differences in expression between recipients of allogeneic BALB/c grafts, and the untreated control mice. Expression of cytokines IL-16 and IL-1 β by allogeneic recipients was significantly increased compared to autologous recipients, while IL-10, IFN γ , and IL-6 were only increased relative to the control. Chemokines with significant expression differences between allogeneic and autologous recipients include CCL5, CXCL11, CCL3, CCL17, CCL1, CCL2, CCL7, and CCL22.

Determining the Role of the Innate and Adaptive Immune Responses in LESC transplant rejection

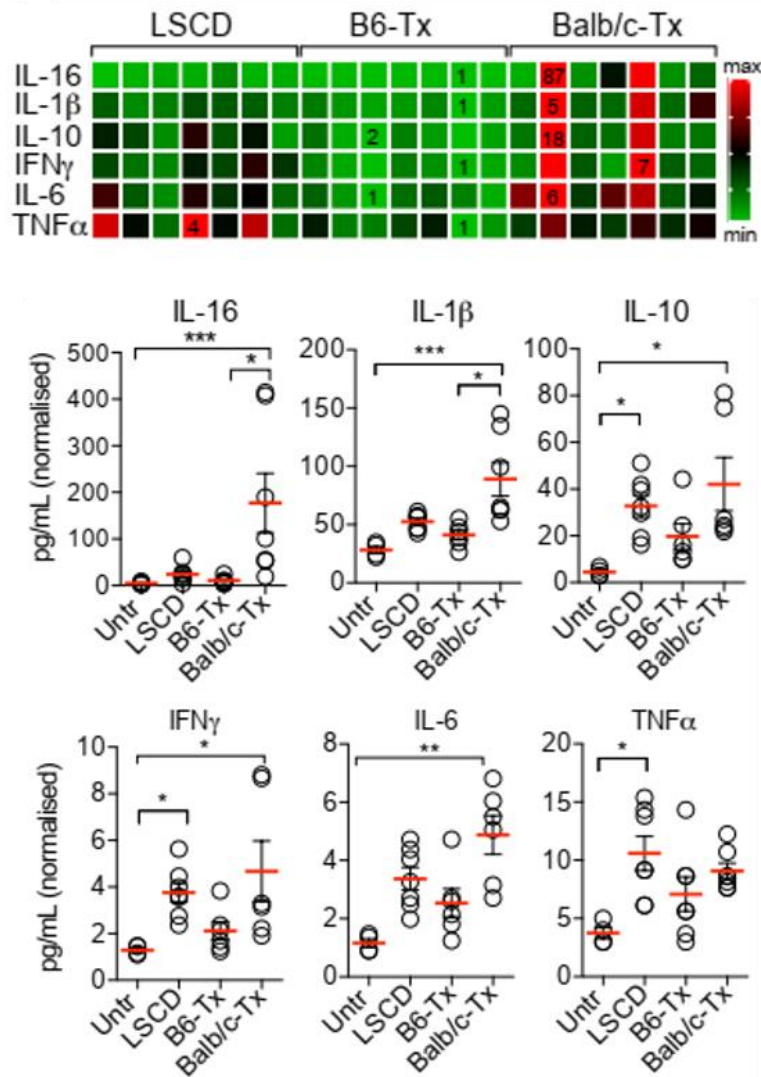


Figure 4.6 Identification of cytokines associated with allospecific graft rejection using Luminex analysis. Luminex analysis of cytokine expression in whole corneal tissues following LSCD induction, or transplantation of limbal epithelial grafts from autologous (B6-Tx) or allogeneic (Balb/c-Tx) mice. Top panel shows fold changes in normalized protein levels relative to untreated control mice, expressed as a heat map of minimum and maximum levels (indicated values) detected for each analyte (n=7 per group). Bottom panels show the concentration of analytes with significantly different protein levels where * $P < 0.05$, ** $P < 0.01$, *** $P < 0.001$, analysed by one-way ANOVA, compared to untreated mice.

Determining the Role of the Innate and Adaptive Immune Responses in LESC transplant rejection

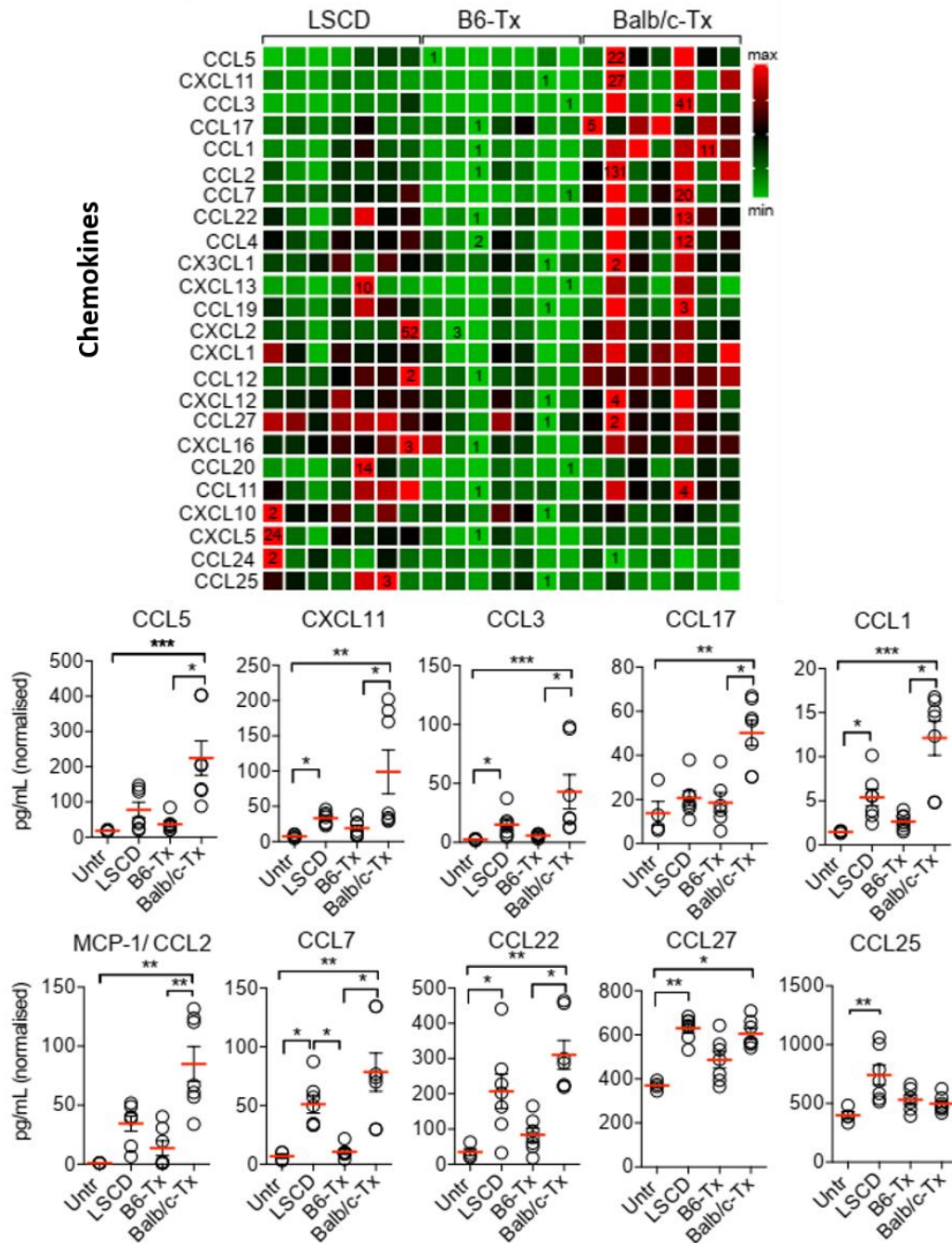


Figure 4.7 Identification of chemokines associated with allospecific graft rejection using Luminex analysis. Luminex analysis of chemokine expression in whole corneal tissues following LSCD induction, or transplantation of limbal epithelial grafts from autologous (B6-Tx) or allogeneic (Balb/c-Tx) mice. Top panel shows fold changes in normalized protein levels relative to untreated control mice, expressed as a heat map of minimum and maximum levels (indicated values) detected for each analyte (n=7 per group). Bottom panels show the concentration of analytes with significantly differentially expressed protein levels where * $P < 0.05$, ** $P < 0.01$, *** $P < 0.001$, analysed by one-way ANOVA, compared to untreated mice.

4.2 2C-TCR+ T cell mediated graft rejection

During early stages of *in vivo* model development, several preliminary experiments were conducted using the limited number of successfully/partially successfully grafted NSG mice, investigating the role of CD8+ T cells in graft rejection (schematic representation of experimental design shown in Figure 4.8). In one such experiment, three NSG mice were transplanted with BALB/c-GFP corneal epithelial cells, which initially expanded to cover approximately 25% of the cornea before growth slowed and stalled. It should be noted that for two of these mice the grafts were morphologically consistent with epithelial cells during *in vivo* imaging, however one showed evidence of engraftment of GFP+ corneal stromal cells which had engrafted into the exposed stroma. At this point CD8+ T cells from 2C-TCR Tg x Rag1 KO mice which have antigen specificity for the MHC Class I BALB/c alloantigen (H2-L^d) expressed by donor grafts were adoptively transferred into the mice which had previously received corneal grafts. The process of subsequent complete graft rejection was visualised and imaged over the following two weeks (Figure 4.9). The two epithelial grafts initially remained stable and even continued to grow until day 8 after adoptive T cell transfer, at which point the density of the graft became visibly reduced. By day 10, the edges of the graft had receded, the density was further decreased, and then by day 13 all signs donor graft cells had disappeared. Graft size was calculated as a proportion of the visible corneal surface, and these percentages are displayed in Figure 4.9.

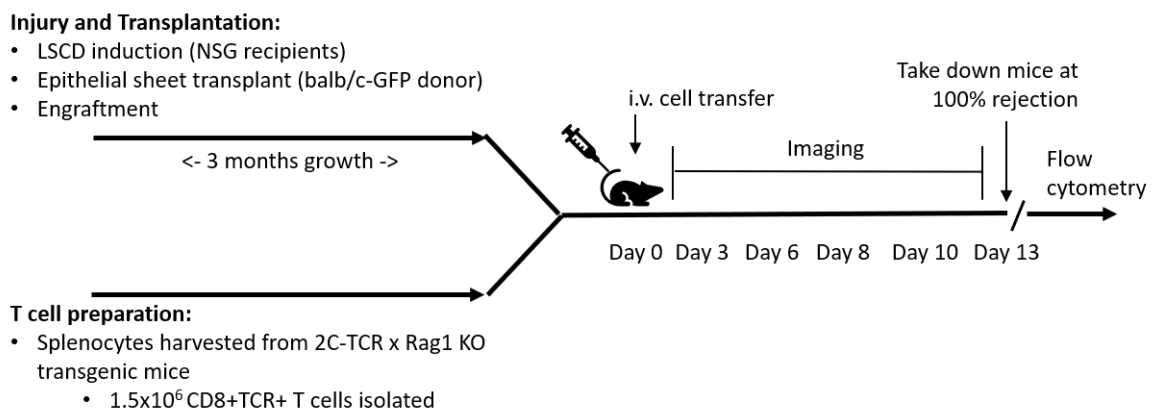


Figure 4.8 Schematic diagram outlining the experimental plan and timeframe of this experiment investigating the role of 2C-TCR+ CD8+ allogeneic T cells in corneal epithelial graft rejection.

Determining the Role of the Innate and Adaptive Immune Responses in LESC transplant rejection

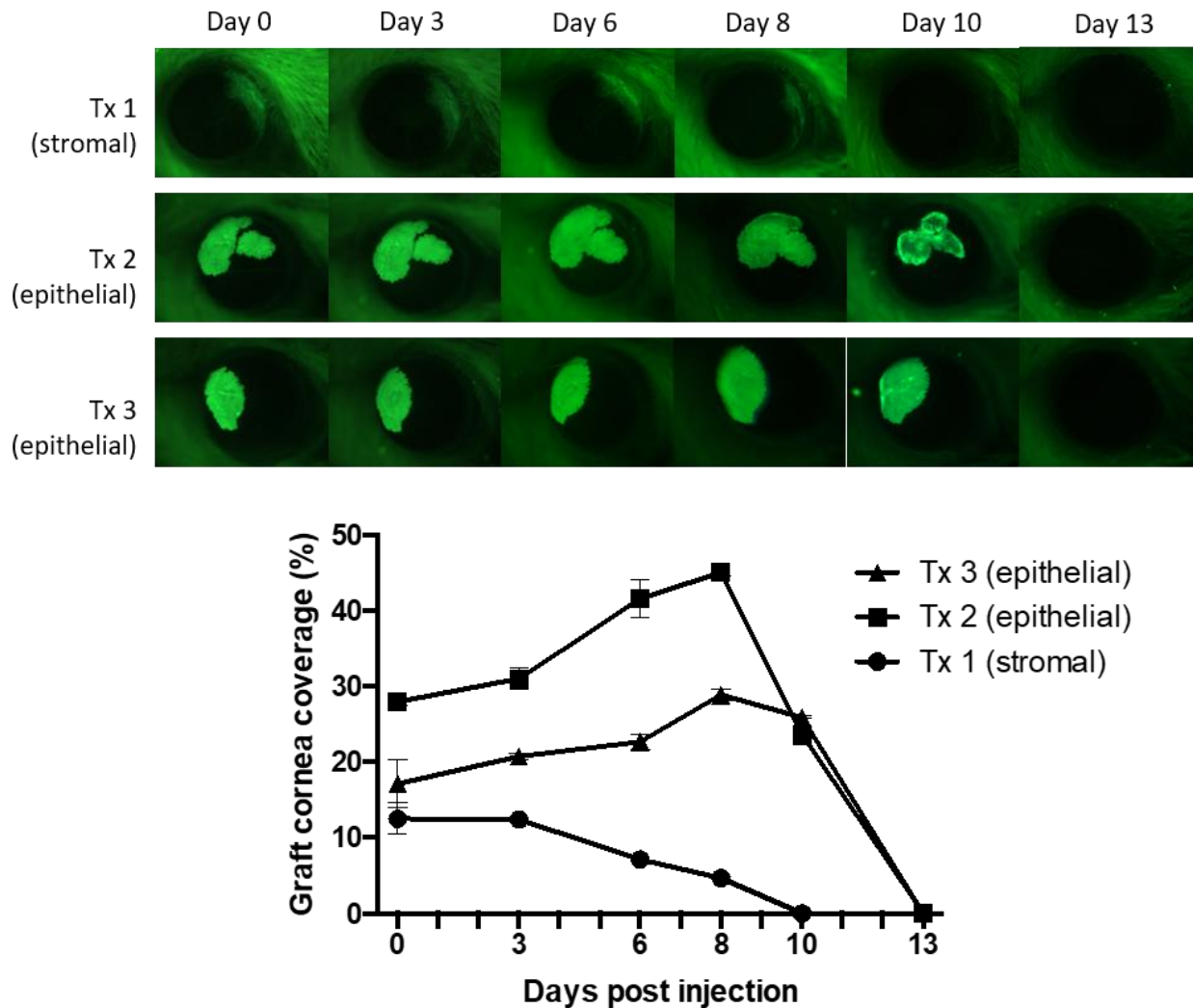


Figure 4.9 Graft rejection timeframe in response to 2C-TCR+ CD8+ allogeneic T cell transfer. Top panel shows images of engrafted GFP+ epithelial or stromal cells in the BALB/c mouse cornea after adoptive transfer of 2C-TCR T cells, throughout graft rejection over the course of 13 days. Bottom panel shows a graph plotting the timeframe of graft rejection above. Graft size calculated and plotted as a percentage of the visible cornea covered by GFP+ fluorescence. N=3 mice (all shown), errors bars shown as SEM.

Determining the Role of the Innate and Adaptive Immune Responses in LESC transplant rejection

Once GFP+ cells were no longer visible on the cornea, mice were taken down, their corneas digested and analysed by flow cytometry. Due to extremely low cell numbers harvested from the isolated corneas no conclusions could be drawn however this served as a useful preliminary experiment. Figure 4.10 shows the proliferation of total corneal epithelial cells (detected by Ki67 and EpCAM staining), for each of the three grafted mice as well as healthy control corneas. Due to the variation between each of the three grafts results were examined individually rather than taking average results. These are plotted relative to the average of three healthy untreated control corneas in the bottom panel, showing that the remaining epithelial cells in the rejected mouse corneas were at similar levels to the healthy control.

While limited due to sample size, investigation of the cellular infiltration in the transplanted corneas was also carried out using flow cytometry after staining and gating for CD11b+ monocytes and macrophages, and CD8+ T cells (Figure 4.11). The results from this corneal tissue analysis indicate that two days after complete graft rejection, between 20-30% of the cells in the injured left cornea were CD8+ T cells, accompanied by large numbers of infiltrating monocytes and macrophages. This infiltration was not observed in the healthy right cornea of the same mice.

Determining the Role of the Innate and Adaptive Immune Responses in LESC transplant rejection

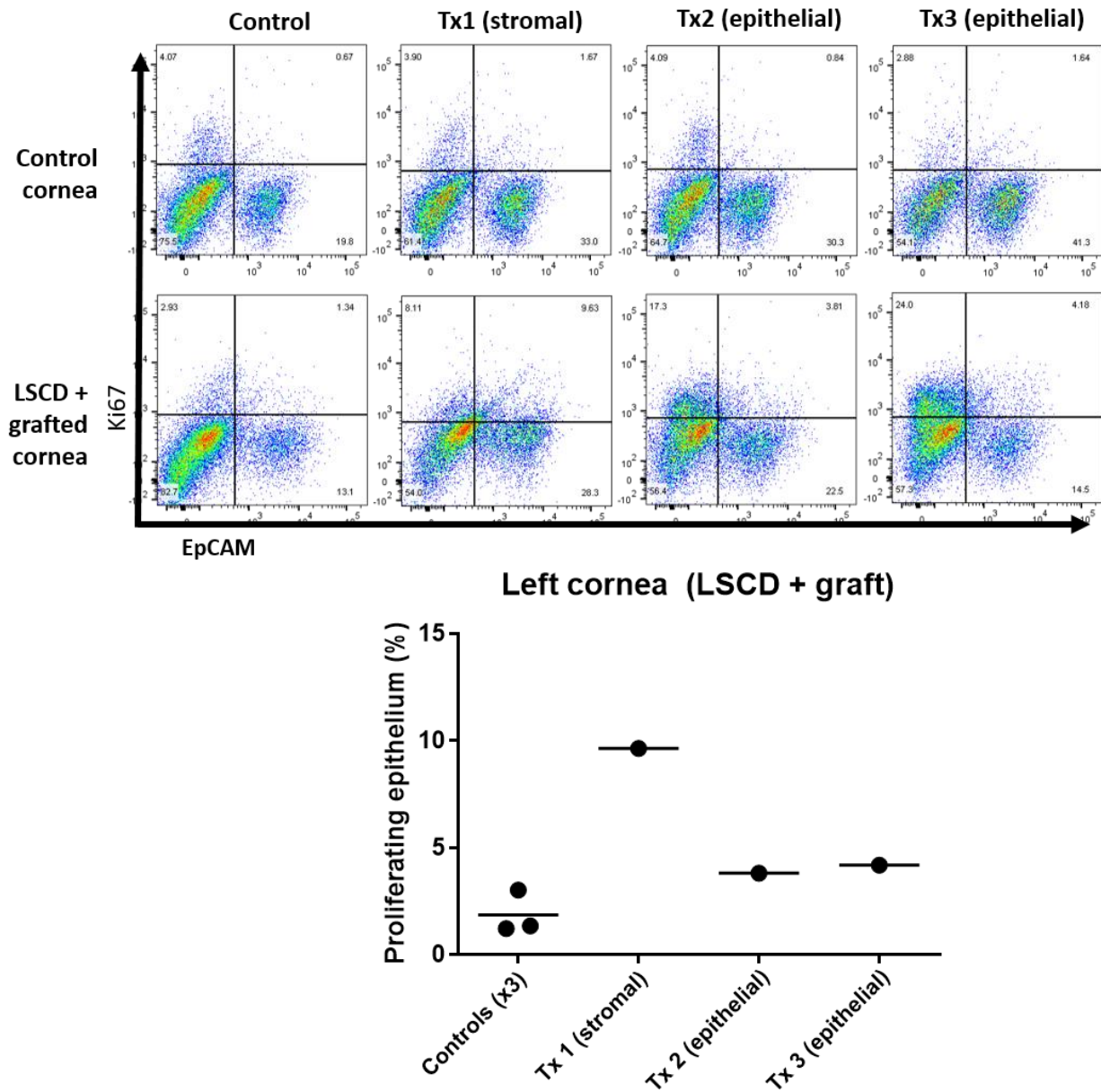


Figure 4.10 Epithelial proliferation in the mouse cornea following rejection of epithelial grafts in response to 2C-TCR allogeneic T cell transfer. Top panel shows FACS plots of the healthy right eye (control) and left eye (LSCD + rejected graft), showing proliferation (Ki67+) of corneal epithelial cells (EpCAM+). Bottom panel shows epithelial proliferation data plotted separately for each of the mice, where N=3. Cells were gated during flow cytometry on forward vs side scatter profile for size and doublets, and live/dead staining.

Determining the Role of the Innate and Adaptive Immune Responses in LESC transplant rejection

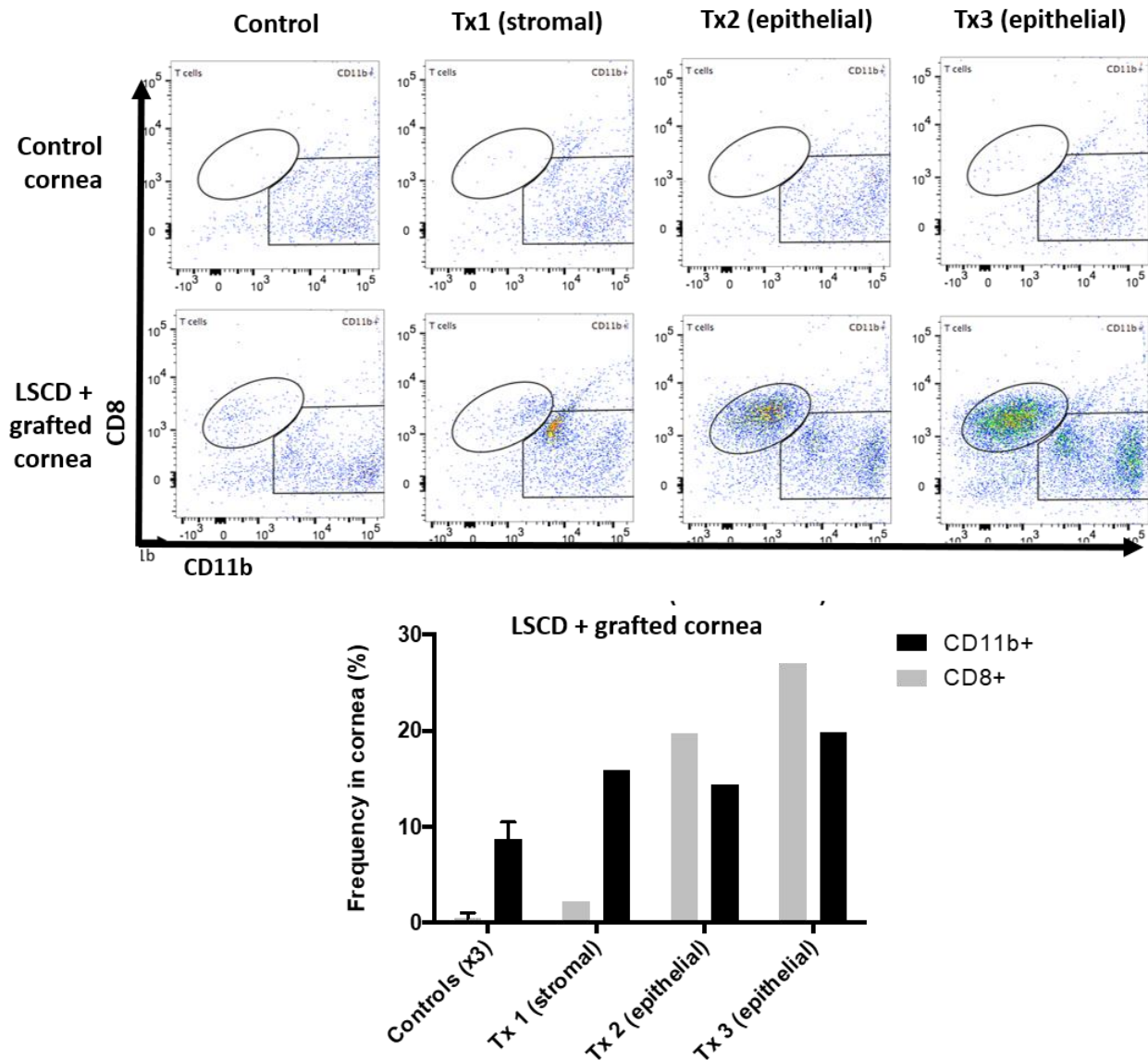


Figure 4.11 Cell infiltration in the mouse cornea following rejection of epithelial grafts in response to 2C-TCR allogeneic T cell transfer. Top panel shows FACS plots of the healthy right eye (control) and left eye (LSCD + rejected graft), showing the infiltration of CD8⁺ T cells and CD11b⁺ monocytes into the cornea. Bottom panel shows infiltration data plotted separately for each of the mice, where N=3. Cells were gated during flow cytometry on forward vs side scatter profile for size and doublets, and live/dead staining.

4.3 CD8+ T cell mediated graft rejection

To continue investigating the role of CD8+ T cells in our mouse model of corneal epithelial graft rejection, an alternative protocol was developed to avoid the use of 2C-TCR transgenic T cells (Figure 4.12). We used NSG mice which had previously received BALB/c-GFP grafts which had expanded and stratified into multiple layers to completely reverse LSCD and regenerate a healthy cornea over the course of 6 months (Figure 3.17). CD8+ T cells stably expressing dsRed fluorescent protein were isolated from CD2-dsRed transgenic mice using negative selection dynabeads (ThermoFisher untouched CD8 mouse kit), and selectively expanded *in vitro* for specificity to the BALB/c alloantigen, through co-culture with BALB/c irradiated splenocytes, using previously described methods [135].

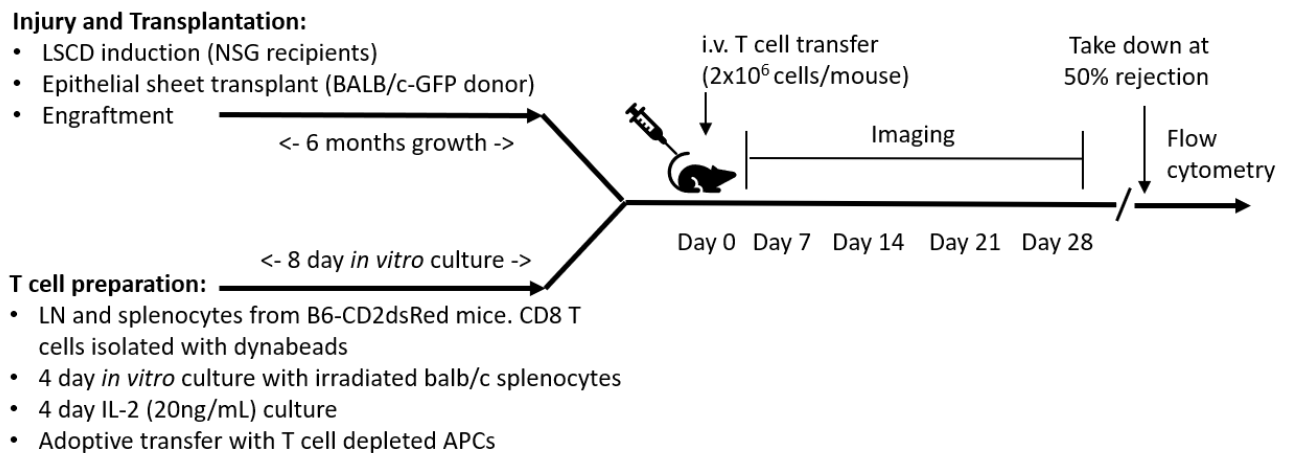


Figure 4.12 Schematic outlining the experimental plan designed to investigate the role of CD8 T cells in corneal epithelial graft rejection.

Determining the Role of the Innate and Adaptive Immune Responses in LESC transplant rejection

CD8⁺ T cells expressing dsRed⁺ were adoptively transferred to the grafted NSG mice, with graft survival tracked and imaged over the following month until the grafts had reached the point of an estimated 50% rejection as measured by percentage cornea area covered (Figure 4.13). All of the mice used in this experiment maintained their body weight, showing no signs of developing graft-vs-host disease (GvHD). Small numbers of single dsRed⁺ T cells were visible at the periphery of the cornea by day 5 post T cell transfer, which steadily infiltrated further into the cornea over the next few weeks, with dense clusters of cells appearing throughout the centre of the graft. By day 31 post-T cell transfer, the epithelium had significantly reduced in both size and density, correlating with the encroachment of the conjunctiva and blood vessels onto the newly exposed stroma. The image containing merged red and green channels make clear the position of T cells relative to the remaining graft tissue, and multiphoton imaging indicating that T cells are capable of penetrating through to the basal layer and not just on the surface of the epithelium.

Determining the Role of the Innate and Adaptive Immune Responses in LESC transplant rejection

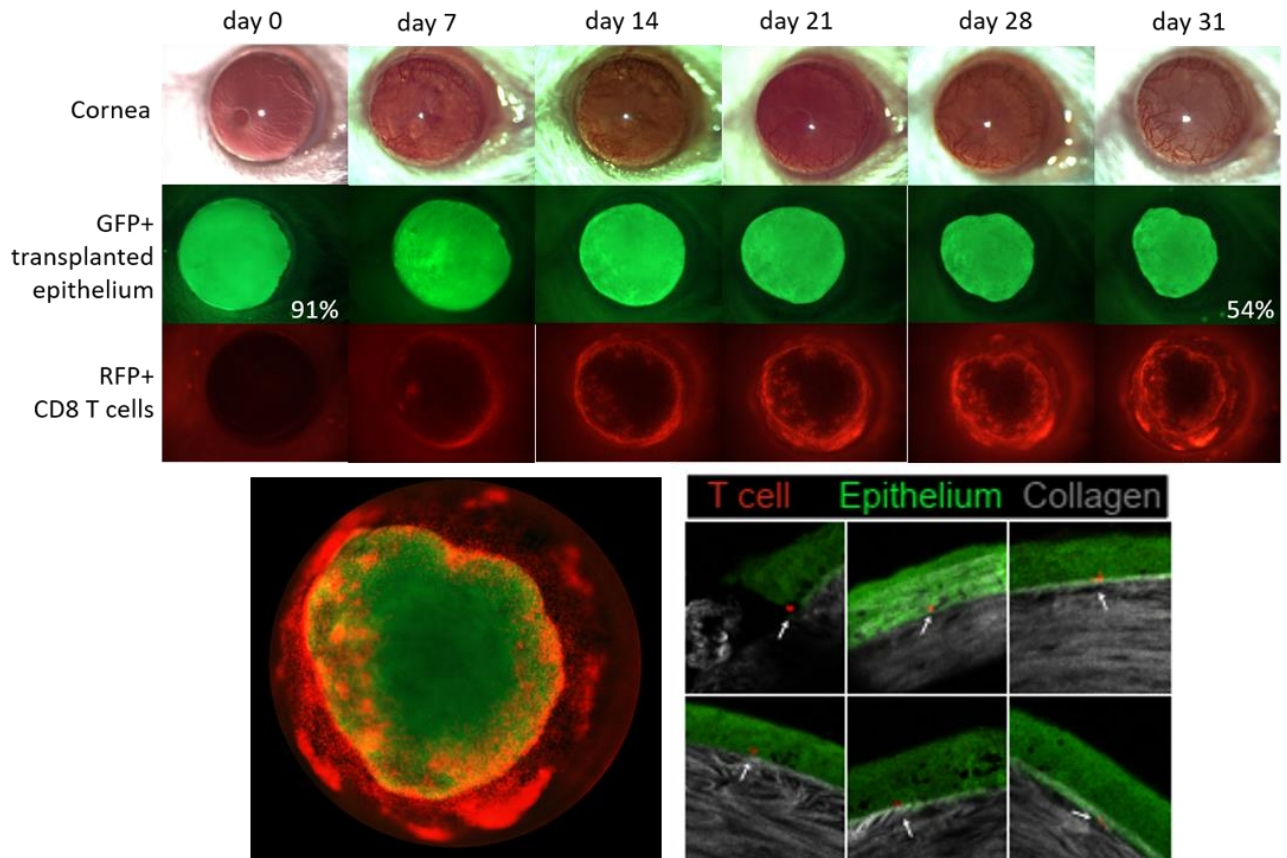


Figure 4.13 Rejection of epithelial grafts following adoptive transfer of dsRed CD8+ T cells in the mouse cornea. Serial imaging of NSG mouse cornea showing transplanted GFP+ epithelial graft rejection and the re-emergence of an LSCD phenotype, following adoptive transfer of RFP+ CD8+ T cells, N=2. Graft size calculated and plotted as a percentage of the visible cornea covered by GFP+ fluorescence. Bottom left panel shows a representative image of the mouse cornea with both red and green channels merged to show T cell position overlaid on remaining graft tissue at day 31. Bottom right panel shows multiphoton microscopy of infiltrating T cells localized to the basal epithelial junction of allogeneic cells, N=3.

Determining the Role of the Innate and Adaptive Immune Responses in LESC transplant rejection

During active graft rejection corneal tissues were harvested for analysis by flow cytometry (Figure 4.14). Untreated contralateral eyes were also analysed as healthy control tissues. Healthy corneas of the two grafted and rejected mice contained 2-3 fold more epithelial cells than in the LSCD corneas, and of the epithelial cells remaining on the grafted corneas, only 4-11% of those epithelial cells were positive for GFP expression. The EpCAM⁺ cells identified in the grafted corneas were likely inflamed epithelial cells or conjunctival cells as they were a much larger in size (as determined by scatter plots) compared to the small cuboidal epithelial cells isolated from healthy corneas. The EpCAM data indicates that there was approximately a 50% reduction in epithelial cells in the left cornea compared to the right, which is as expected given that the eyes were harvested at the time predicted to coincide with 50% rejection. Although markers of conjunctival epithelium and blood vessels were not included in this staining panel, we can see from the imaging in Figure 4.13 that LSCD has indeed progressed, and the space previously occupied by epithelial graft is hazy and highly vascularised. Between 29-38% of the cells in the rejected cornea were CD3⁺dsRed⁺ and therefore CD8⁺ T cells, while the infiltration of CD8⁺ T cells into the healthy right corneas of these mice was negligible. Staining for markers of T cell memory and activation status, CD44 and CD69, in this experiment was inconclusive due to technical and compensation issues, while between 31-36% of dsRed⁺ cells in the injured corneas were positive for Ly6C indicating early activation status. Antibody staining issues were predominantly due to very low cell numbers and a lack of suitable controls for testing the entire panel under experimental conditions.

Determining the Role of the Innate and Adaptive Immune Responses in LESC transplant rejection

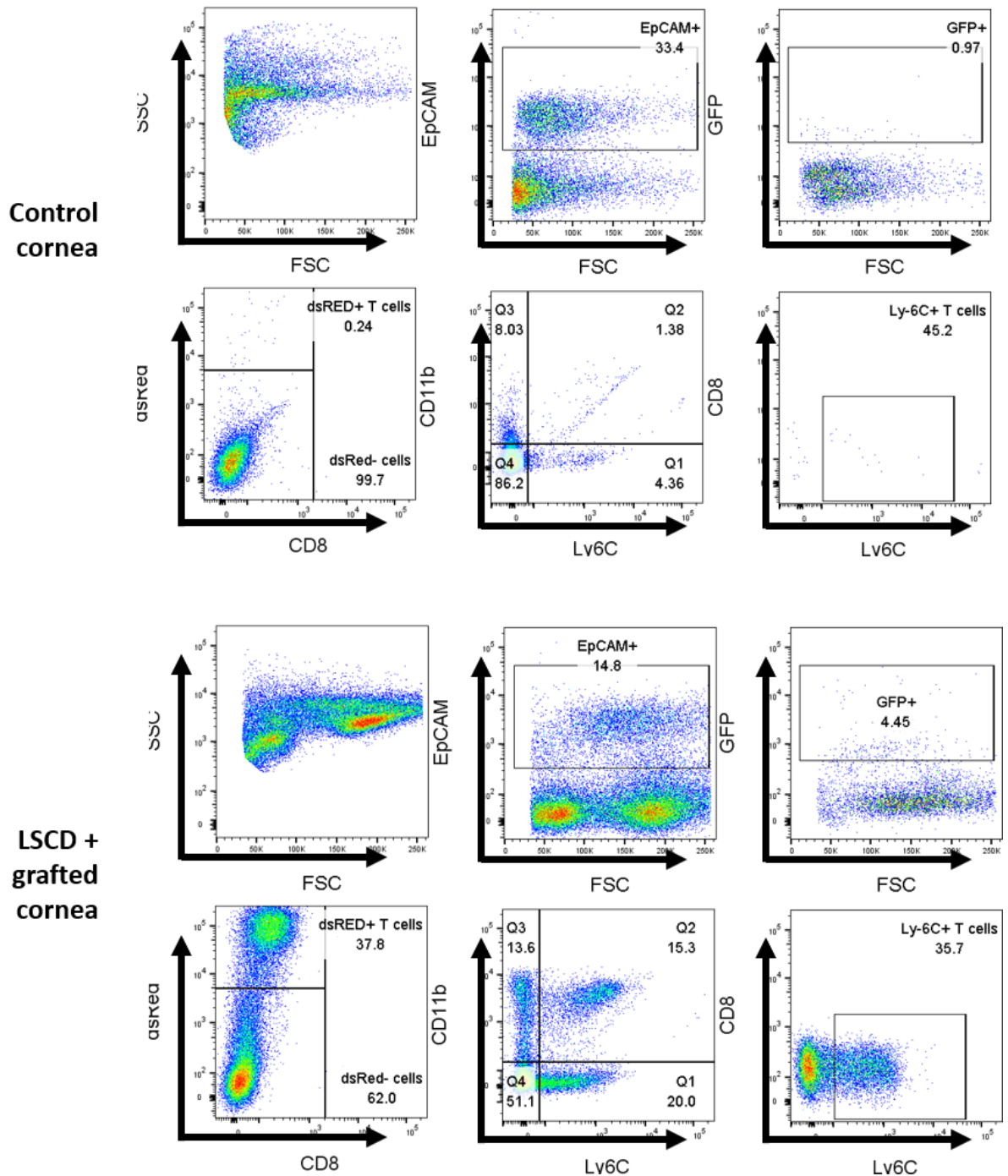


Figure 4.14 Flow cytometry plots of the rejection of epithelial grafts following adoptive transfer of immune cells in the mouse cornea. Representative flow cytometry plots showing cell infiltration in the mouse cornea during graft rejection. Top 6 plots show the healthy control eye, bottom 6 plots show the LSCD + grafted eye. Plots (from L-R) show the following: cell size and granularity, epithelial cell size, presence of GFP+ cells, infiltration of T cells, infiltration of monocytes and macrophages, infiltration of neutrophils. N=2.

4.4 CD4+ T cell mediated graft rejection

We continued to investigate the role of T cells in corneal epithelial graft rejection, specifically CD4+ T cells. Using the previously described protocol, T cells were isolated from a cyan fluorescent protein (CFP) expressing strain of B6 mice and expanded *in vitro* through co-culture with BALB/c splenocytes as an allo-stimulation assay. Subsequently purified CFP+ CD4+ T cells were adoptively transferred to graft recipients and serially imaged throughout the course of the experiment, as outlined in Figure 4.15.

As seen in the representative images of Figure 4.16, there appeared to be no rejection of the GFP+ corneal allograft over the course of the 63 days observed after transfer of allo-stimulated CD4+ T cells. A small cluster of CFP+ cells around day 35, which increased to a larger number of fluorescent cells detected around the peripheral edge of the graft by day 42. However, these disappeared within several days and were not accompanied by either loss of GFP+ cells or the re-emergence of an LSCD phenotype. The reasons for the failure to identify persisting CFP+ CD4+ T cells are unclear, and since blood sampling was not performed we cannot be sure that the transferred T cells survived long enough to cause any graft rejection.

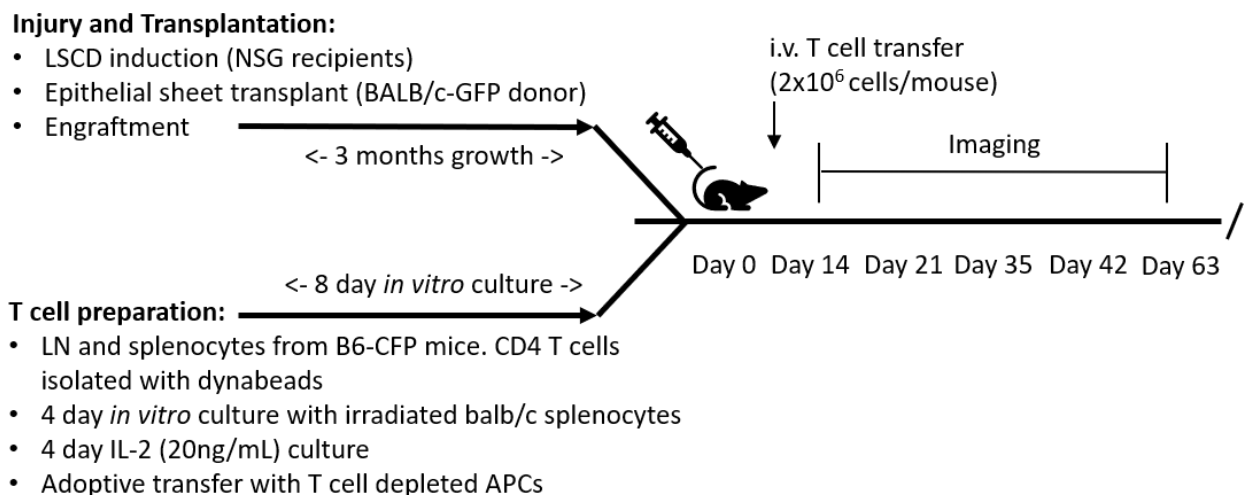


Figure 4.15 Schematic diagram outlining the experimental plan designed to investigate the role of CD4 T cells in corneal epithelial graft rejection.

Determining the Role of the Innate and Adaptive Immune Responses in LESC transplant rejection

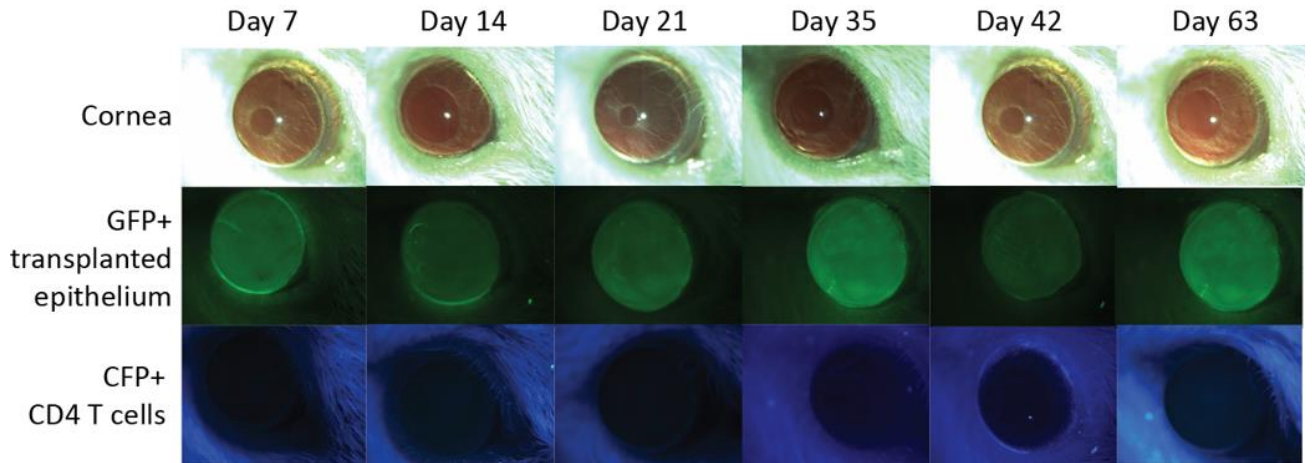


Figure 4.16 Rejection of corneal epithelial grafts following adoptive transfer of immune cells in the mouse cornea. Representative serial imaging of NSG mouse cornea with transplanted GFP+ epithelial graft showing any detected cell infiltration into the cornea following adoptive transfer of CFP+ CD4+ T cells. N=4.

4.5 CD8+ and CD4+ T cell mediated graft rejection

The previous experiments were designed to test the model of allograft rejection and to identify whether CD8+ and CD4+ T cells were important for mediating corneal allograft rejection. The next step was designed to be more representative by transferring both CD4+ and CD8+ T cells along with APCs into the recipient (Figure 4.17).

Mature bone marrow derived dendritic cells (BMDC) were harvested from BALB/c donors, cultured, and matured before being co-cultured with dsRed CD4 and CD8 T cells. Once BMDCs were expanded, LPS treatment was used to mature the cells to increase their expression of co-stimulatory molecules CD80/86, which prime T cells via CTLA4 and CD28 signalling. The stimulatory potential of matured BMDCs would therefore be expected to increase the number of allospecific T cells expanded during subsequent *in vitro* co-culture. Figure 4.18 demonstrates the change in expression of both CD80 and CD86 co-stimulatory molecules as well as MHC class I and II molecules between immature BMDCs and mature BMDCs.

Determining the Role of the Innate and Adaptive Immune Responses in LESC transplant rejection

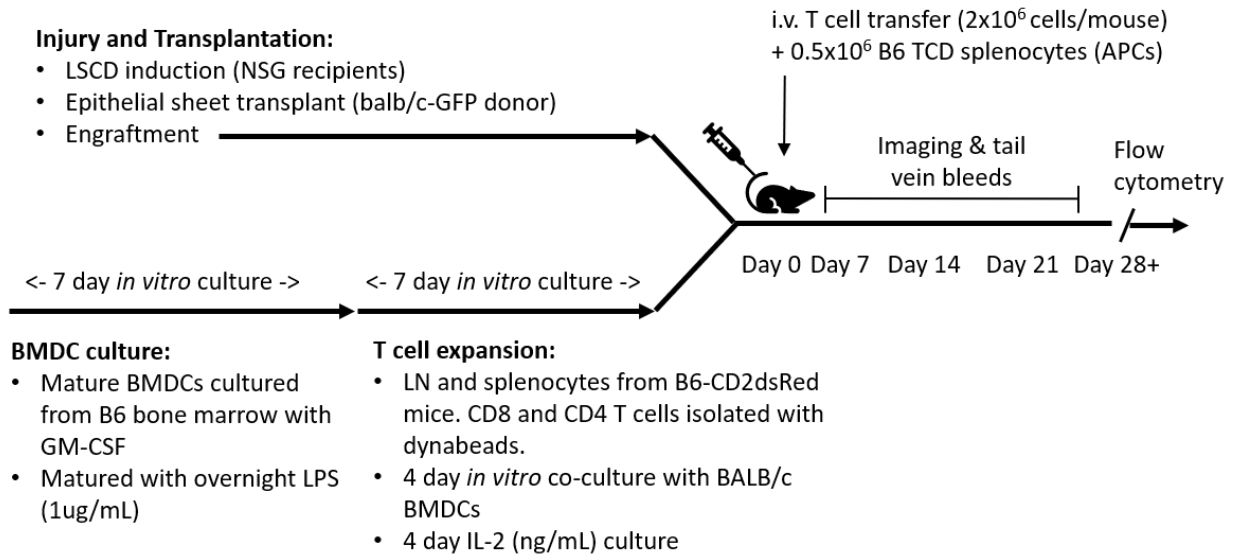
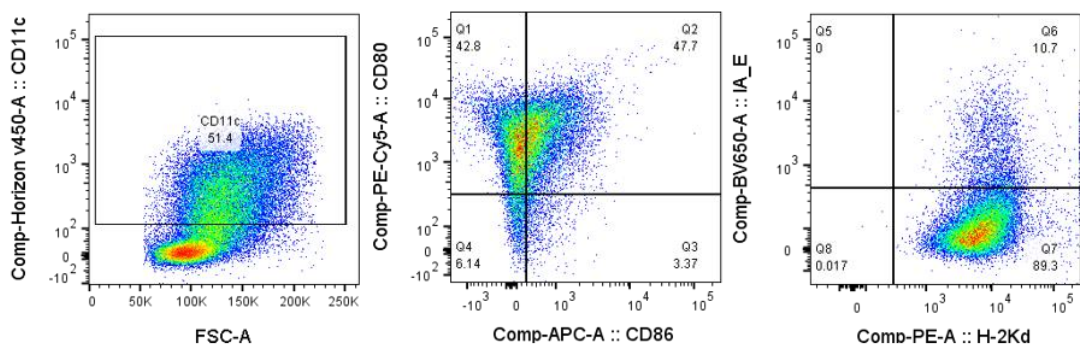


Figure 4.17 Schematic outlining the experimental plan designed to investigate the role of CD4+ and CD8+ T cells in corneal epithelial graft rejection.

Immature BMDC



Mature BMDC

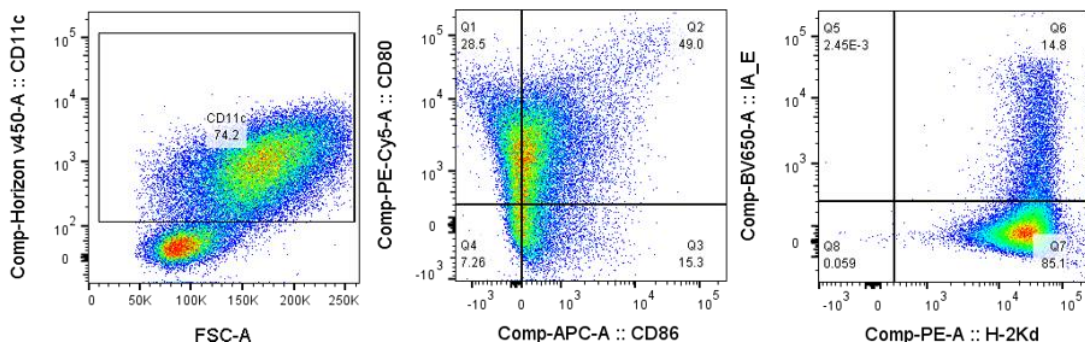


Figure 4.18 Flow cytometry plots of immature and mature BMDCs after LPS stimulation. Representative flow cytometry plots showing the expression of MHC class I and II, as well as the co-stimulatory molecules CD80 and CD86 in BMDCs, gated on cell size, doublets, live/dead staining, and CD11c expression. N=3.

Determining the Role of the Innate and Adaptive Immune Responses in LESC transplant rejection

Once T cells had been expanded *in vitro*, their stimulatory potential was investigated in a mixed lymphocyte reaction assay (MLR). Following stimulation with either allogeneic BALB/c splenocyte, autologous B6 splenocytes, or polyclonal CD3+CD28+ beads, CFSE stained cells were analysed by flow cytometry to assess their proliferation in response to stimulation, shown in Figure 4.19 and summarised in Figure 4.20. Results show that CD4+ T cells show similar levels of proliferation in response to allogeneic cells and polyclonal beads, with little to no response to autologous stimulators, demonstrating that the T cells which had been expanded through *in vivo* culture are those which would respond to the BALB/c antigen of the corneal epithelial grafts. However, the results for CD8+ T cells showed no proliferation. This may indicate issues with their expansion in culture, however given that there is no response to any of the three different sources of stimulation, the problem is more likely to be with the MLR assay or CFSE labelling rather than the *in vitro* stimulation.

Determining the Role of the Innate and Adaptive Immune Responses in LESC transplant rejection

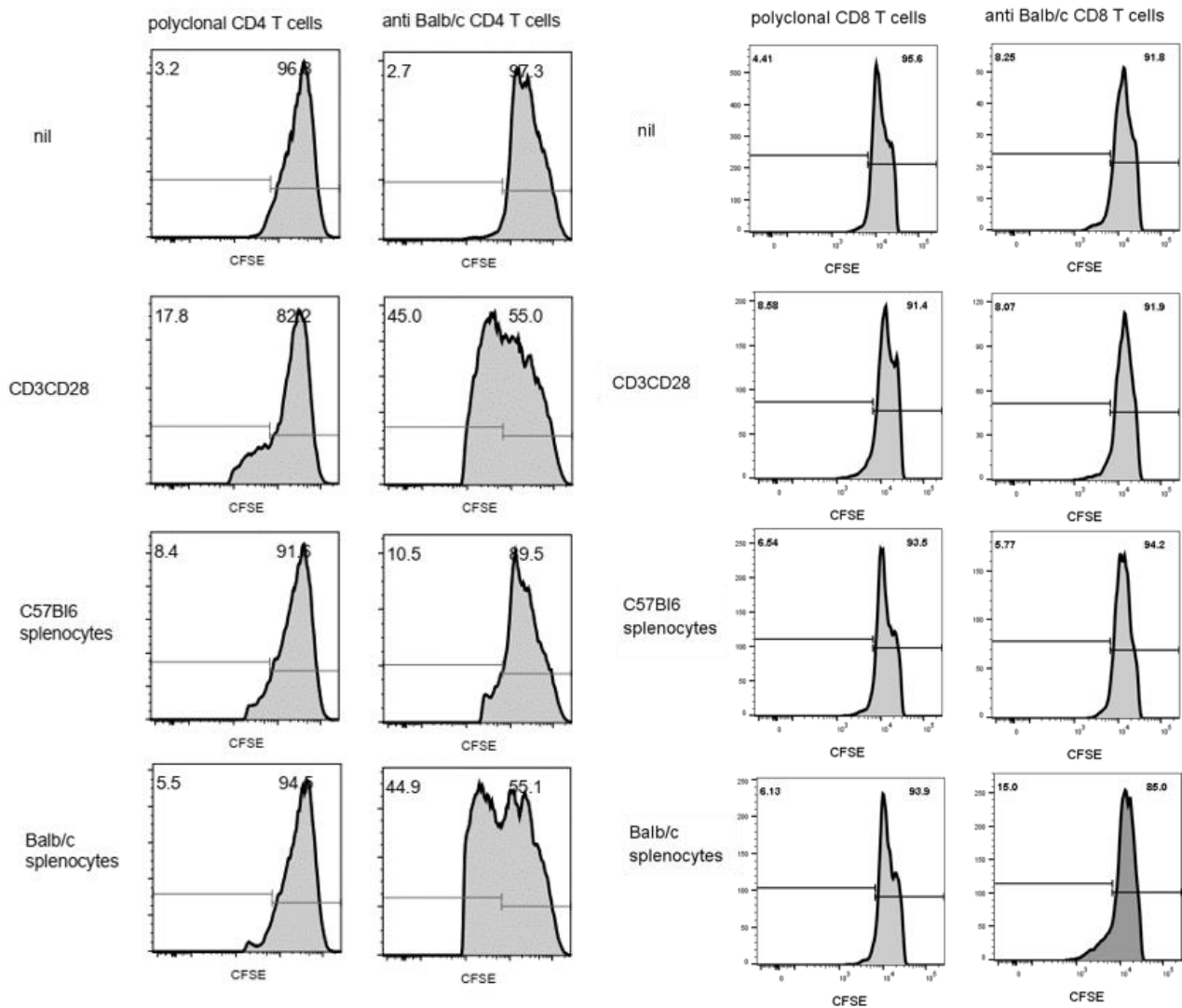


Figure 4.19 Flow cytometry histograms of CD8+ and CD4+ T cells after expansion with allogeneic BMDCs and restimulation in an MLR. Flow cytometry plots showing the proliferation of the expanded CFSE labelled CD4 and CD8 T cells in response to stimulation with either autologous B6 splenocytes, allogeneic BALB/c splenocytes, or polyclonal CD3+ stimulator beads. N=3.

Determining the Role of the Innate and Adaptive Immune Responses in LESC transplant rejection

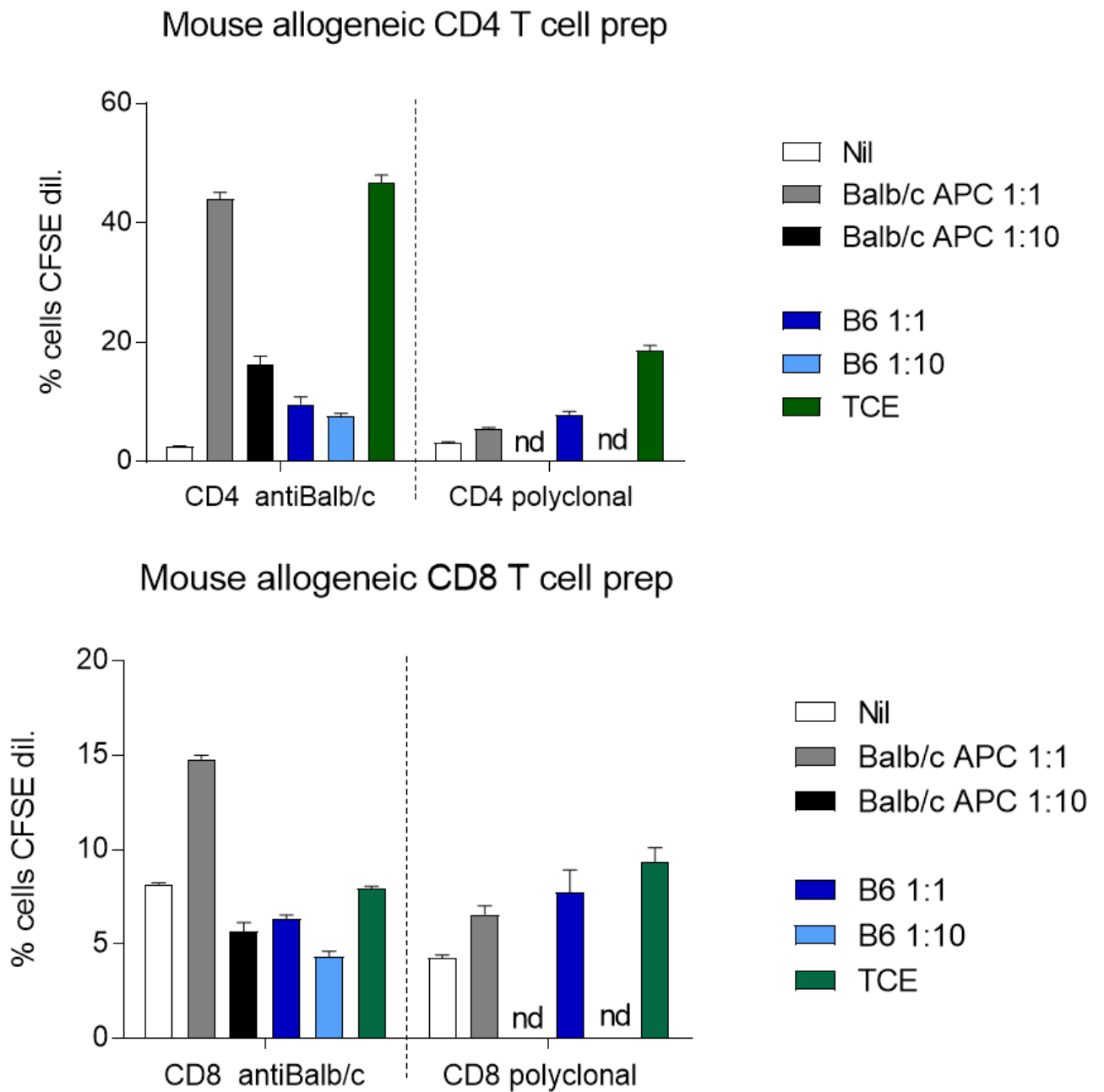
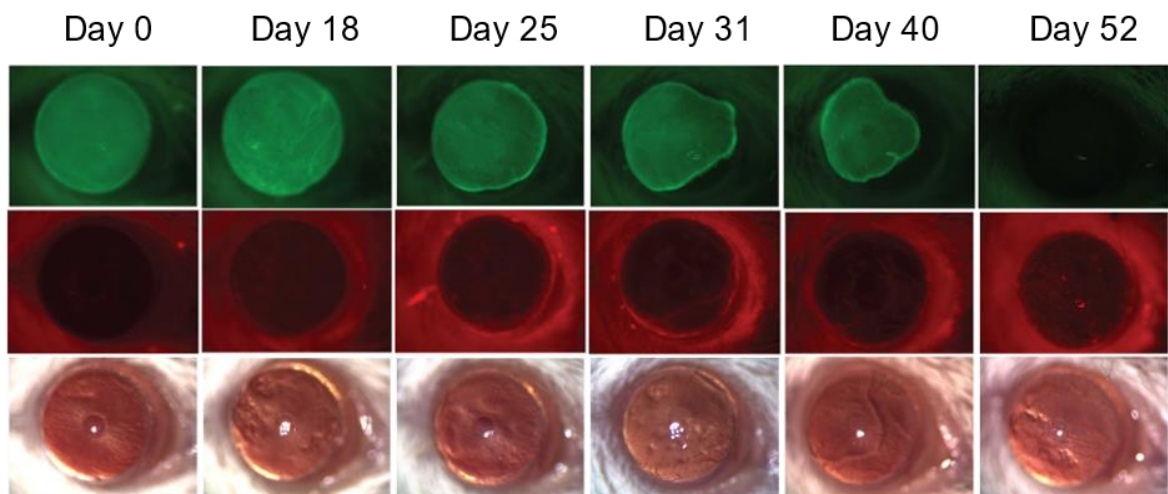


Figure 4.20 Summary of MLR experiments showing the proliferation of allogeneic CD4+ and CD8+ T cells in response to stimulators. Summary of flow cytometry data showing the proliferation of the expanded CFSE labelled CD4 and CD8 T cells in response to stimulation with either autologous B6 splenocytes, allogeneic BALB/c splenocytes, or polyclonal CD3+ stimulator beads. N=3.

Determining the Role of the Innate and Adaptive Immune Responses in LESC transplant rejection

NSG recipient mice received dsRed CD4+ and CD8+ T cells along with APCs generated by depleting B6 whole splenocytes of T cells using dynabeads, recipient mice and controls were serially imaged throughout the course of graft rejection. Generally, two patterns of rejection were observed, shown in Figure 4.21. In several mice, we observed a rapid influx of red fluorescent cells to the cornea followed by the loss of graft tissue and re-emergence of the LSCD phenotype within several days. The alternative pattern of rejection observed involved a much slower infiltration of fluorescent cells and a significantly longer time before any reduction in graft size was observed.

Delayed rejection



Rapid rejection

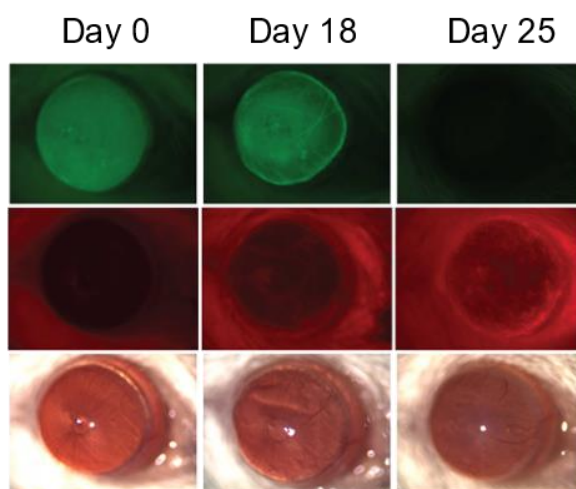


Figure 4.21 Representative images showing two common patterns of graft rejection seen in this experimental transplantation model. Representative images of serial imaging of NSG mouse cornea showing transplanted GFP+ epithelial graft rejection and the re-emergence of an LSCD phenotype, following adoptive transfer of dsRed+ CD8+ and CD4+ T cells, N=4.

Determining the Role of the Innate and Adaptive Immune Responses in LESC transplant rejection

Throughout the time course of this experiment, samples of peripheral blood were taken by tail vein sampling in order to assess the presence of transferred T cells in the recipient mice. Blood samples were stained and gated on cell size, doublets, live/dead markers, as well as dsRed and CD3 markers before being analysed by flow cytometry. Cell numbers obtained were very low and unsuitable for quantifying absolute numbers of cells, however this data has been used to calculate the relative proportions of CD4+ and CD8+ T cells remaining in the blood, shown in Figure 4.22. Ratios remained stable through each of the time points assessed, and any differences were not significant, however this does indicate that cells survived and remained detectable throughout the entire rejection process.

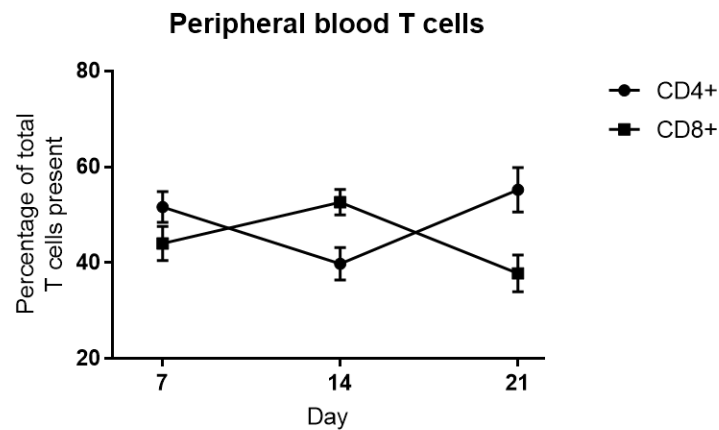


Figure 4.22 Summary of flow cytometry data showing the presence of T cells in peripheral blood during graft rejection. Summary of flow cytometry data from mouse peripheral blood, showing relative proportions of CD4+ and CD8+ T cells present in circulation during corneal epithelial allograft rejection. N=4

Given the relatively unpredictable nature of the rejections occurring in this model, the endpoint was altered from previous experiments in which mice were taken down as 50% graft loss occurred. Instead, corneas, draining and non-draining lymph nodes, and spleen, were harvested within 3 days of complete graft loss. Cell counting beads were included in cell suspensions once digested, in order to quantify absolute cell numbers, and T cells were identified by dsRed+ CD3+ staining as well as using anti-

Determining the Role of the Innate and Adaptive Immune Responses in LESC transplant rejection

CD4 and anti- CD8 antibodies. Also included in this flow cytometry panel were anti-CD44 and anti-CD62L, two markers of T cell activation and differentiation status, to further investigate T cell phenotype. Example flow cytometry in Figure 4.23 demonstrate that the majority of those detected were effector memory cells (CD62L-CD44+), with very few central memory (CD62L+ CD44+) or naïve T cells (CD62L+ CD44-). Cell counting data and the frequency of cells relative to the total live cells are calculated and represented in Figure 4.24, however there are no trends of significance.

Determining the Role of the Innate and Adaptive Immune Responses in LESC transplant rejection

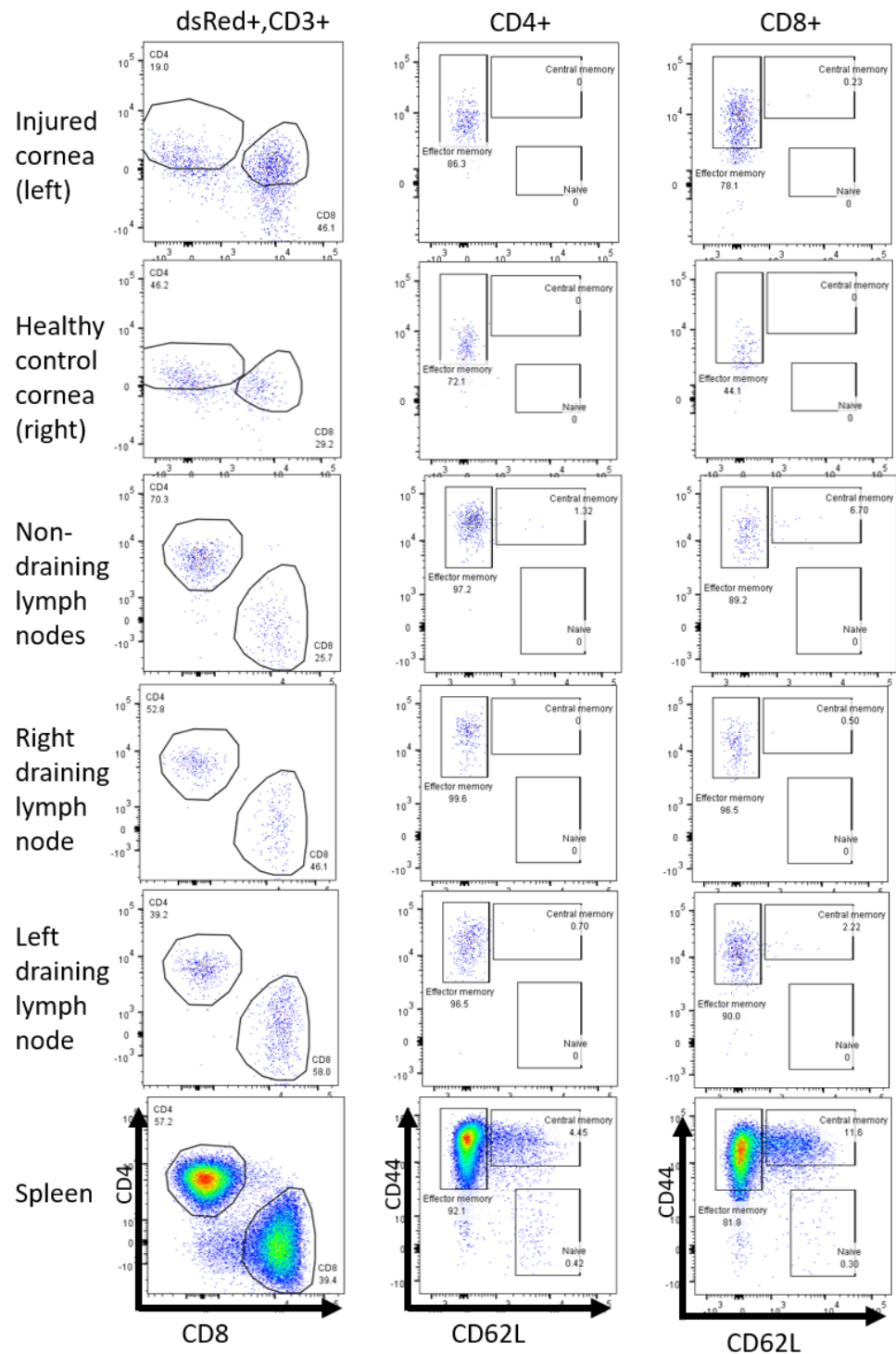


Figure 4.23 Representative flow cytometry plots showing the T cell analysis of tissues from grafted and rejected mice. Representative flow cytometry data showing the infiltration of CD4+ and CD8+ T cells into the graft rejecting cornea, as well as the memory phenotype of those T cells by CD44 and CD62L expression. Tissues examined includes left draining lymph node (LDLN), right draining lymph node (RDLN), non-draining lymph nodes (NDLN), spleen, left and right cornea. N=4.

Determining the Role of the Innate and Adaptive Immune Responses in LESC transplant rejection

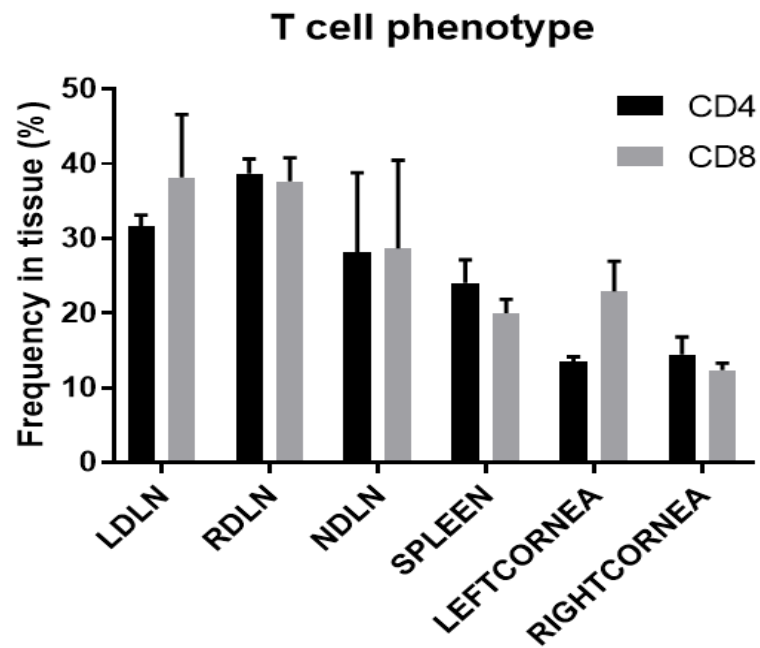


Figure 4.24 Summary of flow cytometry data, comparing the presence of CD4+ and CD8+ T cells in each of the organs examined following corneal graft rejection. Graph showing the relative numbers of CD4+ and CD8+ T cells as a percentage of the total live cells analysed within each tissue, including left draining lymph node (LDLN), right draining lymph node (RDLN), non-draining lymph nodes (NDLN), spleen, left and right cornea. N=4.

4.6 Summary

This chapter documents further developments to our mouse model of corneal epithelial transplantation for the reversal of LSCD, through several experiments which attempted to interrogate the immune response to allografted corneal tissue. Changing from the use of immunodeficient NSG recipients, to fully immunocompetent B6 recipient mice showed the characteristic signs of early graft rejection, and allowed us to calculate the kinetics of complete rejection of donor cells. Flow cytometric analysis of digested corneal tissue obtained during or shortly after graft rejection showed the presence of significant cellular infiltration (including CD3+ T cells, monocytes and macrophages, and neutrophils) into the allografted cornea compared to the healthy control eye. This data suggests that the graft rejection in these mice was a specific targeted response to the detection of alloantigen. Identification of key chemokines and cytokines present in the corneal inflammatory microenvironment was performed through Luminex assay of rejected allograft recipient corneas, showing significantly increased expression of cytokines IL-16 and IL-1 β , and chemokines CCL5, CXCL11, CCL3, CCL17, CCL1, CCL2, CCL7, and CCL22.

The development of multiple adoptive transfer experiments allowed some progress to be made into further understanding the involvement of key cell types in the rejection mechanism, however several practical issues have limited this area of research throughout the project. The loss of our breeding pair of the 2C-TCR Tg mice forced the development of alternate means of producing allospecific T cells which was achieved by isolation and co-culture with mature BALB/c bone marrow derived dendritic cells. Using this method, CD8+ and CD4+ T cells were transferred to mice, both in isolation and combined, along with APCs to observe their effect on stable donor epithelial grafts. Given the extremely small tissue size and low total cell numbers harvested from recipients, data obtained post-rejection was limited, requiring experimental repeats and further investigation.

CHAPTER 5. OPTIMISING CULTURE, IDENTIFICATION, AND ISOLATION OF HUMAN LESC

Limbal epithelial stem cells (LESC) comprise a very rare population of the cornea, with less than 0.5% of cells from freshly isolated human limbal tissue identified as such [8]. Although there are several strategies for phenotyping LESC by examining intracellular markers, holoclone forming potential, dye exclusion, or negative expression of differentiation markers, it is currently an impractical procedure. Indirect methods of isolating potential LESC include centrifugation on a density gradient, magnetic bead selection, or FACS using novel putative LESC markers [17, 18, 136]. With a lack of suitable cell surface markers to identify LESC, isolating this rare cell population is technically challenging although a potentially useful strategy for improving transplantation outcomes.

One suggested hypothesis is that sheet stem cell content is directly related to engraftment success, where higher percentages of LESC improve numbers of cells engrafted and wound healing rates, or low LESC content is linked to graft failure. The licenced tissue engineering product 'Holoclar®' is reported to contain between 1-9% LESC with a success rate for autologous transplants of 72% within 1 year of transplant, however longer-term outcomes are not yet reported. It also unclear regarding the specific stem content of the epithelial sheets and how this affects engraftment or prolonged survival.

This chapter primarily discusses the need for an optimised protocol for the isolation of limbal epithelial stem cells from human corneas, and whether using this to vary the quantity and distribution of LESC within grafts could potentially improve engraftment success. Continued development of the mouse model of LSCD resulted in a humanised model, in which fluorescently labelled primary human corneal epithelial cells could be transplanted without risk of rejection in immunodeficient mice.

5.1 Primary human corneal tissue digestion and culture

To begin to investigate how the phenotype, composition, and number of LSCs within grafts influenced outcome and function, we first sought to establish protocols for the extraction, *ex vivo* culture, and expansion of primary human limbal tissue derived LSCs. Once established, these protocols were used to generate CLET preparations with defined numbers and cell types for study in an *in vivo* model of transplantation to reverse LSCD.

As previously described, the process for *ex vivo* culture of epithelial sheets for transplantation requires the use of human amniotic membrane (HAM), which is difficult and costly to obtain for use in research. As we were unable to source HAM we instead opted to use four alternative strategies for the isolation of LSCs from human corneas, based on collagenase, dispase, or trypsin digestion, or tissue explant culture. Using these protocols, we were able to generate epithelial cultures from primary human tissue. Cell numbers, viability, and cell expansion achieved are detailed in Table 1 of Figure 5.1 .

While several of the methods above produced adequate cell numbers from the digested tissue with good viability, the resulting cultures were often contaminated with stromal cells. These cells adhered to the tissue culture plastic more rapidly than the epithelial cells and then proliferated faster, resulting in overgrowth of the dish. When digested epithelial cells were seeded onto a feeder layer of growth-arrested 3T3 cells, they adhered in the spaces between the cells, and as the cells proliferated, the feeders were pushed outwards from the colonies. Eventually when the culture was completely confluent, few or no feeder cells remained on the dish, as seen in Figure 5.1. If this growth was allowed to continue epithelial cells began to stratify and differentiate, forming 3D structures similar to the structural layers formed *in vivo*.

While trypsin digestion (method 3) proved to be optimal, in terms of maintaining a high degree of viability and the generation of large numbers of corneal epithelial cells, this protocol was not optimised until several enrichment experiments had already

Optimising culture, identification, and isolation of human LESC

been performed. For this reason, overnight collagenase digestion and explant culture methods were used for early LESC enrichment experiments.

	Method (number of attempts)	Post digest cell numbers (viability)	Post culture cell numbers (viability)	Culture phenotype
1	Overnight collagenase digestion (N = >20)	$1 \times 10^5 - 2.5 \times 10^5$ (~60% live)	$5 \times 10^5 - 3 \times 10^6$ (>90% live)	Mixed stromal and epithelial cells.
2	Dispase digestion (N = 3)	<50,000 (<50% live). Incomplete digestion.	n/a	n/a
3	Trypsin digestion (N = 15)	$1.2 \times 10^5 - 1.5 \times 10^5$ (~80% live)	$4 \times 10^6 - 6 \times 10^6$ (>90% live)	Pure epithelial.
4	Explant culture (N = >20)	n/a	$1 \times 10^6 - 3 \times 10^6$ (~75% live)	Mostly epithelial, with signs of differentiation.

Table 1.

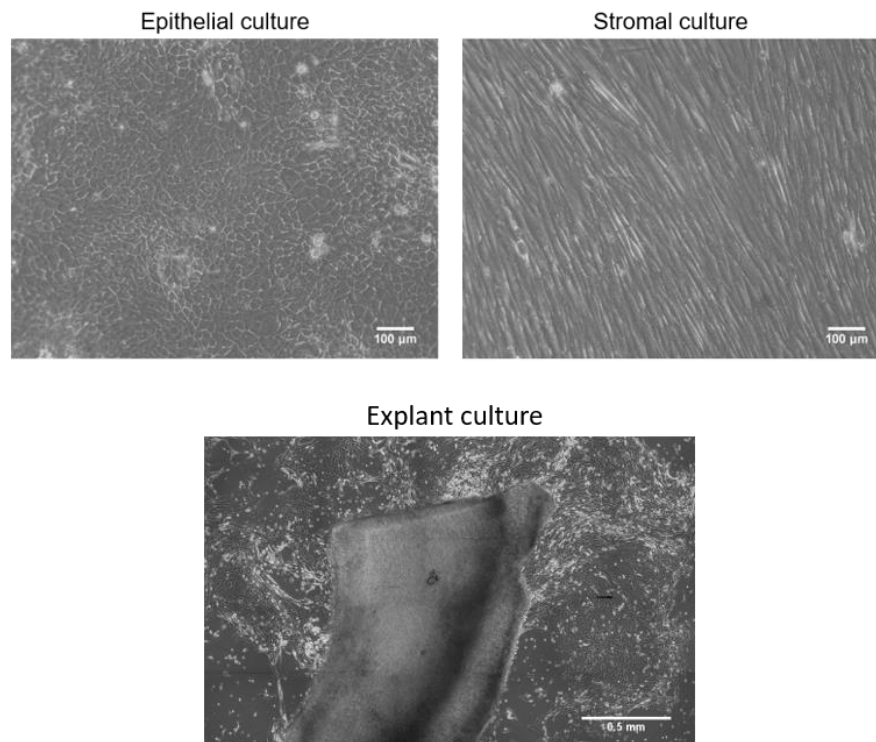


Figure 5.1 Methods of primary human corneal tissue digestion and culture.

Table 1 details four different methods of isolating corneal epithelial cells from primary human corneal tissue, including data on cell numbers and viability post-digestion and culture. Representative images show examples of confluent cells following digestion and culture, in both purely epithelial and stromal cultures as well as epithelial outgrowth from a limbal explant. Image representing explant culture is produced from multiple microscopy images stitched together using ImageJ to show a single explant.

5.2 Primary human corneal epithelial cell inflammatory profile

The treatment of clinical LSCD requires LESC transplantation either by direct grafting of large segments of healthy limbal tissue (autologous or allogeneic) or the transplantation of an *ex vivo* bioengineered sheet of corneal epithelial cells containing 1-10% LESC[33]. To examine the potential impact of the inflammatory LSCD graft bed on subsequent engraftment of LESC transplant, we analysed chemokine and cytokine protein production by cultured human corneal cell populations following exposure to the proinflammatory cytokines IL-1 β , IFN γ , and TNF α , previously identified in our experimental model of LSCD. Separate cultures of stromal and epithelial cells were enriched from primary human corneal tissue and analysed by multiplex immunoassay (Luminex) to determine the concentrations of 40 different inflammatory chemokines (Method 2.2.8) following *ex vivo* stimulation. All assayed proteins were detected above background levels with the exception of CXCL13, IL-2, IL-4, and CCL24, which were therefore excluded from any subsequent analysis. Primary human limbal tissue derived cell cultures were established *in vitro* and specific cell subsets sorted from the expanded populations based on expression of CD105 and EpCAM to identify stromal and epithelial cells respectively. In non-inflammatory conditions the proteins secreted by purified stromal and epithelial cells were similar except for several potent chemo attractants including CXCL12, IL-1 β , IL-6, IL-8, IL-16, CCL2, CCL17, CCL21, and CCL27. They were present at significantly higher concentrations in stromal cell cultures compared to epithelial cultures (Figure 5.2).

Exposure to proinflammatory cytokines resulted in significant increase in the levels of proinflammatory mediators produced by both epithelial and stromal cells (Figure 5.3). Significant differences in expression of CXCL2 and GM-CSF between epithelial and stromal cells were also detected, suggesting that the stromal compartment may drive early inflammatory cell recruitment and activation following LSCD. While both epithelial and stromal cells significantly upregulated production of IL-8, CXCL5, CXCL6, CXCL10, and CXCL11, epithelial cells produced more CX3CL1, IL-6, MIP1 α , CCL2, and CCL3 on proinflammatory cytokine stimulation. Many of the chemokines

Optimising culture, identification, and isolation of human LESC

and cytokines expressed by human corneal stromal and epithelial cells following the inflammatory response to LSCD can induce remodelling of the corneal tissue while also providing potent chemotaxis signals to infiltrating inflammatory cells.

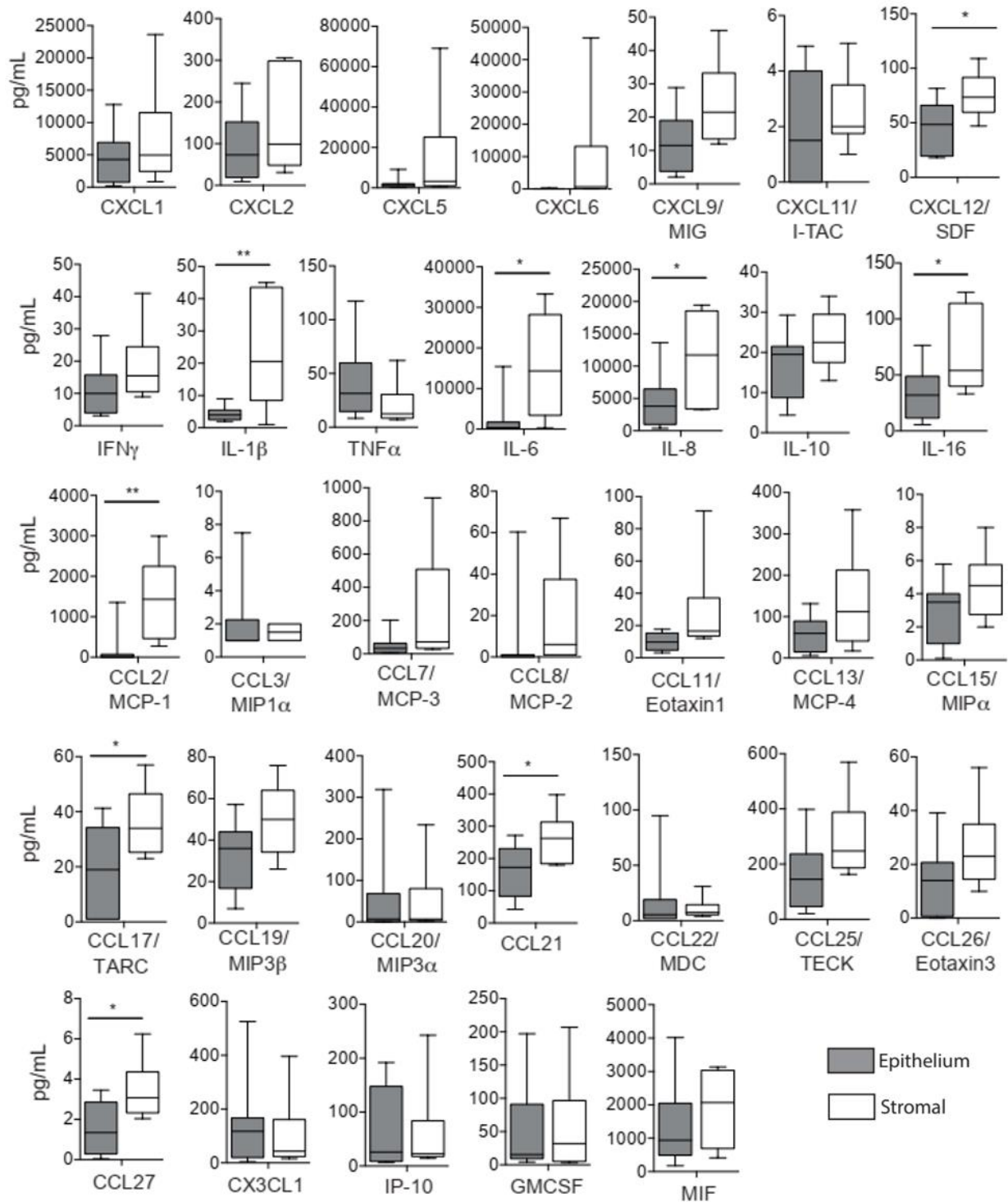


Figure 5.2 Basal expression of chemokine & cytokines by cultured human corneal stromal and epithelial subsets *in vitro*. Supernatants from human limbal tissue derived stromal (white bars) or epithelial cells (grey bars) were screened for chemokine and cytokine mediators by multiplex immunoassay. Several other factors were undetected (CXCL13, Eotaxin-2/CCL24, IL-2, IL-4, CXCL11/I-TAC). Data shows mean concentration and boxplots whiskers of 10-90th percentile of n=10 individual limbal donor tissue derived cell cultures. Statistical significance calculated by two-way ANOVA (* $P < 0.05$, ** $P < 0.01$).

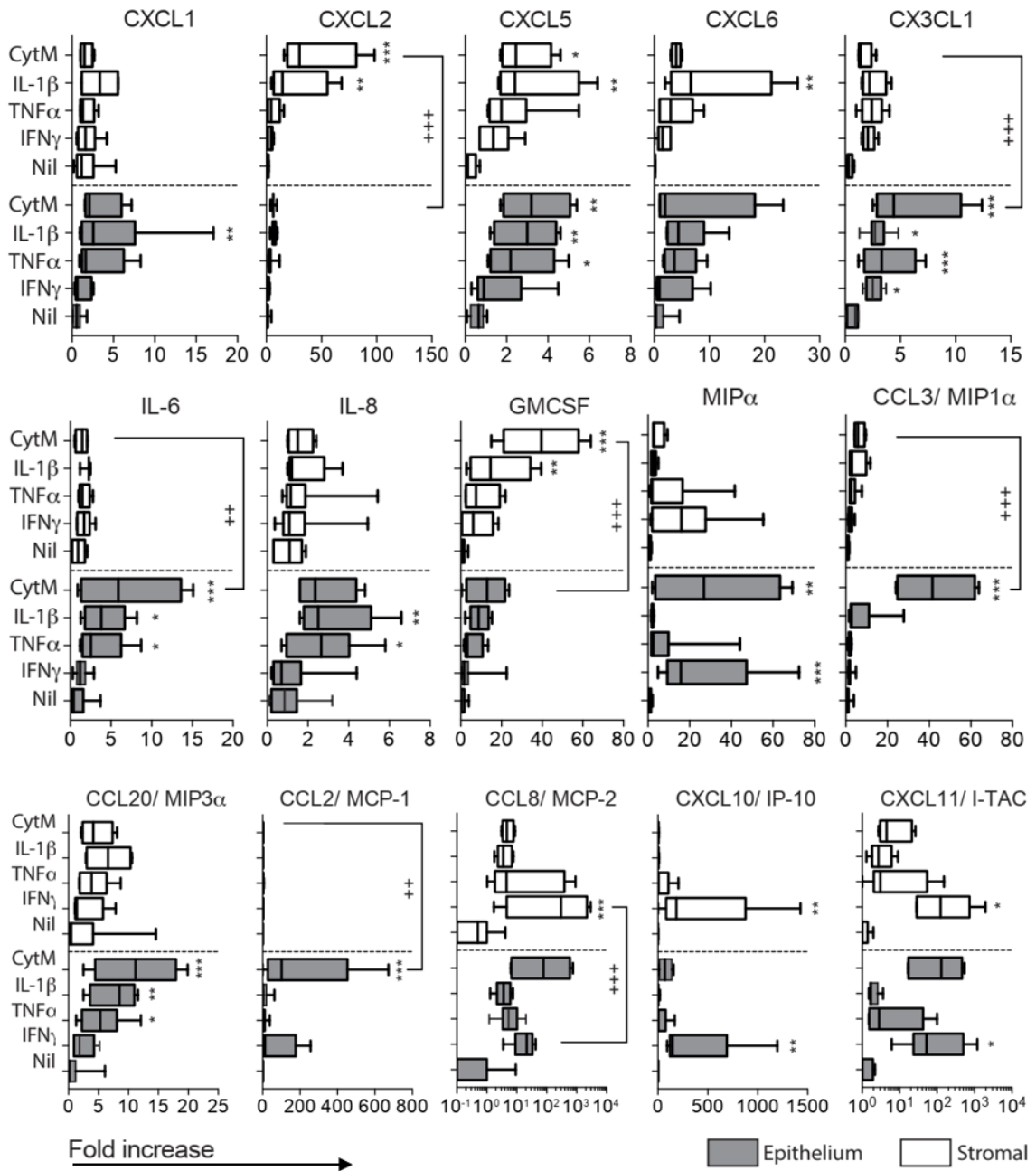


Figure 5.3 Primary human limbal CLET derived cells produce chemokine and cytokine mediators following proinflammatory cytokine stimulation. Supernatants from human limbal tissue derived stromal (white bars) or epithelial cells (grey bars) cultured in the presence of proinflammatory cytokines IL-1b, IFN γ and TNF α or a combination of all three cytokines (CytM) were screened for the presence of chemokine and cytokine mediators by multiplex immunoassay. Data shows the fold-increase in detected protein concentrations relative to unstimulated control cell cultures. Boxplots show mean and whiskers 10-90th percentile of n=10 individual limbal donor tissue derived cell cultures. Statistical significance compared to unstimulated (*), or between stromal and epithelial cultures (+) calculated by two-way ANOVA (* $P < 0.05$, ** $P < 0.01$, *** $P < 0.001$).

5.3 Enrichment of human corneal epithelial cells

Once protocols for the digestion and culture of human corneal epithelial cells had been optimised, we began investigating methods to isolate LESC from primary human corneal cell digests.

5.3.1 Percoll density gradient centrifugation

Human limbal tissue was digested using an overnight collagenase digestion protocol followed by Percoll gradient centrifugation for further enrichment of LESC. This method has been previously described using mouse limbal cells, where a population of cells retained within the densest fraction (80% Percoll) were enriched for the LESC markers ABCG2 and Lgr5, and exhibited a side population phenotype associated with LESC [136]. Digested corneal cells obtained from three individual donors were separated by Percoll gradient, and cells of the 40% and 80% Percoll fractions were then seeded for a colony forming efficiency (CFE) assay on a feeder layer of irradiated 3T3 fibroblasts. Flow cytometry data shown in Figure 5.4 shows the relative live cell proportions of EpCAM⁺ epithelial cells, CD90⁺ stromal cells, and PAX6⁺ABCB5⁺ LESC. Scatter plots show the difference in size between the 40% and 80% fractions, with larger cells in the 40% as expected. No statistically significant difference in epithelial, stromal, or LESC populations were detected either between each of the fractions, or relative to unsorted controls. It should also be noted that cells were fixed in PFA in order to stain with the intracellular PAX6 antibody, which was used to identify potential LESC along with an antibody against ABCB5. Cells seeded for CFE assays were fixed and stained with Toluidine Blue in order to identify and quantify holoclone-like cells, which are known to be LESC if they retain their proliferative potential and holoclone forming ability during single cell sub-culture. Figure 5.4 shows that although the CFE for all groups was extremely low, that of the densest 80% fraction was significantly higher compared to the 40% fraction.

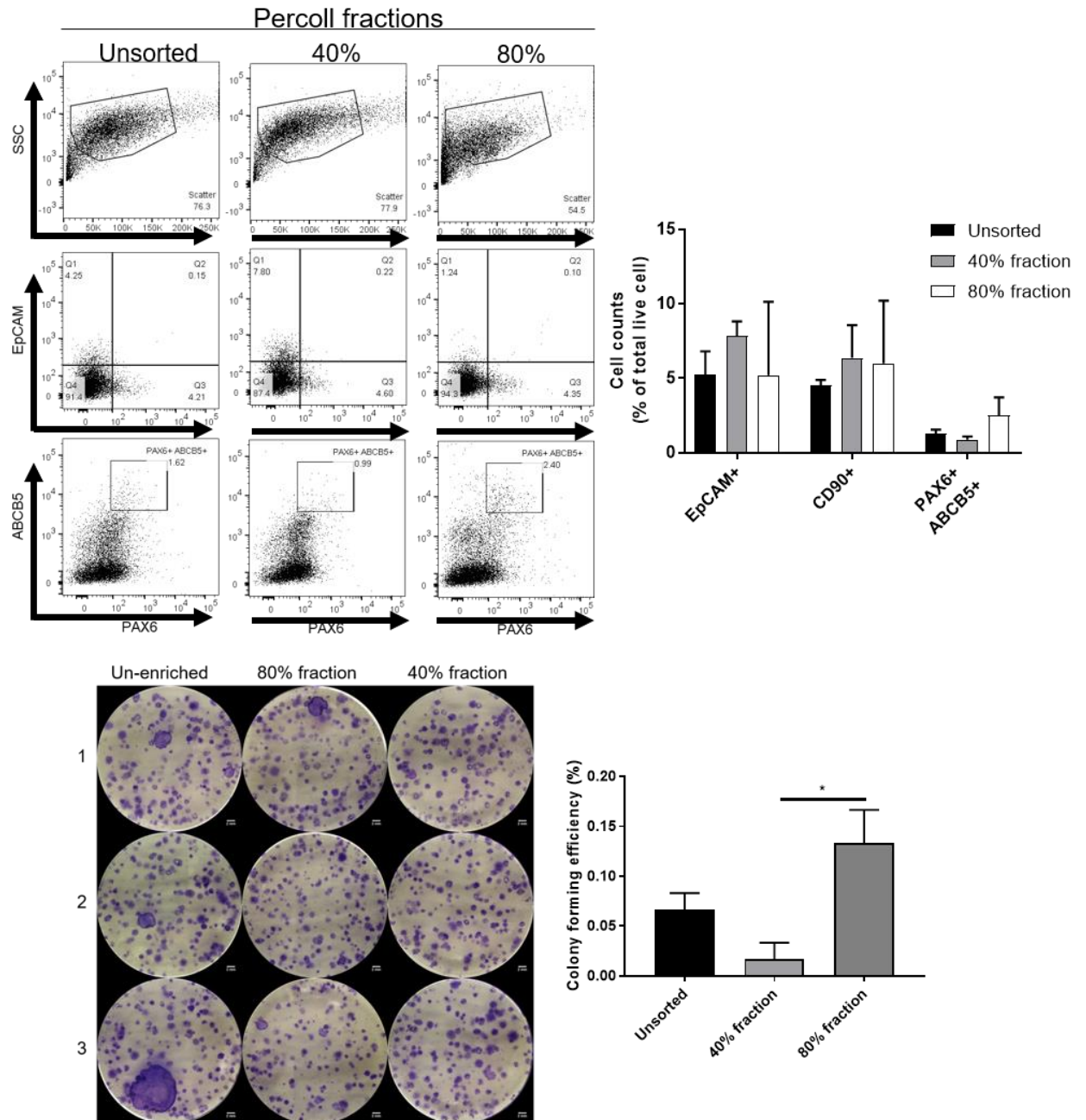


Figure 5.4 Enrichment of primary human limbal epithelial cells on a Percoll density gradient analysed by flow cytometry. Representative flow cytometry plots of human corneal cells centrifuged on a Percoll density gradient and collected from either the 40% or 80% fraction and analysed for expression of stromal marker CD90, epithelial marker EpCAM, and LESC markers ABCB5 and PAX6 after fixation and antibody staining. Data is quantified and presented as a mean percentage of the total live cell counts, compared to an unsorted control sample (\pm SEM). N=3. Microscopy images show results of a colony forming assay to assess holoclone-like cells, plated of cells from each fraction (\pm SEM). Statistical significance between 40% and 80% fractions, calculated by t test (* $p < 0.05$) N=3.

This experiment was repeated using three different corneal donors using the same method with results analysed by qPCR, looking at the expression of several key corneal markers and the results are shown in Figure 5.5. ABCG2, ABCB5, K14, LGR5, CD34, and CD200 were all included as potential markers of LESC or limbal basal epithelial cells. There was a 5-fold increase in the expression of LGR5, a G-coupled protein receptor present in multiple stem cell niches including the limbus in the 80% fraction. This increase was relative to the unsorted cell population although failed to reach statistical significance. Other markers included conjunctival and differentiated epithelial markers which also showed no significant change in expression. qPCR data from cells of the 40% fraction was not included as the RNA quality of isolated cells was too poor to perform DNA synthesis. The CFE assays contained multiple holoclone colonies, with far fewer meroclones or paraclones compared to that of Figure 5.4, and showed a significantly higher holoclone forming efficiency, indicating an LESC content 9 times higher in the 80% fraction compared to the unsorted cells.

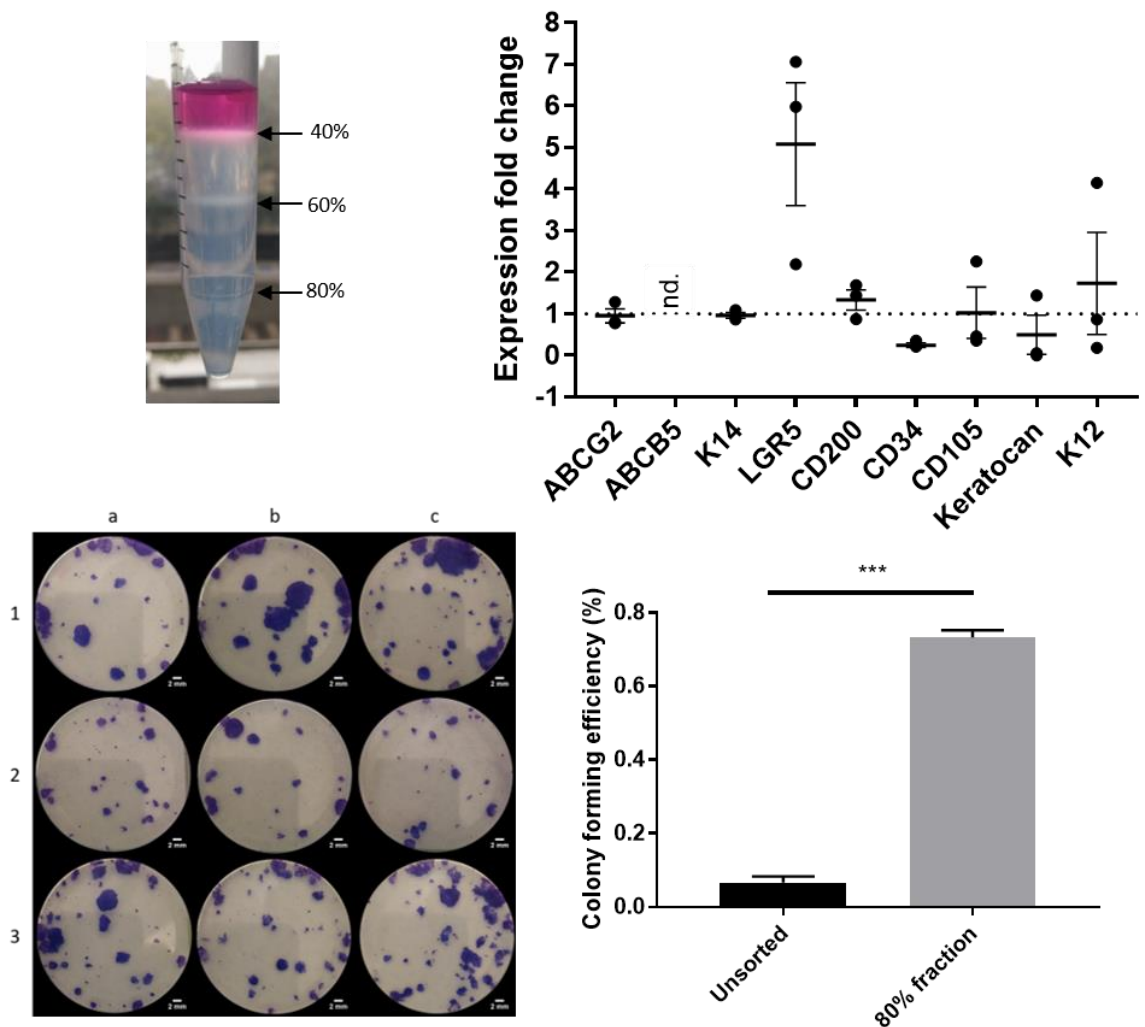


Figure 5.5 Enrichment of primary human limbal epithelial cells on a Percoll density gradient analysed by qPCR. qPCR summary data of human corneal cells centrifuged on a Percoll density gradient and collected from the 80% fraction and analysed for expression of epithelial and LESC markers. Data is presented as mean fold change in gene expression relative to an unsorted control (\pm SEM). No expression changes of significance. N=3. Microscopy images show results of a colony forming assay to assess holoclone-like cells, plated of cells from the 80% fraction. Statistical significance between control and 80% fractions, calculated by t test (***) $p < 0.001$ N=3.

5.3.2 Magnetic activated cell sorting

An alternative technique for enrichment using magnetic activated cell sorting (MACS) was also tested for positive selection of cells expressing LESC markers. Digested corneal cells were labelled with an antibody against the cell surface marker ABCB5 and passed through a positive selection MACS column to isolate those expressing the LESC marker. The flow cytometry plots in Figure 5.6 demonstrate a large increase in the population of ABCB5+ cells, however, the expression of PAX6 in this population was the same as in the ABCB5- population indicating that these were unlikely to be LESC. Given the large percentage of ABCB5+ cells in the unsorted control it is likely that there was an issue with the specificity of the antibody and/or the gating strategy used. Both enriched and control populations were processed for RNA isolation, cDNA synthesis, and qPCR analysis for the expression of key LESC genes relative to an unsorted control population of cells. Also included in this qPCR panel were ABCB5, CD34, and Keratocan, however they were excluded from the analysis due to insufficient Ct values from experimental samples and controls, resulting in no expression data. Genes for LESC or basal epithelial cells ABCG2, Lgr5, and PAX6 showed a 2-4 fold upregulation in expression; K14 showed no change; while K12, a marker of differentiated epithelium, showed a 2.9- fold change in the enriched population compared to the unenriched control cells. However, the qPCR data further confirmed no significant change in any gene expression in the enriched population, and several markers including ABCB5 were not detected in the sample. Due to these results CFE assays were not subsequently performed with these samples.

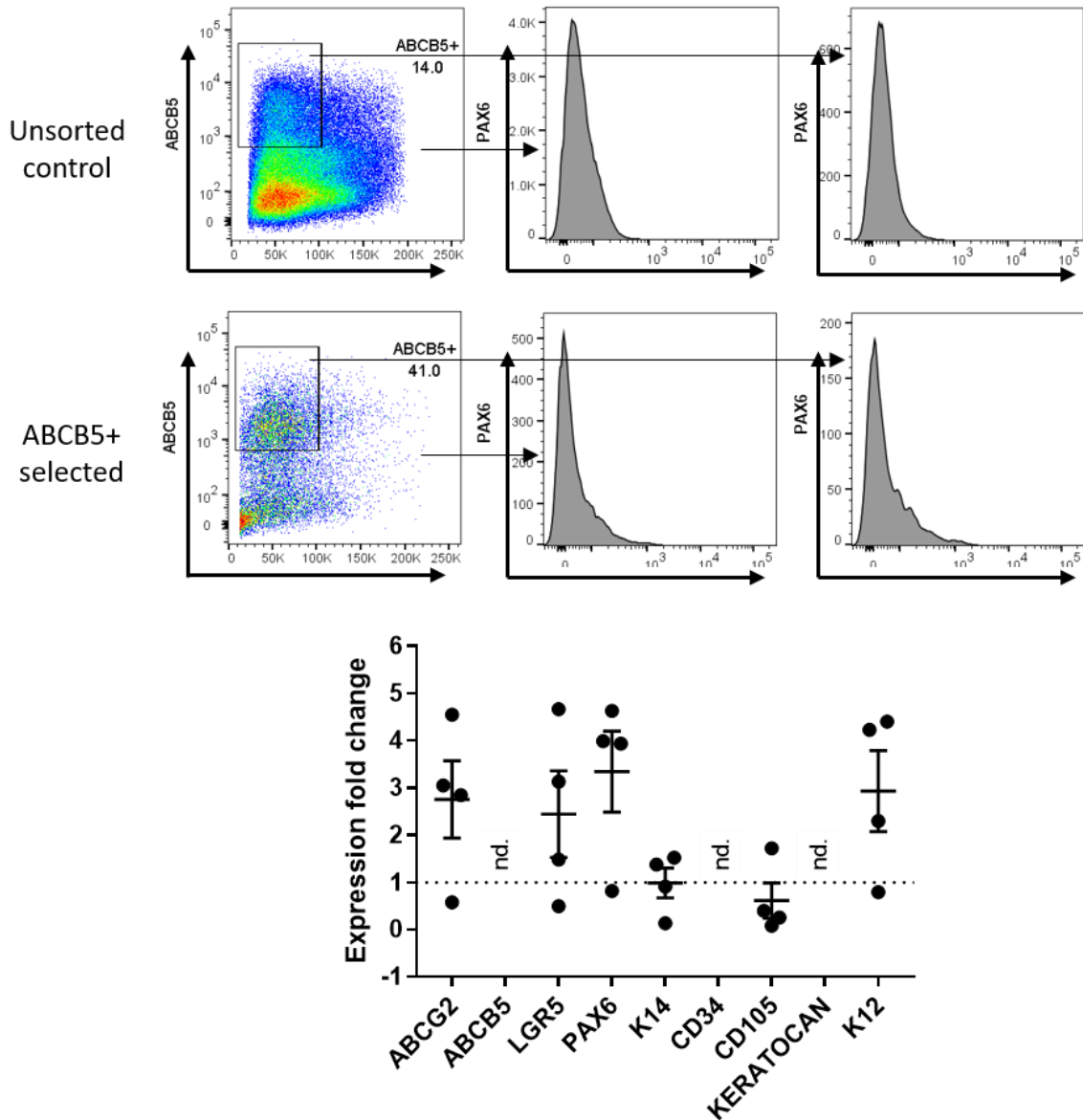


Figure 5.6 Enrichment of primary human limbal epithelial cells by MACS positive selection column analysed by flow cytometry and qPCR. Representative flow cytometry plots of human corneal cells positively selected for ABCB5 expression on a MACS positive selection column, showing histograms of PAX6 expression. qPCR summary data shows cells analysed for expression of epithelial and LESC markers. Data is presented as mean fold change in gene expression relative to an unsorted control (\pm SEM). No expression changes of significance analysed by t test . N=4

5.3.3 Fluorescence activated cell sorting

The third enrichment strategy attempted was cell sorting by flow cytometry. While this can be a powerful method for isolating small populations of rare cells, its success relies on the use of antibodies specific for the target cells. As shown in Figure 5.6, as well as the results of many optimisation experiments, ABCB5 is not suitable for this purpose with the antibodies commercially available at the time. Recently published data from our collaborators in the Lako laboratory at the University of Newcastle has shown that CD200 is a novel cell surface marker for LSCs [18]. This cell surface marker was used to sort cells from digested four human limbal rings which had been cultured and expanded *in vitro*. The gating strategy represented in Figure 5.7 shows how after scatter, singlet, and live/dead gates, CD200 is plotted against an empty channel to exclude autofluorescence. This population is then gated on CD200-high, FSC-low to identify the LSCs. CD200+ sorted cells were analysed by qPCR for several key LSC and epithelial markers, however the results show that the only gene with significantly higher expression was CD200, with ABCB5 not detected suggesting a technical problem with the antibody or staining protocol.

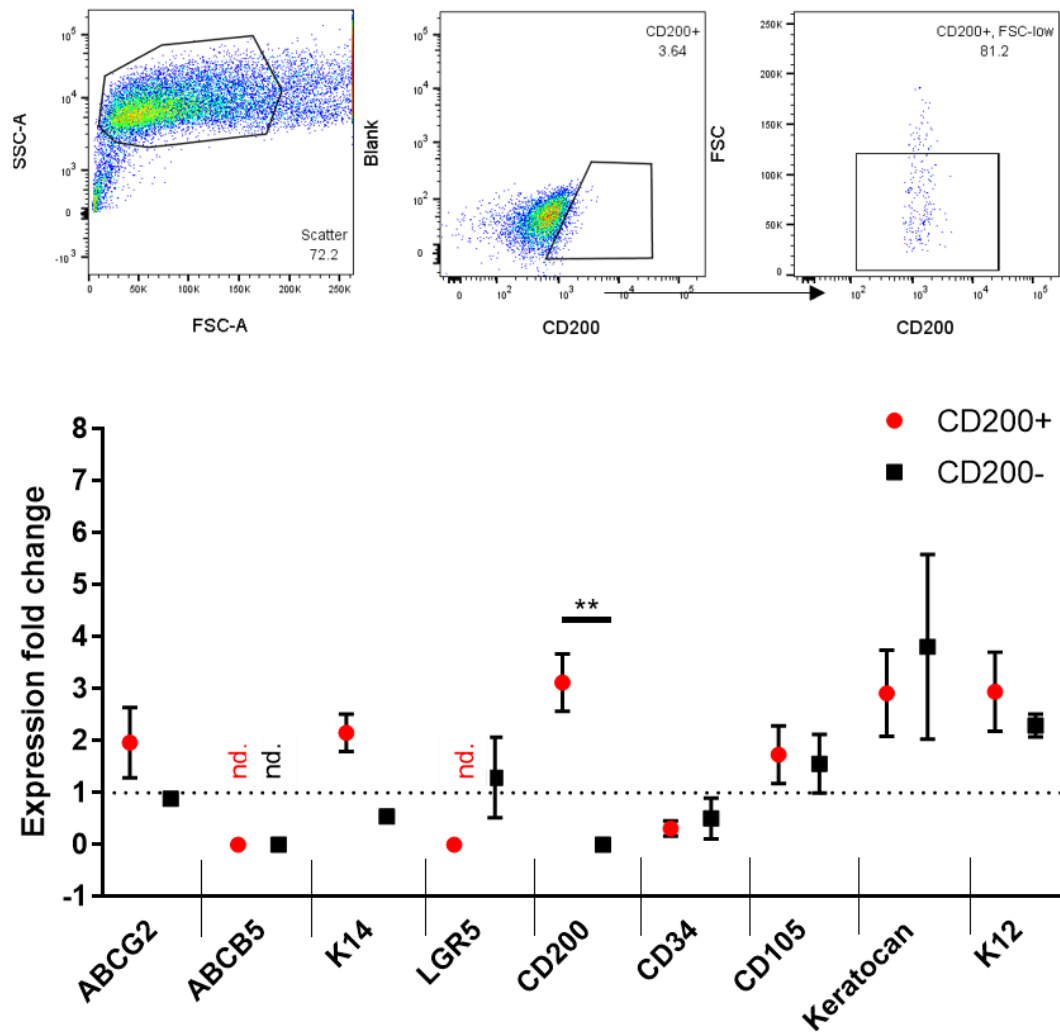


Figure 5.7 Enrichment of primary human limbal epithelial cells by cell sorting for CD200 expression analysed by qPCR. Representative flow cytometry plots showing gating strategy for selection of CD200+ human corneal epithelial cells, including gating for single cells and a live/dead stain (data not shown). qPCR summary data of human corneal cells sorted by CD200+ or CD200- populations, analysed for expression of epithelial and LESC markers. Data is presented as mean fold change in gene expression relative to an unsorted control (\pm SEM). Statistical significance in CD200 expression between positive and negative populations (** $p < 0.1$), as analysed by multiple comparison two-way ANOVA. N=4.

5.4 Development of a humanised mouse model of LESC transplantation

As well as developing strategies to enrich a stem cell population from human limbal tissue, we also chose to further develop our mouse model of LSCD and transplantation. By using immunodeficient NSG mice as recipients, human cells would be able to be grafted without risk of rejection. By generating a stock of GFP lentivirus we were able to begin optimising a protocol for the *ex vivo* transduction of primary human corneal epithelial cells. Figure 5.8 shows flow cytometry plots of human cells which were transduced with a range of virus concentrations calculated as multiplicity of infection (MOI) following titration, demonstrating that an MOI of 10 was the most effective, achieving transduction efficiencies of >65% (as determined by GFP expression). Near uniform expression of GFP by microscopy confirmed that transduction was successful.

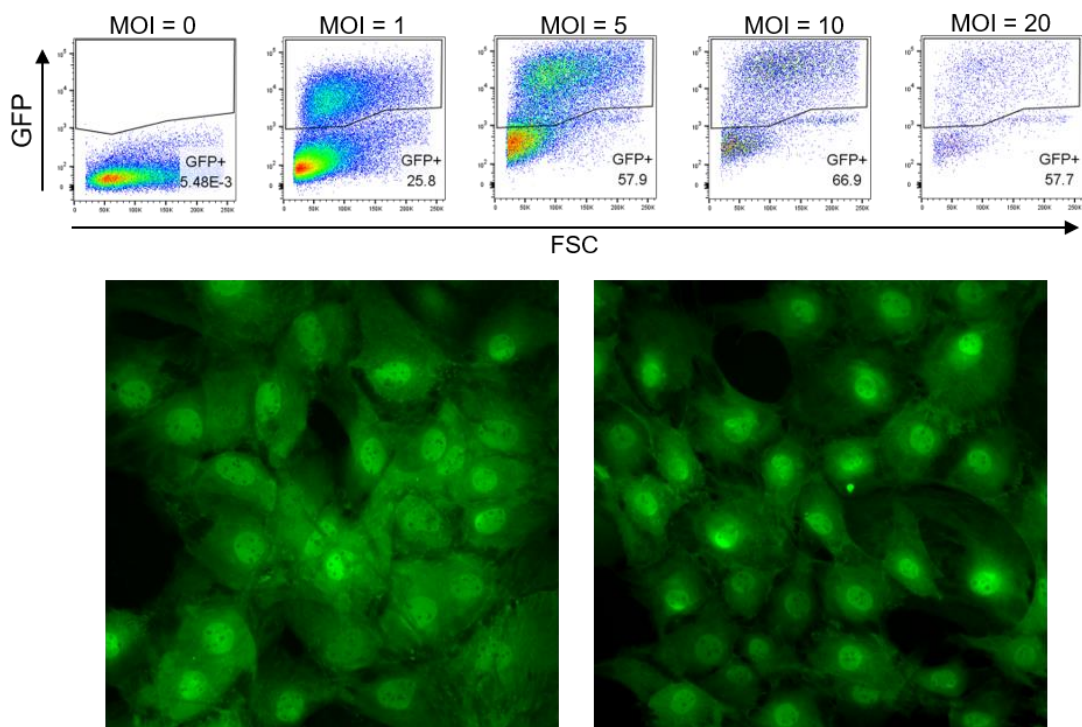


Figure 5.8 GFP+ lentiviral transduction of primary human corneal epithelial cells *in vitro* culture. Flow cytometry plots showing the expression of GFP in primary cultured human corneal epithelial cells transduced by a GFP lentivirus at varying concentrations (also gated by cell size, singles, and live/dead stain). Representative images show transduced corneal epithelial cells expressing GFP in culture.

Sheets of lenti-GFP primary human limbal epithelial cells were generated by culturing limbal digests on temperature sensitive tissue culture dishes until confluent. At this point, GFP expression was confirmed by microscopy and intact epithelial sheets were harvested by lowering the temperature of the dish to $<25^{\circ}\text{C}$ causing the adherent cells to cleanly detach from the dish without trypsin. These sheets were transplanted into prepared LSCD NSG recipient mice as either single or multiple layers of sheets. This was due to imperfect technique resulting in breakages of the delicate epithelial sheets. Once grafts were applied, the protective lenses were placed on top and eyes were sutured closed. The images shown in Figure 5.9 show the placement of the sheets during surgery. However, at day 4 most of the grafted cells were attached to the protective lens and disappeared when the lens was removed. By day 7 no sign of the small remaining clusters of grafted cells remained, and severe LSCD developed shortly after in all recipients including the LSCD control.

In a separate subsequent experiment three human limbal rings were digested, cultured to confluency before being harvested and sorted by flow cytometry for CD200 expression using the previously described gating technique. Cells of each group (CD200+ or CD200-) were then seeded onto a thin layer of pre-prepared fibrin gel and left to adhere for 3 hours in tissue culture. Prior to transplantation cells were labelled with CFSE (instead of GFP transduction) to reduce the steps involved in the protocol. Single intact sheets were then transplanted onto each of the LSCD NSG recipients, in one of four groups: CD200+ sorted cells; CD200- sorted cells; or unsorted cells; while the contralateral eye was used as an untreated control. The presence of engrafted cells were confirmed by *in vivo* imaging during surgery (shown in Figure 5.10), and while very few were visible on day 4 upon removing the protective lens this was possibly due to the CFSE label having diluted rather than graft failure. Corneas were imaged and visually graded using three criteria: corneal haze, epithelial irregularity, and vascularisation. The mean scores at the point of takedown in Figure 5.10 showed no significant differences between any of the experimental treatment groups.

Optimising culture, identification, and isolation of human LESC

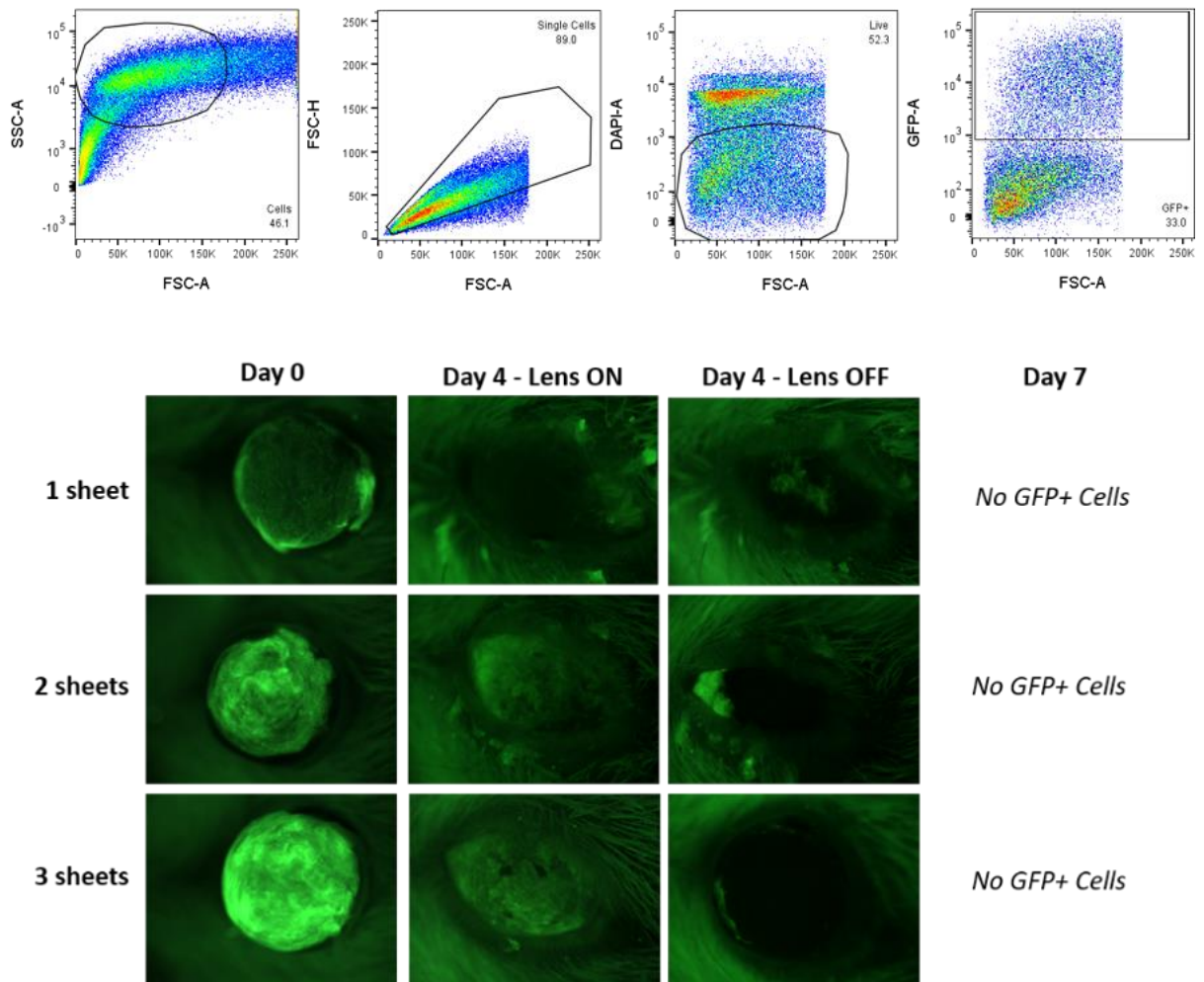


Figure 5.9 Transplantation of GFP+ human corneal epithelial cells into a mouse model of LSCD. Representative flow cytometry plots showing the gating and expression of GFP in cultured human corneal epithelial cells following lentiviral transduction. Representative *in vivo* imaging shows sheets of GFP+ cultured human corneal epithelial cells transplanted onto the LSCD cornea of recipient NSG mice in multiple layers over the course of 7 days. N= 3 mice per treatment group.

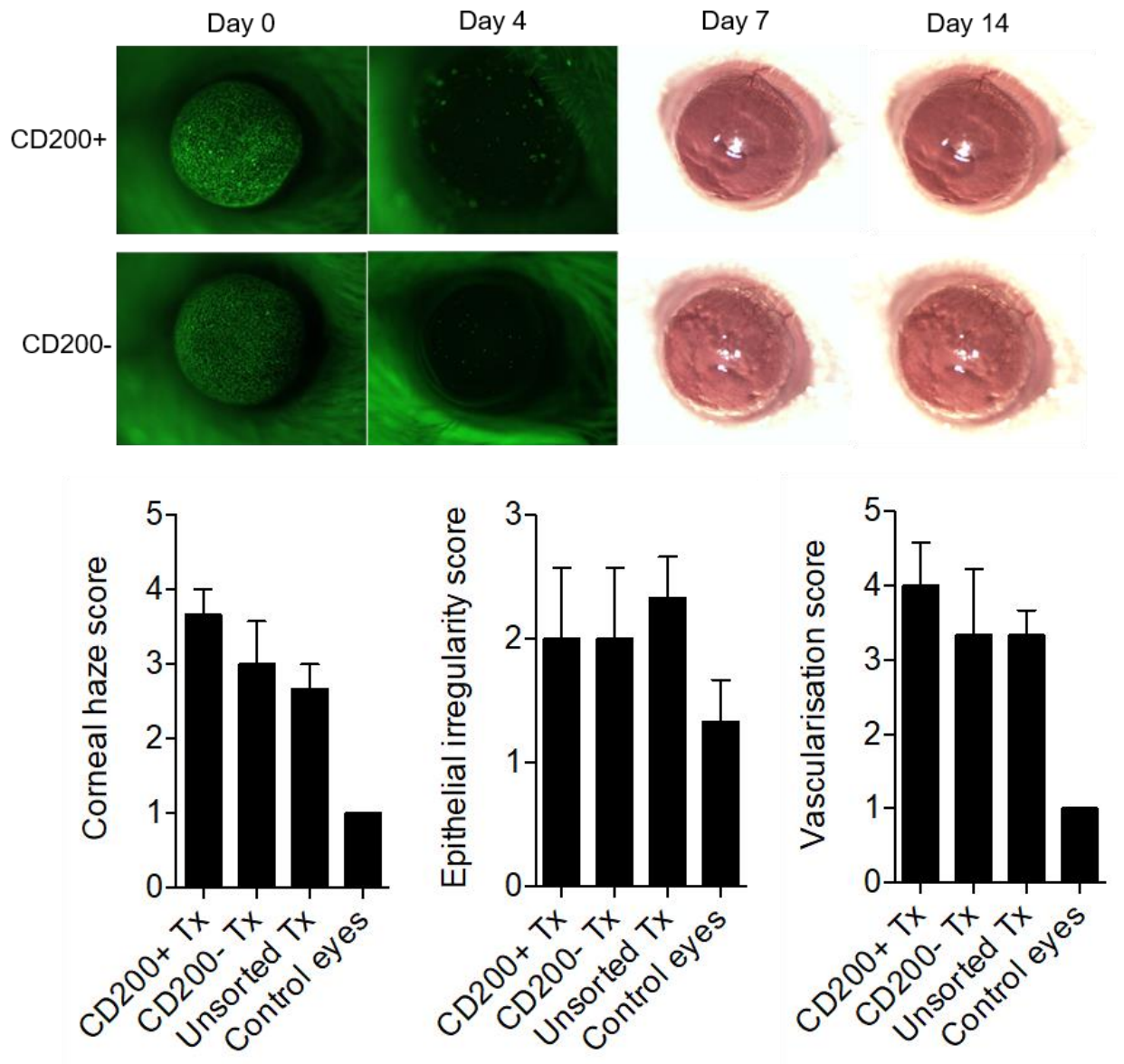


Figure 5.10 Transplantation of CD200+ CFSE labelled human corneal epithelial cells into a mouse model of LSCD. Representative *in vivo* imaging of CFSE labelled human corneal epithelial cells sorted for expression of CD200 by flow cytometry transplanted onto the LSCD cornea of recipient NSG mice. Imaged over the course of 14 days and visually graded for corneal haze, epithelial irregularity, and vascularisation. Scores are averaged and summarised from day 14 post transplant, plotted as mean \pm SEM. N=3 mice per treatment group.

Mice were taken down after two weeks, the corneas digested, and analysed by flow cytometry. Vascularisation and epithelialisation were assessed through antibody staining against murine vascular cell adhesion molecule (VCAM) and murine EpCAM, shown in Figure 5.11. Assessing these factors by flow cytometry was a more quantitative measure of vascularisation and epithelialisation than the visual assessment method. Cells were quantified using FACS counting beads and presented as cell numbers per cornea, although the data showed little variation between experimental groups and none of significance. Corneas were also assessed for levels of expression of MHC class I and II, as an upregulation of Class I would be indicative of epithelial activation, although no changes of statistical significance were observed.

Infiltration of myeloid cells into the cornea was assessed and quantified by CD45, CD11b, and Ly6G with counting beads in Figure 5.12. The representative flow plots showed very little difference in the presence of CD45+ cells between the three experimental groups, confirmed by the calculated means. Neutrophil presence was determined by the CD11b+ Ly6G+ population, and showed far greater levels of neutrophil infiltration in the CD200- grafted group compared to both the CD200+ and unsorted control groups, however again, there was no statistical significance.

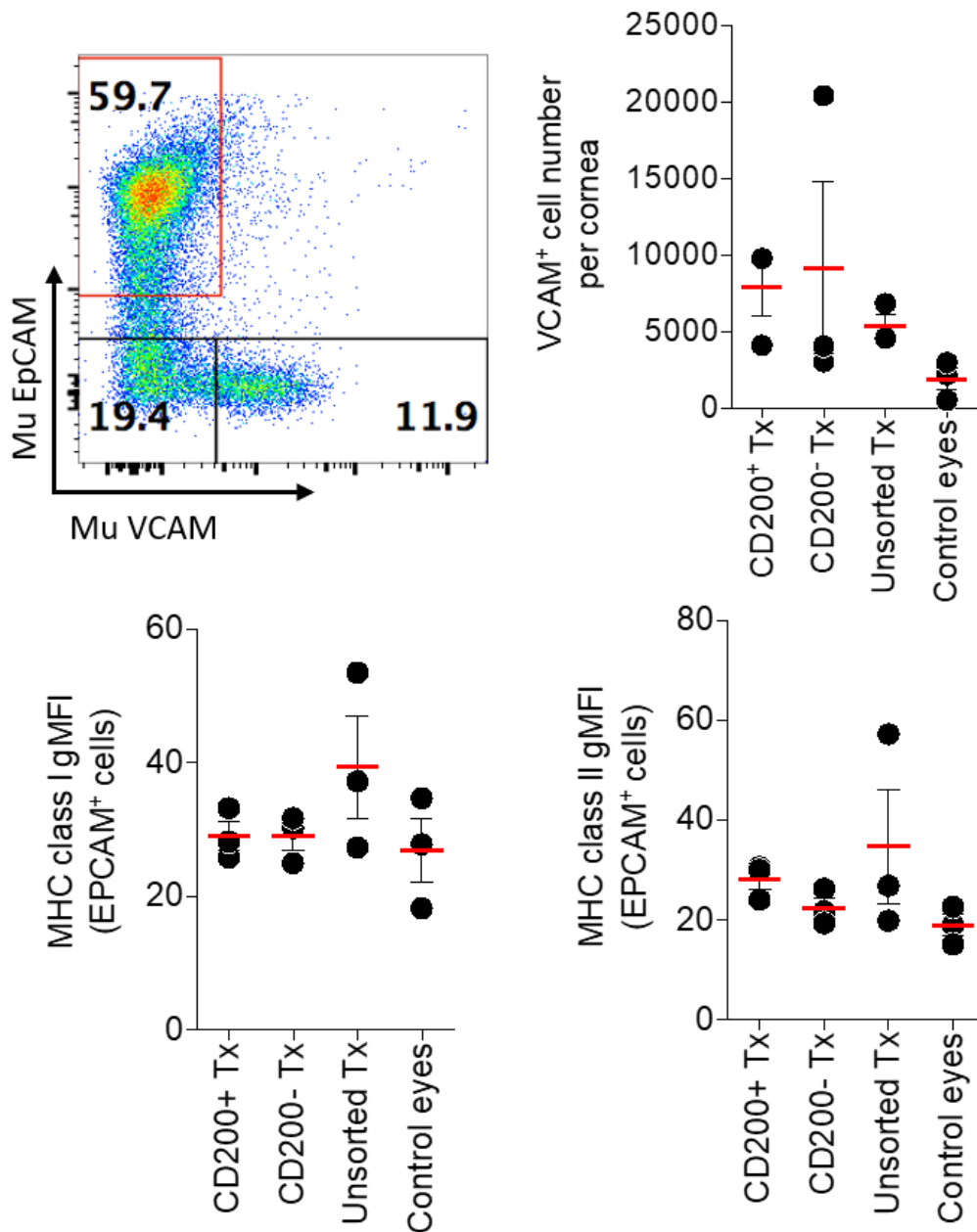


Figure 5.11 Vascularisation and epithelialisation of the LSCD mouse cornea following transplantation of CD200+ CFSE labelled human corneal epithelial cells. Representative flow cytometry plot showing gating strategy for EpCAM and VCAM following digestion of LSCD treated mouse corneas. Cell numbers are quantified by FACS counting beads and plotted as mean cell number (\pm SEM) for VCAM+ cells. MHC class I and II EpCAM+ cells are shown as mean gMFI (\pm SEM). N=3 mice per treatment group.

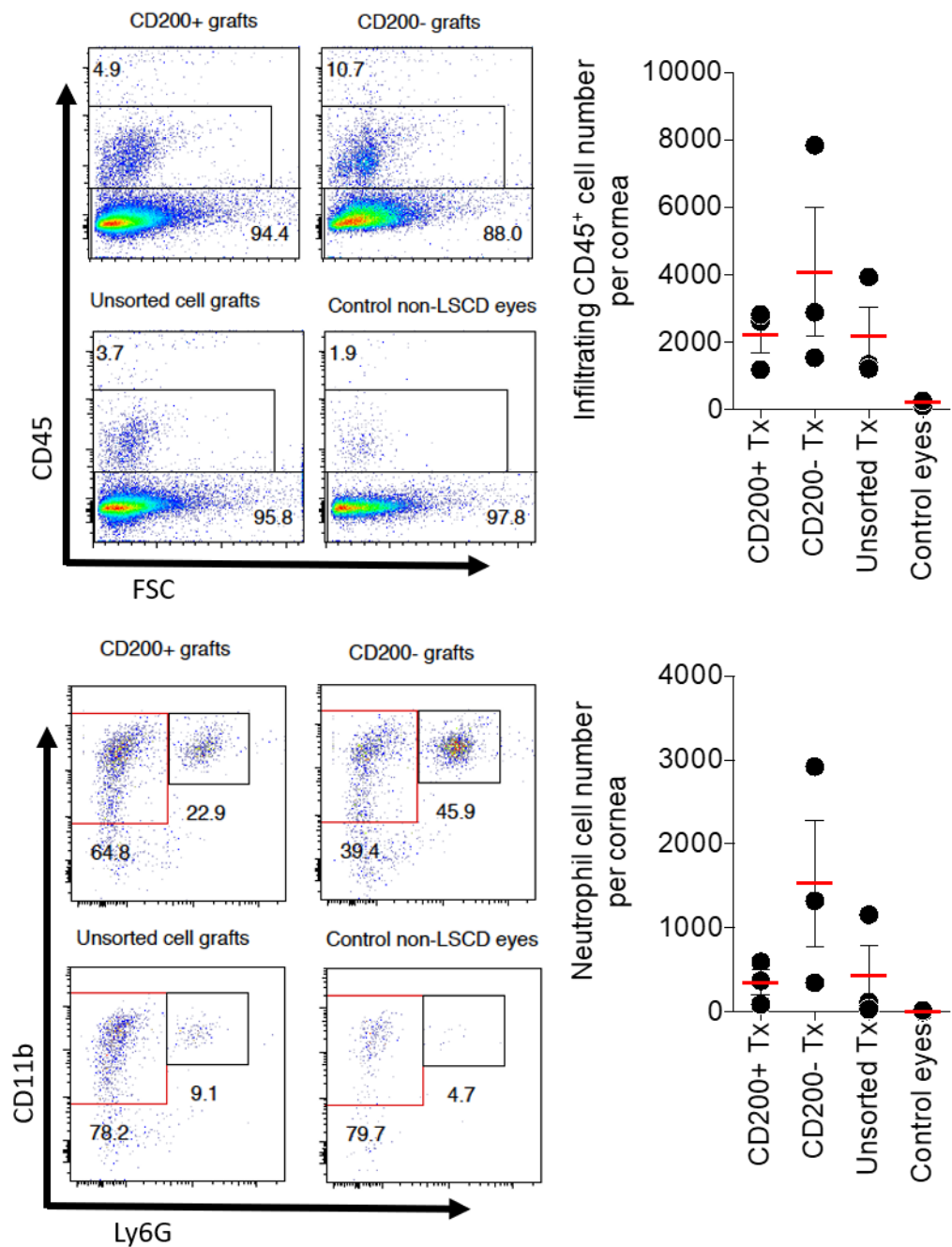


Figure 5.12 Myeloid cell infiltration in the LSCD mouse cornea following transplantation of CD200+ CFSE labelled human corneal epithelial cells. Representative flow cytometry plots showing gating strategy for identifying infiltrating CD45+ cells and CD11b+ Ly6G+ neutrophils into the digested LSCD mouse cornea following CD200+ human epithelial cell transplantation. Cell numbers are quantified by FACS counting beads and plotted as mean cell number (\pm SEM). N=3 mice per treatment group.

By using CFSE as an *in vivo* label rather than GFP we were unable to see if any transplanted donor cells had remained in the recipient cornea throughout the study. To assess this, corneal cells were stained with Human EpCAM and HLA-ABC antibodies, but only negligible cell numbers were detected. One single recipient mouse in the unsorted transplant group showed significantly higher numbers of cells expressing human antigens indicating that some cells, or a small cluster, had survived. Given that no other means of assessing the transplant outcomes had shown any evidence of this, and it was clear from imaging of the cornea that LSCD had progressed unchecked, it is unlikely that these were any engrafted cells, rather residual cells which had remained attached to the cornea from surgery.

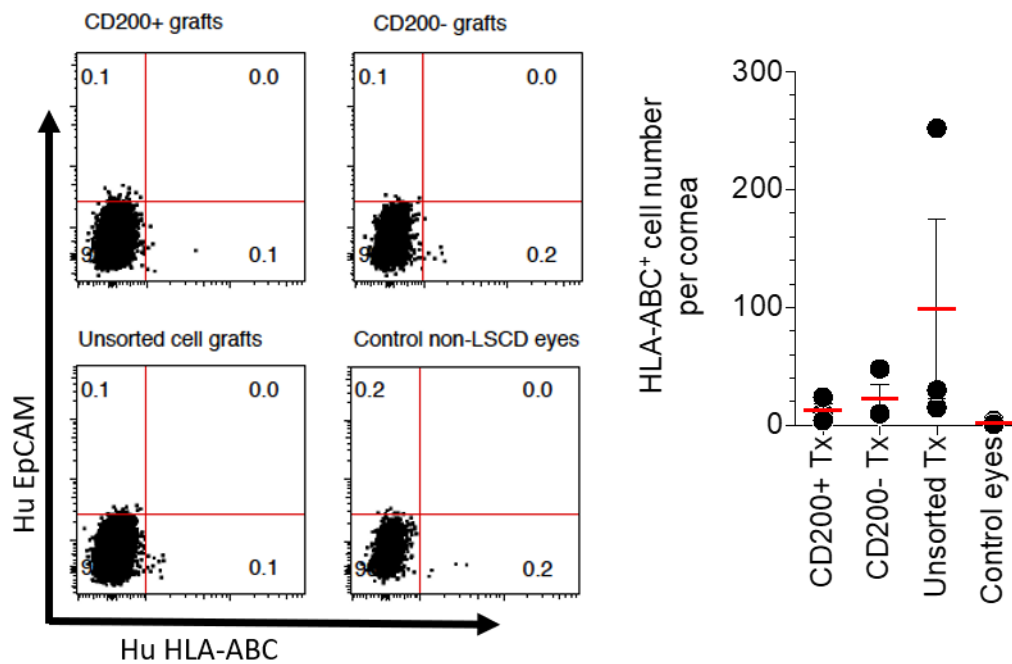
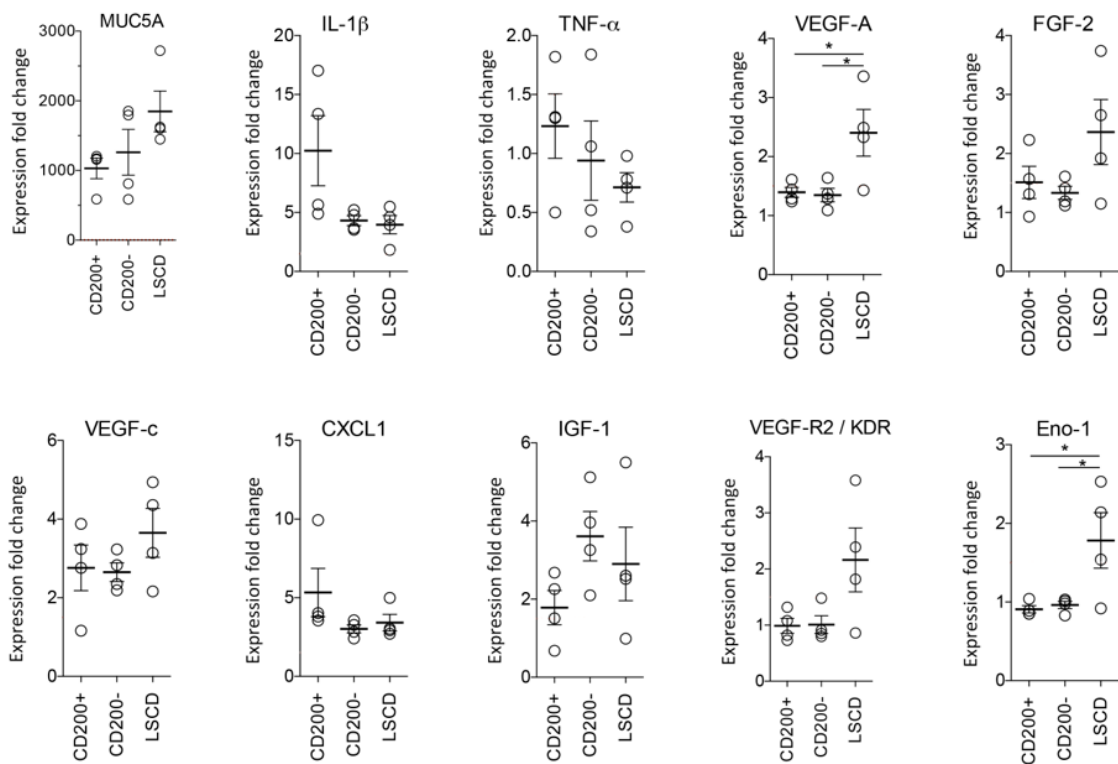


Figure 5.13 Human epithelial cell presence in the LSCD mouse cornea following transplantation of CD200+ CFSE labelled human corneal epithelial cells. Representative flow cytometry plots showing gating strategy for identifying any remaining human epithelial cells in the digested LSCD mouse cornea following CD200+ human epithelial cell transplantation. Cell numbers are quantified by FACS counting beads and plotted as mean cell number (\pm SEM). N=3 mice per treatment group.

Finally, expression of genes associated with corneal inflammation were assessed by qPCR in samples of cells taken from corneal digests. Data shown in Figure 5.14 shows fold change in gene expression relative to the healthy control for each of the three experimental groups. Expression of vascular endothelial growth factor-A (VEGF-A), a marker of vascularisation, was significantly higher in the LSCD control group relative to both the CD200+ and CD200- groups, suggesting that transplantation may have had an ameliorating effect on slowing LSCD progression compared to no treatment. Expression of enolase (ENO-1), a marker of epithelial cell differentiation, was also significantly higher in the LSCD control group. No other inflammatory or vascular markers showed significant increases in expression for any of the groups, and genes IFN γ , IL-10, IL-4, and CD8 α were analysed but no expression was detected.



IFN γ , IL-10, IL-4, CD8 α not detected

Figure 5.14 Gene expression of corneal markers of inflammation following transplantation of GFP+ human corneal epithelial cells sorted for expression of CD200 into a mouse model of LSCD. Summary of qPCR data of digested mouse corneas following CD200+ human epithelial cell transplantation, analysed for expression of key markers of corneal inflammation. Data is presented as mean fold change in gene expression relative to an untreated healthy control group (\pm SEM). IFN γ , IL-10, IL-4, CD8 α expression analysed but not detected. Statistical significance is shown in gene expression for VEGF-A and Eno-1 (** $p < 0.1$), as analysed by two-way ANOVA (* $P < 0.05$). N=3.

5.5 Summary

This chapter has focused on the development of strategies to successfully isolate and culture limbal epithelial cells from human cadaveric limbal tissue, and enrich a population of L ESCs from these cultures. It was determined that digestion of limbal rings using a short incubation in trypsin was the most efficient at generating cultures of viable epithelial cells. Using this approach, we were able to produce human epithelial or stromal cultures reliably in large quantities which allowed the investigation of their basal inflammatory chemokine and cytokine profile *in vitro*, as well as the response to stimulation by pro-inflammatory cytokines. These results demonstrated significantly upregulated expression of potent chemoattractants and those involved in tissue remodelling responses.

Developing methods of isolating and enriching L ESCs from limbal epithelial digests proved to be a major technical and experimental challenge, which together with a general shortage of available human tissue limited the scope of these enrichment experiments. Centrifugation of cells on a Percoll density gradient, positive selection of ABCB5+ cells by MACS, and cell sorting for CD200+ expression were all found to be potentially useful methods for studying L ESCs. As no significant conclusions could be drawn from this data, further development of these methods will be required before their effectiveness can be confirmed.

Although several attempts at developing a humanised mouse model of LSCD and LESC transplantation were made, we did not observe any long term engraftment of human cells. Results from the transplantation of CD200+ human cells did not show any reduction in cell infiltration or inflammation in the cornea and failed to prevent the re-emergence of the LSCD phenotype.

CHAPTER 6. DISCUSSION

Limbal stem cell deficiency is a painful and debilitating cause of blindness which has a significant effect on quality of life. For patients with LSCD, transplantation of donor derived LSCs can be an effective treatment, however the use of both auto- and allogeneic tissue has high degree of failure despite systemic immune suppression, for which the reasons are poorly understood. Through this project we have sought to investigate key variables in determining transplantation success, including graft bed inflammation and characterising the recipient immune response to allogeneic grafts. The findings from each results chapter are discussed independently below.

6.1 Establishing a mouse model of LSCD and LESC transplantation

Despite several different animal models of LSCD existing in the literature, each has several limitations, and few are able to accurately simulate the LESC transplant procedure performed in humans. We sought to develop a reliable and reproducible mouse model of both LSCD and LESC transplantation with which to further investigate the innate and adaptive cellular immune response. Development of the protocol for induction of LSCD and transplantation of allogeneic donor LSCs was a lengthy and challenging process, with many of the strategies and modifications adopted having little or no effect. The use of ethanol and mechanically debriding the cornea proved to be effective in the development of an LSCD phenotype in recipient mice, with the cornea displaying the characteristic features of the injury as seen in humans, including epithelial defects, neovascularisation, conjunctival migration. This was demonstrated through fluorescent *in vivo* imaging, multiphoton imaging, immunohistochemistry, and qPCR gene expression analysis to detail the loss of differentiated epithelium and invasion of CK-19 expressing conjunctival epithelium along with Muc5A expressing goblet cells. These results are in line with data from *in vivo* models in the published literature which used alternative protocols for LSCD induction, indicating this method and model was effective at simulating the human

LSCD injury phenotype [113, 114]. This LSCD injury model also caused cellular infiltration into the cornea and the secretion of inflammatory mediators which we analysed using qPCR, ELISA, and flow cytometric analysis of corneal tissues.

CXCL-1 expressed by corneal epithelium & stroma in response to insult induces neutrophil & monocyte infiltration. Neutrophils play a key role in pathogen clearance in corneal infections but can also cause inflammation and tissue damage. Studies have shown that neutrophil recruitment to the cornea is reduced in a CXCL1 knockout mouse model of viral keratitis, indicating it is likely one of the key drivers of early cellular infiltration seen in the cornea following LSCD, along with IL-1 β , IFN γ , and TNF α [117, 137]. This coincides with the LSCD environment gene expression and ELISA data (Figure 3.11 and Figure 3.12) which also shows significant increases in expression of these same genes, and biphasic pattern of elevated expression of IFN γ at days 3 and 14 most likely due to tissue infiltrating myeloid cells recruited to the cornea at these time points. Production of these proinflammatory factors immediately following injury is likely derived from residual stromal and epithelial compartments, while the continued elevated IL-1 β suggests a continuous low level of corneal inflammation compartments [120-122].

Several angiogenic and lymphangiogenic genes (VEGF-A, VEGF-C, and VEGF-R2, and FGF2) also displayed significant increases in gene expression which are reported as acute stromal stress and epithelial wound healing responses in the cornea, as well as key drivers of blood vessel growth associated with the corneal neovascularisation seen in LSCD [117-119]. Elevated levels are seen up to day 3 post-injury in our qPCR gene expression data of LSCD mouse corneas (Figure 3.11) before lowering to non-significant levels from days 3 onwards suggesting an initial drive towards neovascularisation in response to the initial LSCD injury.

When cultured *in vitro* in the presence of IL-1 β , primary mouse corneal cell stromal cells secreted high concentrations of CXCL1 and CXCL2 into the culture supernatant, while the epithelial cell response in the same conditions was more limited suggesting that activated stromal cells play a larger role in LSCD graft bed inflammation. Levels

of chemokines CCL5 and CCL7 were also elevated when stimulated by IFN γ or a combination of IL-1 β , TNF α , and IFN γ (CytM), both of which act as potent chemoattractants, promoting leukocyte migration to inflammation sites. Significant levels of CCL5 were detected in stimulated epithelial and stromal cultures, while CCL7 was only elevated in stromal cultures.

There continues to be debate in the literature regarding the location of LESC in the cornea, and whether or not they are exclusively confined to the limbal niche, or as suggested by Mayo *et al.* (2008), that they are actually distributed throughout the ocular surface[138]. Most evidence in the literature disagrees with this hypothesis[139-142]. We observed in our transplant model that small clusters of GFP+ donor cells which successfully engrafted in the central cornea were able to survive and proliferate to partially regenerate the epithelial surface despite the lack of a supporting limbal niche microenvironment. This supports evidence from Chang *et al.* (2008) as the outward centrifugal growth of these cells is similar to results where cells of the central cornea were also able to grow centrifugally despite removal of the limbus in *ex vivo* human corneas. It may be that the centrifugal growth of single cells grafted in the centre of the cornea, as observed in our experiments supports the claim that LESC may be scattered throughout the ocular surface, however there are a number of caveats. For example when grafting, the epithelial sheets are not always perfectly flat and there can be movement post-grafting which can artificially alter the position of LESC in these experimental conditions. Further, the edges of the sheets usually experience some degradation, with single cells and small fragments breaking off to settle on other parts of the cornea where they engraft and proliferate.

6.2 Determining the role of the innate and adaptive immune response in LESC transplant rejection

Results in this chapter focused on the development of our mouse model of corneal epithelial transplantation and several experiments designed to interrogate the

immune response to allograft tissue. *in vivo* imaging showed characteristic signs of graft rejection in immunocompetent recipient mice, and flow cytometric analysis of digested corneal tissues post-rejection detailed demonstrated significant cellular infiltration of immune cell subsets into the allografted cornea. Furthermore, the cytokines and chemokines present in the corneal inflammatory microenvironment were determined through Luminex assay, showing significant differences in expression between allogeneic and autologous recipients. Establishing protocols for the adoptive transfer of purified immune cell subsets into allografted NSG recipient mice proved a technical challenge. Several experiments to investigate the role of fluorescently labelled CD8+ and CD4+ T cells in allograft rejection showed the accumulation and infiltration of CD8+ T cells at the peripheral allograft edge as well as throughout the epithelial surface during rejection. Unfortunately practical issues have limited this area of research, and as such experimental repeats and further optimised investigation is required before conclusions can be drawn.

Current clinical management of patients with acute ocular surface injuries aims to minimise inflammation as well as preventing continued epithelial and stromal damage, and to promote re-epithelialisation. Treatments include anti-inflammatory therapies such as topical corticosteroids to reduce inflammatory cell infiltration. LSCT is not recommended during active inflammation and should be delayed until ocular surface inflammation has subsided or is well controlled with medications [36]. The corneal epithelium is the most antigenic of all ocular tissues although *in vitro* cell culture reduces immunoreactivity [143]. Post-operative steroids are essential for patients receiving cultured limbal allografts to prevent rejection which can be both chronic and acute and is the most commonly reported complication [144]. Late acute rejection can also occur after initial engraftment success, indicating long term local and systemic immunosuppression is required [37].

Data from our mouse model of auto- and allografts show that autograft epithelial sheets are able to survive long term despite the inflammatory LSCD environment and without immunosuppressants. In comparison, the mice which received allografts begin to immediately show signs of acute rejection which without intervention

progressively worsened over the course of 35 days. Epithelial rejection in this mouse model closely resembled the smooth curved rejection line seen in both humans and rabbits [145]. The Kaplan-Meier graft survival plot generated from these pooled experiments demonstrate the long-term survival of autografts as well as initial allograft survival for around 20 days followed by a gradual but complete failure of all transplanted tissue. Differences in survival time between our *in vivo* mouse model and reported post-transplant patient data can be explained predominantly by the use of various immunosuppressant therapeutic regimes, such as regular cyclosporine eyedrops, in treating human patients. For example, the peak time of immune rejection in 10 allogeneic CLET patients was between 1-3 months post-transplantation in 70% cases [35, 143].

The descriptions of the immune response in patients who receive CLET allografts has been limited and most immunohistological rejection data in humans and animal models has focused on the stroma. Our allograft rejection data from the immunocompetent B6 mouse model of rejection shows that the predominantly infiltrating cell type through the donor epithelium were CD3⁺ lymphocytes, along with monocytes and neutrophils, supporting existing published data in both rats and rabbits [146]. The significant number of monocytes also detected in the rejecting corneal epithelial allograft may be attributed to the cell debris phagocytosis function of macrophages rather than as a primary cause of damage.

The initial experiment (Figure 4.9) designed to investigate allogeneic graft rejection only used two grafted 2C-TCR recipient mice which had not completely regenerated the cornea, due to the challenges encountered developing the transplantation model. However, this was a useful preliminary experiment to indicate engraftment kinetics. While the information gathered from the flow cytometric analysis of the corneas was limited, it demonstrated the presence of substantial numbers of CD8⁺ T cells, monocytes, and macrophages confirming their involvement in the graft rejection as predicted. Due to lack of the ongoing availability of the 2C-TCR transgenic strain of mice, subsequent experiments used transgenic B6-CD2dsRed mice as donors. These mice have red fluorescent T cells which enabled us to visualise the

rejection process and the experimental end point was set as the point where roughly 50% of the graft surface area had been rejected.

The prolonged kinetics of graft rejection observed in this second experiment (Figure 4.13) were likely multifactorial: firstly the size of the donor grafts are significantly larger, covering not only the whole cornea but also forming multiple layers of epithelium; and secondly, the T cells used in this experiment had been expanded *in vitro* for specificity to BALB/c alloantigen from within a polyclonal T cell population. In comparison, T cells from the 2C-TCR strain express the transgenic T cell receptor with specificity for the mouse MHC Class I H-2L^d alloantigen. Since the dsRed T cells were pre-stimulated with allogeneic cells, an alloreactive effector cell population was expanded and transferred, whereas the 2C-TCR mice used previously were not pre-stimulated and so possessed alloreactive effector, memory, and naïve T cells. Technical difficulties with CD8 antibody staining during post rejection tissue analysis prevented the identification of T cells in the corneal tissue, possibly because CD8 can be cleaved off from T cells during collagenase digestion [147]. The majority of the dsRed⁻ CD11b⁺ population observed were likely endogenous NSG recipient cells, as although these are immunodeficient mice they possess neutrophils and monocytes as well as dendritic cells and macrophages, however these are functionally defective due to the NOD genetic background [148].

Adoptive transfer of primed CD8⁺ T cells along with APCs to immunodeficient allograft recipients successfully showed long term survival of the transferred T cells, as well as localisation to the allogeneic corneal epithelium and rapid onset of graft rejection within 7 days. Adoptive transfer of primed CD4⁺ T cells in similar conditions failed to provoke the same reaction, with no presence of transferred cells detected post-transplant and epithelial grafts continued to survive unaffected. Similar results were obtained with a combination of both CD4⁺ and CD8⁺ T cells were transferred, detecting only the presence of CD8⁺ in rejecting corneal epithelial allografts. The most likely explanation for these results is that the expanded CD4⁺ T cells did not survive the transfer process or engraftment into the host. Cell numbers and viability

were confirmed prior to injection, however as blood sampling was not performed during graft rejection, we cannot confirm T cell survival in these mice.

Graft rejection tracking through the use of fluorescent markers showed a clear pattern of CD8+ T cell localisation at the graft edge indicating entry to the cornea via conjunctival and limbal vasculature. It was interesting to note that the initial areas of graft loss were at the outer edge of the conjunctiva where neovascularisation mostly occurs, as these blood vessels provide access for circulating immune cells to reach the graft. As LSCD developed over time, increasing numbers of T cells were observed to be infiltrating into the centre of the cornea indicating that this was the predominant route of entry in this model, supporting the idea of migration of circulating T cells into the epithelial layer. Where initially this would occur at the vascularised limbus, in cases of LSCD where neovascularisation has developed the process is accelerated and infiltration may also invade through the corneal stroma [149]. Access to the epithelial layer is increasingly available as epithelial basement membrane becomes disrupted and discontinuous with the progression of rejection and redevelopment of LSCD. Limiting or halting neovascularisation in the cornea through the use of anti-angiogenic agents could form the basis of a potential new therapy to prevent graft rejection.

The essential role of LESC in corneal epithelial wound healing has been supported by a number of published studies [150-152]. When limbal cells are damaged or absent, wound healing in the cornea is altered or does not occur. Deficiencies of or damage to LESC result in partial or total LSCD. This leads to serious corneal problems, such as delayed wound healing, stromal neovascularization and ingrowth of conjunctival cells, which may ultimately cause corneal opacity and visual loss. Limbal transplantation is able to restore wound healing and epithelial resurfacing of the entire corneal epithelium, and removal of the central epithelium leads to complete wound repopulation by limbal cells. It should be noted that central corneal cells significantly contribute to healing of small wounds, but large wounds require limbal cell involvement, although it may be delayed for several days [153, 154]. Data from our model of LSCD show the complete removal of both central and limbal corneal

epithelial cells prevented any regeneration occurring, even when allowing for delayed responses, which resulted in the development of the LSCD phenotype.

Signals activating LESC activation, proliferation, differentiation, and migration into the wound site are poorly understood, and it is believed that growth factors, cytokines, and chemokines (including those secreted by infiltrating inflammatory cells and ECM degradation products) contribute to wound healing. Corneal epithelial damage triggers limbal fibroblasts to upregulate keratinocyte growth factor expression, which combined with elevated expression the KGF receptor, suggests a key role wound healing [64].

The tear film has an important role in normal homeostasis of the corneal epithelium, contributing to an extracellular microenvironment critical to functions including wound healing and inflammatory responses as the lacrimal fluid is known to contain both anti- and pro-inflammatory cytokines [155]. IL-6, a pro-inflammatory cytokine is produced by a variety of infiltrating immune cell types, particularly macrophages and monocytes, and is reported to be significantly elevated in patients with dry eye disease. This appears to support our data showing both significant increases in IL-6 levels detected by Luminex analysis of rejecting corneal tissue and the large infiltration of macrophages and monocytes into the same tissue by flow cytometry. While the role of IL-6 in inflammation is well established it has also been more recently reported that the involvement of both IL-6 and IL-10 in a human corneal epithelial wound healing response has been demonstrated [64], and that IL-6 enhances wound healing and cellular migration in a rabbit corneal epithelial cells while the anti-inflammatory cytokine IL-10 is elevated in human patients with corneal graft rejection [156-159]. In allogeneic transplanted mice we observed significant infiltration of multiple cell types including macrophages and monocytes as well as increases in both IL-6 and IL-10, pointing to the role IL-6 plays in cellular migration. In LSCD only controls, and mice which received autografts the same trend was not observed, with no significant increase in cellular infiltration and only increased IL-10 expression in the injury only controls.

6.3 Optimising culture, identification, and isolation of human LESC

The development of strategies to enrich LESC from human corneoscleral rims requires access to fresh tissue. Currently there is a global shortage of available tissue, and that which is sporadically available to the research community has often been stored in organ culture medium for excess of 4 weeks[103]. Most published literature regarding the LESC obtained from these rims used tissue obtained within several days of enucleation[104, 160], as it is known that the efficiency and success of limbal epithelial cell isolation is negatively impacted by long term storage[161, 162]. When digestion protocols described in the literature were used in this project the numbers of viable cells obtained were significantly lower than expected, likely due to prolonged storage of the corneal tissue. Originally, the aim had been to use freshly digested cells for enrichment to develop a simple, rapid strategy for isolating LESC. However, with low starting numbers of viable cells, subsequent flow cytometric analysis and enrichment proved technically challenging. After attempting several other protocols unsuccessfully, we adopted the explant culture method to generate larger quantities of cells for experimental use. However again we faced technical challenges such as cells growing slowly, exhibiting a differentiated phenotype, and half of all seeded cultures never sprouting from the original limbal explant segment; likely another consequence of using older stored tissue. This approach continued to be used until the optimisation of trypsin digestion and feeder subculture method began to produce large healthy cultures of viable, undifferentiated, corneal epithelial cells. It was determined that this protocol will be used for all future experiments.

The supernatant concentrations of 40 different inflammatory chemokines from *in vitro* cultures of primary human corneal epithelial and stromal cells were analysed by Luminex immunoassay in a similar experiment shown in Figure 3.13. Some differences were observed between mouse and human corneal cell responses to inflammatory cytokine stimulation, for example concentrations of CXCL1 and CCL2 were significantly higher in mouse stromal cultures compared to epithelial, whereas in human cells the opposite was true. It should be noted that in the cultures where statistically significant differences were detected, basal expression was higher in

stromal cultures compared to epithelial, pointing to a more significant role of neutrophil and leukocyte recruitment for the corneal stroma during LSCD which is as expected given the absence of epithelium in this injury.

Percoll density gradients have been successfully used to isolate LSCs from mouse cornea by other investigators, however this method has not been published for human cells. Our results support the hypothesis that human LSCs can be collected within the 80% Percoll gradient fraction, however firm conclusions cannot be drawn at this time as further investigation is needed. The results of the colony forming efficiency (CFE) assay indicated twice as many holoclone-like cells were present in the target fraction compared to the control, although colony numbers were very small and these results may be unreliable. In future experiments, greater starting numbers of viable cells should be plated in a larger 10cm dish at a higher density rather than the 6-well plates we used, in order to allow for an improved chance of forming holoclones rather than the larger, more differentiated para- or meroclones. Furthermore the identification of true holoclones requires sub-culture of single cells harvested from these first holoclone-like colonies, a step which should be included for future CFE assays.

ABCB5 is a limbal stem cell gene required for corneal development and repair, as reported by Ksander *et al.* (2014)[17]. The expression of ABCB5 in the limbus, its key role in LESC function, and requirement for restoration of the corneal epithelium in a mouse model of CLET have all been demonstrated in several publications from this same group. These results were demonstrated using a specific monoclonal antibody developed in their own laboratory, however it is currently commercially unavailable.

Despite the potential of ABCB5, the reproducibility of results from these publications has been limited. It is worth noting that data from the same authors sheds doubt on the role in stem cell and tissue maintenance, as ABCB5 knockout mice did not show epithelial repair defects or the absence of corneal epithelium [29]. Furthermore, RNA sequencing analysis of slow cycling cells isolated from a transgenic mouse model by Sartaj *et al.* (2017) did not identify ABCB5 within this population [163]. We were also

unable to identify ABCB5 expression in our enriched LESC populations despite using three different commercially available polyclonal rabbit antibodies and were therefore unable to corroborate the findings.

The use of these antibodies resulted in a high degree of non-specific and background staining possibly due to the presence of large, differentiated cells present normally on the surface of the cornea. These cells tend to stain positive for most markers regardless of their true phenotype, and so their presence may partially explain the ABCB5 staining profile we observed. We also included intracellular PAX6 analysis which is established as a reliable marker of LESC and to provide sufficient cells for accurate flow cytometric analysis we pooled cells isolated from three separate experiments [164, 165]. However, we were unable to detect PAX6⁺ within the ABCB5⁺ population most likely due to the large quantity of dead or differentiated cells also present in the sample, therefore no firm conclusions can be drawn at this time as the data is very preliminary.

The preliminary qPCR analysis performed on explant cultured cells enriched by MACS depletion was used to investigate the efficiency of each method and the results demonstrated increased expression of several LESC genes. We had planned to perform flow cytometric cell sorting of LESC as a suitable robustly expressed cell surface marker had been identified. Unfortunately, we were not able to optimise staining for ABCB5 as our candidate marker based on previous publications, so turned our focus to CD200. Data from flow cytometry screening of an expanded population of limbal epithelial cells proposed the cell surface marker CD200 as a novel proliferative marker of LESC, expressing several established markers including ΔNp63, as well as exhibiting holoclone forming efficiency *in vitro* [18]. Due to time constraints we only had time to perform a single experiment using this antibody and staining protocol. Future work should develop improved trypsin digestion and subculture methods for producing large numbers of epithelial cells to allow better comparison between enrichment methods by qPCR and flow cytometry.

Being able to visualise, transplant, and image the growth of human corneal epithelial cells in our humanised mouse model was essential. This can be done using tracer dyes such as CFSE, however their brightness is reduced with every cell division so typically only lasts several generations. An excellent alternative was to transduce the cells to stably express GFP. Given the shortage of human tissue available we initially attempted this using the hTCEpi immortalised cell line and achieved an excellent transduction efficiency. However, when transplanted as either a suspension or cultured on fibrin gels, we could not achieve durable engraftment. The reasons for this were unclear since the cells adhered and grew rapidly on untreated tissue culture plastic, and with up to 1 million cells were grafted to a single recipient cornea protected by fixed mouse contact lenses during engraftment. We speculate that perhaps these cells are more susceptible to the inflammatory environment than the successful mouse epithelial sheets, or possibly the absence of primary LESC in the immortalised cell line cultures prevents engraftment. Future experiments to establish *in vitro* co-cultures between the mouse stromal cells and human hTCEpi epithelium, stimulated with inflammatory cytokines could help identify the cause, and further analysis by flow cytometry and qPCR is needed to understand the phenotype of this cell line.

The transduction of actively growing limbal explants, if successful, could be extremely useful for generating large numbers of GFP⁺ cells, however despite using extremely high concentration of lentivirus we failed to transduce the proliferating LESC in *in vitro* cultures. The transduction of trypsin digested cells in early stages of culture showed potential, and although only 20% of cells expressed GFP at an MOI = 1 these cells were sorted by flow cytometry and reseeded for further culture. Although using a higher MOI resulted in greater transduction efficiency, cultures with an MOI of >5 produced significantly fewer viable cells. While this entire process was lengthy, it provided large cultures of GFP⁺ epithelial cultures for transplantation without the need for CFSE labelling.

The qPCR data presented demonstrated a large increase in expression of LESC markers after sorting on CD200 expressing cells. When these were grafted into the

humanised mouse using the suspension transplant method there was surprisingly no observable difference in engraftment success or prevention of LSCD onset between the positive and negative populations.

CHAPTER 7. CONCLUSIONS

We hypothesised that a combination of intrinsic (graft related) and extrinsic (recipient microenvironment and immunological) factors determine the success of LESC transplant engraftment and ocular surface regeneration. Three primary aims were established in order to investigate this effectively.

Firstly, we aimed to develop a mouse model of LSCD. In summary, we have successfully developed a simple, novel method for induction of LSCD which results the same clinical injury phenotype observed in human patients, including epithelial defects, neovascularisation, cellular infiltration, conjunctival migration, and inflammatory mediator secretion. Furthermore, transplantation of donor derived epithelial sheets containing LESC to the injured corneas is capable of regenerating the lost epithelial surface and reversing the LSCD phenotype in this mouse model. The use of fluorescently labelled donor epithelial cells allowed visualisation and tracking of engraftment and growth kinetics as LESC repair the damaged mouse cornea. Publication of this model and data will aid continued research into the understanding of LSCD and LESC transplantation.

Secondly, we wished to investigate the role of the innate and adaptive immune response to allogeneic LESC grafts. Transplantation into fully immunocompetent recipient mice demonstrated characteristic signs of early corneal graft rejection, and flow cytometric analysis detailed significant cellular infiltration into the allografted eye along with identification of cytokines and chemokines of the inflammatory microenvironment present during rejection. This is important as it will allow researchers to interrogate the immune response while developing strategies for suppression or amelioration. Examples of further experimentation could include potential therapies such as the use of a neutrophil blocking antibody to prevent neutrophil recruitment in the cornea during injury, or VEGF blocking antibody to inhibit neovascularisation in response to LSCD inflammation. Our use of adoptive transfer experiments allowed some progress to be made into further understanding the cell types involved in the allograft rejection mechanism, by transferring purified

activated T cell subsets (CD8+ and CD4+) into immunodeficient recipient mice with corneal allografts. Unfortunately, several technical issues hindered these experiments and limit the conclusions which can be drawn until protocol optimisation can be achieved.

Finally, we were also interested in identifying the variables which determine LESC transplant success, such as stem cell content and graft composition. Strategies to investigate this revolved around optimising a protocol for the digestion, isolation, and culture of LESC from primary human corneal tissue. Using a trypsin digestion-based protocol produced large quantities of human epithelial and stromal cells for analysis *in vitro* which determined a significant increase in expression of chemoattractants in response to stimulation by pro-inflammatory cytokines, which was in line with similar results obtained from mouse cells. Optimising methods of isolating and enriching LESC from corneal digests proved to be a major technical challenge, which together with a general shortage of available human corneal tissue limited progression on achieving this aim. Enrichment of LESC populations by sorting for the novel marker CD200 allowed us to attempt transplantation into a humanised NSG mouse model, however no long-term engraftment of human cells was observed and there was no marked reduction in corneal inflammation or LSCD severity. This is an exciting potential avenue to pursue, as the prospect of a readily available cell surface marker for LESC would greatly improve isolation protocols for generating CLET sheets with higher stem cell content. One further suggestion for future experiments is that digested human corneal epithelial cells could be sorted by flow cytometry for expression of proposed LESC markers such as ABCB5 and CD200. These sub-populations could then be analysed by more sensitive methods to account for extremely low cell numbers, for example RNA sequencing to determine the genetic profile and relation to putative intracellular markers of LESC.

In summary, excellent progress has been made in understanding the role of inflammation and the immune system in graft rejection and despite several technical challenges the mouse model of LSCD and LESC transplantation shows great potential for further advancement of the field.

CHAPTER 8. BIBLIOGRAPHY

- [1] Rolfsen, M.L., Frisard, N.E., Stern, E.M., Foster, T.P., Bhattacharjee, P.S., McFerrin Jr, H.E., Clement, C., Rodriguez, P.C., Lukiw, W.J., Bergsma, D.R., *et al.* (2013). Corneal neovascularization: a review of the molecular biology and current therapies. *Expert Review of Ophthalmology* 8, 167-189.
- [2] Shaharuddin, B., Ahmad, S., Meeson, A., and Ali, S. (2013). Concise review: immunological properties of ocular surface and importance of limbal stem cells for transplantation. *Stem cells translational medicine* 2, 614-624.
- [3] Müller, L.J., Marfurt, C.F., Kruse, F., and Tervo, T.M. (2003). Corneal nerves: structure, contents and function. *Exp Eye Res* 76, 521-542.
- [4] Thoft, R.A., and Friend, J. (1983). The X, Y, Z hypothesis of corneal epithelial maintenance. *Investigative ophthalmology & visual science* 24, 1442-1443.
- [5] Shortt, A.J., Secker, G.A., Munro, P.M., Khaw, P.T., Tuft, S.J., and Daniels, J.T. (2007). Characterization of the limbal epithelial stem cell niche: novel imaging techniques permit in vivo observation and targeted biopsy of limbal epithelial stem cells. *Stem cells (Dayton, Ohio)* 25, 1402-1409.
- [6] Grieve, K., Ghoubay, D., Georgeon, C., Thouvenin, O., Bouheraoua, N., Paques, M., and Borderie, V.M. (2015). Three-dimensional structure of the mammalian limbal stem cell niche. *Experimental Eye Research* 140, 75-84.
- [7] Bath, C., Yang, S., Muttuvelu, D., Fink, T., Emmersen, J., Vorum, H., Hjortdal, J., and Zachar, V. (2013). Hypoxia is a key regulator of limbal epithelial stem cell growth and differentiation. *Stem Cell Research* 10, 349-360.
- [8] Notara, M., Alatza, A., Gilfillan, J., Harris, A.R., Levis, H.J., Schrader, S., Vernon, A., and Daniels, J.T. (2010). In sickness and in health: Corneal epithelial stem cell biology, pathology and therapy. *Experimental Eye Research* 90, 188-195.
- [9] Romano, A.C., Espana, E.M., Yoo, S.H., Budak, M.T., Wolosin, J.M., and Tseng, S.C.G. (2003). Different Cell Sizes in Human Limbal and Central Corneal Basal Epithelia Measured by Confocal Microscopy and Flow Cytometry. *Investigative ophthalmology & visual science* 44, 5125-5129.
- [10] Cotsarelis, G., Cheng, S.-Z., Dong, G., Sun, T.-T., and Lavker, R.M. (1989). Existence of slow-cycling limbal epithelial basal cells that can be preferentially stimulated to proliferate: Implications on epithelial stem cells. *Cell* 57, 201-209.
- [11] Chen, Z., Evans, W.H., Pflugfelder, S.C., and Li, D.Q. (2006). Gap junction protein connexin 43 serves as a negative marker for a stem cell-containing population of human limbal epithelial cells. *Stem cells (Dayton, Ohio)* 24, 1265-1273.
- [12] Chen, Z., de Paiva, C.S., Luo, L., Kretzer, F.L., Pflugfelder, S.C., and Li, D.Q. (2004). Characterization of putative stem cell phenotype in human limbal epithelia. *Stem cells (Dayton, Ohio)* 22, 355-366.

- [13] Barbaro, V., Testa, A., Di Iorio, E., Mavilio, F., Pellegrini, G., and De Luca, M. (2007). C/EBP δ regulates cell cycle and self-renewal of human limbal stem cells. *The Journal of cell biology* 177, 1037-1049.
- [14] Schlötzer-Schrehardt, U., and Kruse, F.E. (2005). Identification and characterization of limbal stem cells. *Experimental Eye Research* 81, 247-264.
- [15] de Paiva, C.S., Chen, Z., Corrales, R.M., Pflugfelder, S.C., and Li, D.-Q. (2005). ABCG2 Transporter Identifies a Population of Clonogenic Human Limbal Epithelial Cells. *Stem cells (Dayton, Ohio)* 23, 63-73.
- [16] Di Iorio, E., Barbaro, V., Ruzza, A., Ponzin, D., Pellegrini, G., and De Luca, M. (2005). Isoforms of DeltaNp63 and the migration of ocular limbal cells in human corneal regeneration. *Proceedings of the National Academy of Sciences of the United States of America* 102, 9523-9528.
- [17] Ksander, B.R., Kolovou, P.E., Wilson, B.J., Saab, K.R., Guo, Q., Ma, J., McGuire, S.P., Gregory, M.S., Vincent, W.J.B., Perez, V.L., *et al.* (2014). ABCB5 is a limbal stem cell gene required for corneal development and repair. *Nature* 511, 353-357.
- [18] Bojic, S., Hallam, D., Alcada, N., Ghareeb, A., Queen, R., Pervinder, S., Buck, H., Amitai Lange, A., Figueiredo, G., Rooney, P., *et al.* (2018). CD200 Expression Marks a Population of Quiescent Limbal Epithelial Stem Cells with Holoclone Forming Ability. *Stem cells (Dayton, Ohio)* 36, 1723-1735.
- [19] Rosenblum, M.D., Olasz, E.B., Yancey, K.B., Woodliff, J.E., Lazarova, Z., Gerber, K.A., and Truitt, R.L. (2004). Expression of CD200 on epithelial cells of the murine hair follicle: a role in tissue-specific immune tolerance? *The Journal of investigative dermatology* 123, 880-887.
- [20] Nubile, M., Curcio, C., Dua, H.S., Calienno, R., Lanzini, M., Iezzi, M., Mastropasqua, R., Agnifili, L., and Mastropasqua, L. (2013). Pathological changes of the anatomical structure and markers of the limbal stem cell niche due to inflammation. *Mol Vis* 19, 516-525.
- [21] Hayashi, R., Yamato, M., Sugiyama, H., Sumide, T., Yang, J., Okano, T., Tano, Y., and Nishida, K. (2007). N-Cadherin Is Expressed by Putative Stem/Progenitor Cells and Melanocytes in the Human Limbal Epithelial Stem Cell Niche. *Stem cells (Dayton, Ohio)* 25, 289-296.
- [22] Dziasko, M.A., Armer, H.E., Levis, H.J., Shortt, A.J., Tuft, S., and Daniels, J.T. (2014). Localisation of Epithelial Cells Capable of Holoclone Formation In Vitro and Direct Interaction with Stromal Cells in the Native Human Limbal Crypt. *PLoS ONE* 9, e94283.
- [23] Vazirani, J., Nair, D., Shanbhag, S., Wurity, S., Ranjan, A., and Sangwan, V. (2018). Limbal Stem Cell Deficiency - Demography And Underlying Causes. *Am J Ophthalmol*.

- [24] Agency, E.M. (2015). Ex vivo expanded autologous human corneal epithelium containing stem cells for the treatment of corneal lesions, with associated corneal (limbal) stem cell deficiency, due to ocular burns.
- [25] Bobba, S., Di Girolamo, N., Mills, R., Daniell, M., Chan, E., Harkin, D.G., Cronin, B.G., Crawford, G., McGhee, C., and Watson, S. (2017). Nature and incidence of severe limbal stem cell deficiency in Australia and New Zealand. *Clinical & Experimental Ophthalmology* 45, 174-181.
- [26] Ghareeb, A.E., Lako, M., and Figueiredo, F.C. (2020). Recent Advances in Stem Cell Therapy for Limbal Stem Cell Deficiency: A Narrative Review. *Ophthalmology and Therapy* 9, 809-831.
- [27] Niederkorn, J.Y. (2013). Corneal Transplantation and Immune Privilege. *International reviews of immunology* 32, 10.3109/08830185.08832012.08737877.
- [28] Shortt, A.J., Secker, G.A., Rajan, M.S., Meligonis, G., Dart, J.K., Tuft, S.J., and Daniels, J.T. (2008). Ex vivo expansion and transplantation of limbal epithelial stem cells. *Ophthalmology* 115, 1989-1997.
- [29] Pellegrini, G., Lambiase, A., Macaluso, C., Pocobelli, A., Deng, S., Cavallini, G.M., Esteki, R., and Rama, P. (2016). From discovery to approval of an advanced therapy medicinal product-containing stem cells, in the EU. *Regenerative Medicine* 11, 407-420.
- [30] Kheirkhah, A., Raju, V.K., and Tseng, S.C.G. (2008). Minimal conjunctival limbal autograft for total limbal stem cell deficiency. *Cornea* 27, 730-733.
- [31] Sangwan, V.S., Basu, S., MacNeil, S., and Balasubramanian, D. (2012). Simple limbal epithelial transplantation (SLET): a novel surgical technique for the treatment of unilateral limbal stem cell deficiency. *The British journal of ophthalmology* 96, 931-934.
- [32] Imanishi, J., Kamiyama, K., Iguchi, I., Kita, M., Sotozono, C., and Kinoshita, S. (2000). Growth factors: importance in wound healing and maintenance of transparency of the cornea. *Progress in Retinal and Eye Research* 19, 113-129.
- [33] Shortt, A.J., Tuft, S.J., and Daniels, J.T. (2011). Corneal stem cells in the eye clinic. *British medical bulletin* 100, 209-225.
- [34] Sangwan, V., Jain, R., Basu, S., Bagadi, A., Sureka, S., Mariappan, I., and MacNeil, S. (2014). Transforming ocular surface stem cell research into successful clinical practice. *Indian Journal of Ophthalmology* 62, 29-40.
- [35] Shortt, A.J., Bunce, C., Levis, H.J., Blows, P., Dore, C.J., Vernon, A., Secker, G.A., Tuft, S.J., and Daniels, J.T. (2014). Three-year outcomes of cultured limbal epithelial allografts in aniridia and Stevens-Johnson syndrome evaluated using the Clinical Outcome Assessment in Surgical Trials assessment tool. *Stem cells translational medicine* 3, 265-275.
- [36] Shortt, A.J., Tuft, S.J., and Daniels, J.T. (2010). Ex vivo cultured limbal epithelial transplantation. A clinical perspective. *The ocular surface* 8, 80-90.

- [37] Eslani, M., Haq, Z., Movahedan, A., Moss, A., Baradaran-Rafii, A., Mogilishetty, G., Holland, E.J., and Djalilian, A.R. (2017). Late Acute Rejection After Allograft Limbal Stem Cell Transplantation: Evidence for Long-Term Donor Survival. *Cornea* 36, 26-31.
- [38] Rama, P., Matuska, S., Paganoni, G., Spinelli, A., De Luca, M., and Pellegrini, G. (2010). Limbal Stem-Cell Therapy and Long-Term Corneal Regeneration. *New England Journal of Medicine* 363, 147-155.
- [39] Lencova, A., Pokorna, K., Zajicova, A., Krulova, M., Filipec, M., and Holan, V. (2011). Graft survival and cytokine production profile after limbal transplantation in the experimental mouse model. *Transplant immunology* 24, 189-194.
- [40] Maruyama, K., Yamada, J., Sano, Y., and Kinoshita, S. (2003). Th2-Biased Immune System Promotion of Allogeneic Corneal Epithelial Cell Survival after Orthotopic Limbal Transplantation. *Investigative ophthalmology & visual science* 44, 4736-4741.
- [41] Mills, R.A.D., Coster, D.J., and Williams, K.A. (2002). Effect of Immunosuppression on Outcome Measures in a Model of Rat Limbal Transplantation. *Investigative ophthalmology & visual science* 43, 647-655.
- [42] Swift, G.J., Aggarwal, R.K., Davis, G.J., Coster, D.J., and Williams, K.A. (1996). Survival of rabbit limbal stem cell allografts. *Transplantation* 62, 568-574.
- [43] Xu, K.P., Wu, Y., Zhou, J., and Zhang, X. (1999). Survival of rabbit limbal stem cell allografts after administration of cyclosporin A. *Cornea* 18, 459-465.
- [44] Sanchez, R.F., and Daniels, J.T. (2016). Mini-Review: Limbal Stem Cells Deficiency in Companion Animals: Time to Give Something Back? *Current Eye Research* 41, 425-432.
- [45] Hovav, A.H. (2018). Mucosal and Skin Langerhans Cells - Nurture Calls. *Trends in immunology* 39, 788-800.
- [46] Liu, J., and Li, Z. (2021). Resident Innate Immune Cells in the Cornea. *Frontiers in Immunology* 12.
- [47] Acuto, O., and Michel, F. (2003). CD28-mediated co-stimulation: a quantitative support for TCR signalling. *Nature Reviews Immunology* 3, 939-951.
- [48] Ayala García, M.A., González Yebra, B., López Flores, A.L., and Guaní Guerra, E. (2012). The Major Histocompatibility Complex in Transplantation. *Journal of Transplantation* 2012, 842141.
- [49] Samelson, L.E. (2011). Immunoreceptor signaling. *Cold Spring Harb Perspect Biol* 3, a011510.
- [50] Wong, P., and Pamer, E.G. (2003). CD8 T Cell Responses to Infectious Pathogens. *Annual review of immunology* 21, 29-70.
- [51] Luckheeram, R.V., Zhou, R., Verma, A.D., and Xia, B. (2012). CD4⁺T cells: differentiation and functions. *Clin Dev Immunol* 2012, 925135-925135.

- [52] Stein-Streilein, J. (2008). Immune regulation and the eye. *Trends in immunology* 29, 548-554.
- [53] Griffith, T.S., Brunner, T., Fletcher, S.M., Green, D.R., and Ferguson, T.A. (1995). Fas ligand-induced apoptosis as a mechanism of immune privilege. *Science* (New York, NY) 270, 1189-1192.
- [54] Sugita, S., Futagami, Y., Smith, S.B., Naggar, H., and Mochizuki, M. (2006). Retinal and ciliary body pigment epithelium suppress activation of T lymphocytes via transforming growth factor beta. *Exp Eye Res* 83, 1459-1471.
- [55] Sugita, S., Ng, T.F., Lucas, P.J., Gress, R.E., and Streilein, J.W. (2006). B7+ iris pigment epithelium induce CD8+ T regulatory cells; both suppress CTLA-4+ T cells. *Journal of immunology* (Baltimore, Md : 1950) 176, 118-127.
- [56] Medawar, P.B. (1948). Immunity to homologous grafted skin; the fate of skin homografts transplanted to the brain, to subcutaneous tissue, and to the anterior chamber of the eye. *British journal of experimental pathology* 29, 58-69.
- [57] Cousins, S.W., Trattler, W.B., and Streilein, J.W. (1991). Immune privilege and suppression of immunogenic inflammation in the anterior chamber of the eye. *Curr Eye Res* 10, 287-297.
- [58] Hori, J. (2008). Mechanisms of immune privilege in the anterior segment of the eye: what we learn from corneal transplantation. *Journal of Ocular Biology, Diseases, and Informatics* 1, 94-100.
- [59] Niederkorn, J.Y., and Mellon, J. (1996). Anterior chamber-associated immune deviation promotes corneal allograft survival. *Investigative ophthalmology & visual science* 37, 2700-2707.
- [60] Hori, J., Taniguchi, H., Wang, M., Oshima, M., and Azuma, M. (2010). GITR ligand-mediated local expansion of regulatory T cells and immune privilege of corneal allografts. *Investigative ophthalmology & visual science* 51, 6556-6565.
- [61] Cunnusamy, K., Paunicka, K., Reyes, N., Yang, W., Chen, P.W., and Niederkorn, J.Y. (2010). Two different regulatory T cell populations that promote corneal allograft survival. *Investigative ophthalmology & visual science* 51, 6566-6574.
- [62] Cunnusamy, K., Chen, P.W., and Niederkorn, J.Y. (2010). IL-17 promotes immune privilege of corneal allografts. *Journal of immunology* (Baltimore, Md : 1950) 185, 4651-4658.
- [63] McDermott, A.M. (2013). Antimicrobial compounds in tears. *Experimental Eye Research* 117, 53-61.
- [64] Ljubimov, A.V., and Saghizadeh, M. (2015). Progress in corneal wound healing. *Progress in Retinal and Eye Research* 49, 17-45.
- [65] Lee, H.T., Lee, J.G., Na, M., and Kay, E.P. (2004). FGF-2 Induced by Interleukin-1 β ; through the Action of Phosphatidylinositol 3-Kinase Mediates

Endothelial Mesenchymal Transformation in Corneal Endothelial Cells *. *Journal of Biological Chemistry* 279, 32325-32332.

[66] Seghezzi, G., Patel, S., Ren, C.J., Gualandris, A., Pintucci, G., Robbins, E.S., Shapiro, R.L., Galloway, A.C., Rifkin, D.B., and Mignatti, P. (1998). Fibroblast growth factor-2 (FGF-2) induces vascular endothelial growth factor (VEGF) expression in the endothelial cells of forming capillaries: an autocrine mechanism contributing to angiogenesis. *The Journal of cell biology* 141, 1659-1673.

[67] Tran, M.T., Tellaetxe-Isusi, M., Elnor, V., Strieter, R.M., Lausch, R.N., and Oakes, J.E. (1996). Proinflammatory cytokines induce RANTES and MCP-1 synthesis in human corneal keratocytes but not in corneal epithelial cells. Beta-chemokine synthesis in corneal cells. *Investigative ophthalmology & visual science* 37, 987-996.

[68] Hamrah, P., Yamagami, S., Liu, Y., Zhang, Q., Vora, S.S., Lu, B., Gerard, C.J., and Dana, M.R. (2007). Deletion of the Chemokine Receptor CCR1 Prolongs Corneal Allograft Survival. *Investigative ophthalmology & visual science* 48, 1228-1236.

[69] Kumbala, D., and Zhang, R. (2013). Essential concept of transplant immunology for clinical practice. *World J Transplant* 3, 113-118.

[70] Lakkis, F.G., and Sayegh, M.H. (2003). Memory T cells: a hurdle to immunologic tolerance. *Journal of the American Society of Nephrology : JASN* 14, 2402-2410.

[71] Opelz, G., Wujciak, T., Döhler, B., Scherer, S., and Mytilineos, J. (1999). HLA compatibility and organ transplant survival. Collaborative Transplant Study. *Reviews in immunogenetics* 1, 334-342.

[72] Warren, E.H., Greenberg, P.D., and Riddell, S.R. (1998). Cytotoxic T-lymphocyte-defined human minor histocompatibility antigens with a restricted tissue distribution. *Blood* 91, 2197-2207.

[73] Boardman, D.A., Jacob, J., Smyth, L.A., Lombardi, G., and Lechler, R.I. (2016). What Is Direct Allorecognition? *Curr Transplant Rep* 3, 275-283.

[74] Veerapathran, A., Pidala, J., Beato, F., Yu, X.Z., and Anasetti, C. (2011). Ex vivo expansion of human Tregs specific for alloantigens presented directly or indirectly. *Blood* 118, 5671-5680.

[75] Benichou, G., Gonzalez, B., Marino, J., Ayasoufi, K., and Valujskikh, A. (2017). Role of Memory T Cells in Allograft Rejection and Tolerance. *Frontiers in Immunology* 8.

[76] Lonsdorf, A.S., Hwang, S.T., and Enk, A.H. (2009). Chemokine Receptors in T-Cell-Mediated Diseases of the Skin. *Journal of Investigative Dermatology* 129, 2552-2566.

[77] Rosenberg, A.S., and Singer, A. (1992). Cellular basis of skin allograft rejection: an in vivo model of immune-mediated tissue destruction. *Annual review of immunology* 10, 333-358.

- [78] Boisg rault, F., Liu, Y., Anosova, N., Ehrlich, E., Dana, M.R., and Benichou, G. (2001). Role of CD4+ and CD8+ T Cells in Allorecognition: Lessons from Corneal Transplantation. *The Journal of Immunology* 167, 1891-1899.
- [79] He, Y.G., Ross, J., and Niederkorn, J.Y. (1991). Promotion of murine orthotopic corneal allograft survival by systemic administration of anti-CD4 monoclonal antibody. *Investigative ophthalmology & visual science* 32, 2723-2728.
- [80] Yamada, J., Ksander, B.R., and Streilein, J.W. (2001). Cytotoxic T Cells Play No Essential Role in Acute Rejection of Orthotopic Corneal Allografts in Mice. *Investigative ophthalmology & visual science* 42, 386-392.
- [81] Hegde, S., and Niederkorn, J.Y. (2000). The Role of Cytotoxic T Lymphocytes in Corneal Allograft Rejection. *Investigative ophthalmology & visual science* 41, 3341-3347.
- [82] Ksander, B.R., Sano, Y., and Streilein, J.W. (1996). Role of donor-specific cytotoxic T cells in rejection of corneal allografts in normal and high-risk eyes. *Transplant immunology* 4, 49-52.
- [83] Niederkorn, J.Y., Stevens, C., Mellon, J., and Mayhew, E. (2006). Differential Roles of CD8+ and CD8- T Lymphocytes in Corneal Allograft Rejection in 'High-Risk' Hosts. *American Journal of Transplantation* 6, 705-713.
- [84] Niederkorn, J.Y., Stevens, C., Mellon, J., and Mayhew, E. (2006). CD4+ T-Cell-Independent Rejection of Corneal Allografts. *Transplantation* 81, 1171-1178.
- [85] Yamada, J., Kurimoto, I., and Streilein, J.W. (1999). Role of CD4+ T Cells in Immunobiology of Orthotopic Corneal Transplants in Mice. *Investigative ophthalmology & visual science* 40, 2614-2621.
- [86] Goslings, W.R., Yamada, J., Dana, M.R., Streilein, J.W., van Beelen, E., Prodeus, A.P., Carroll, M.C., and Jager, M.J. (1999). Corneal transplantation in antibody-deficient hosts. *Investigative ophthalmology & visual science* 40, 250-253.
- [87] Hegde, S., Mellon, J.K., Hargrave, S.L., and Niederkorn, J.Y. (2002). Effect of alloantibodies on corneal allograft survival. *Investigative ophthalmology & visual science* 43, 1012-1018.
- [88] Wynn, T.A., Chawla, A., and Pollard, J.W. (2013). Macrophage biology in development, homeostasis and disease. *Nature* 496, 445-455.
- [89] Brissette-Storkus, C.S., Reynolds, S.M., Lepisto, A.J., and Hendricks, R.L. (2002). Identification of a Novel Macrophage Population in the Normal Mouse Corneal Stroma. *Investigative ophthalmology & visual science* 43, 2264-2271.
- [90] Yamagami, S., Ebihara, N., Usui, T., Yokoo, S., and Amano, S. (2006). Bone Marrow-Derived Cells in Normal Human Corneal Stroma. *JAMA Ophthalmology* 124, 62-69.
- [91] Yamamoto, N., Einaga-Naito, K., Kuriyama, M., Kawada, Y., and Yoshida, R. (1998). CELLULAR BASIS OF SKIN ALLOGRAFT REJECTION IN MICE: Specific Lysis of Allogeneic Skin Components by Non-T cells¹. *Transplantation* 65, 818-825.

- [92] Slegers, T.P.A.M., Torres, P.F., Broersma, L., van Rooijen, N., van Rij, G., and van der Gaag, R. (2000). Effect of Macrophage Depletion on Immune Effector Mechanisms during Corneal Allograft Rejection in Rats. *Investigative ophthalmology & visual science* *41*, 2239-2247.
- [93] Mayadas, T.N., Cullere, X., and Lowell, C.A. (2014). The Multifaceted Functions of Neutrophils. *Annual Review of Pathology: Mechanisms of Disease* *9*, 181-218.
- [94] Edwards, S. (1994). The development and structure of mature neutrophils. In *Biochemistry and Physiology of the Neutrophil*, S.W. Edwards, ed. (Cambridge: Cambridge University Press), pp. 33-76.
- [95] Summers, C., Rankin, S.M., Condliffe, A.M., Singh, N., Peters, A.M., and Chilvers, E.R. (2010). Neutrophil kinetics in health and disease. *Trends in immunology* *31*, 318-324.
- [96] Yang, F., Feng, C., Zhang, X., Lu, J., and Zhao, Y. (2017). The Diverse Biological Functions of Neutrophils, Beyond the Defense Against Infections. *Inflammation* *40*, 311-323.
- [97] Braza, F., Brouard, S., Chadban, S., and Goldstein, D.R. (2016). Role of TLRs and DAMPs in allograft inflammation and transplant outcomes. *Nature reviews Nephrology* *12*, 281-290.
- [98] Leliefeld, P.H., Koenderman, L., and Pillay, J. (2015). How Neutrophils Shape Adaptive Immune Responses. *Front Immunol* *6*, 471.
- [99] Jones, N.D., Brook, M.O., Carvalho-Gaspar, M., Luo, S., and Wood, K.J. (2010). Regulatory T cells can prevent memory CD8+ T-cell-mediated rejection following polymorphonuclear cell depletion. *European journal of immunology* *40*, 3107-3116.
- [100] Mandal, A., and Viswanathan, C. (2015). Natural killer cells: In health and disease. *Hematology/Oncology and Stem Cell Therapy* *8*, 47-55.
- [101] Glas, R., Franksson, L., Une, C., Eloranta, M.-L., Öhlén, C., Örn, A., and Kärre, K. (2000). Recruitment and Activation of Natural Killer (Nk) Cells in Vivo Determined by the Target Cell Phenotype: An Adaptive Component of Nk Cell-Mediated Responses. *Journal of Experimental Medicine* *191*, 129-138.
- [102] Niederkorn, J.Y. (2010). Chapter Twenty-Nine - NK cells in the eye. In *Natural Killer Cells*, M.T. Lotze, and A.W. Thomson, eds. (San Diego: Academic Press), pp. 385-401.
- [103] Tovell, V.E., Massie, I., Kureshi, A.K., and Daniels, J.T. (2015). Functional limbal epithelial cells can be successfully isolated from organ culture rims following long-term storage. *Investigative ophthalmology & visual science* *56*, 3531-3540.
- [104] Zhang, Z.-H., Liu, H.-Y., Liu, K., and Xu, X. (2016). Comparison of Explant and Enzyme Digestion Methods for Ex Vivo Isolation of Limbal Epithelial Progenitor Cells. *Current Eye Research* *41*, 318-325.

- [105] Tananuvat, N., Bumroongkit, K., Tocharusa, C., Mevatee, U., Kongkaew, A., and Ausayakhun, S. (2017). Limbal stem cell and oral mucosal epithelial transplantation from ex vivo cultivation in LSCD-induced rabbits: histology and immunologic study of the transplant epithelial sheet. *International Ophthalmology* 37, 1289-1298.
- [106] Ti, S.-E., Anderson, D., Touhami, A., Kim, C., and Tseng, S.C.G. (2002). Factors Affecting Outcome Following Transplantation of Ex vivo Expanded Limbal Epithelium on Amniotic Membrane for Total Limbal Deficiency in Rabbits. *Investigative ophthalmology & visual science* 43, 2584-2592.
- [107] Lin, Z., He, H., Zhou, T., Liu, X., Wang, Y., He, H., Wu, H., and Liu, Z. (2013). A Mouse Model of Limbal Stem Cell Deficiency Induced by Topical Medication With the Preservative Benzalkonium Chloride. *Investigative ophthalmology & visual science* 54, 6314-6325.
- [108] Richardson, A., Park, M., Watson, S.L., Wakefield, D., and Di Girolamo, N. (2018). Visualizing the Fate of Transplanted K14-Confetti Corneal Epithelia in a Mouse Model of Limbal Stem Cell Deficiency. *Investigative ophthalmology & visual science* 59, 1630-1640.
- [109] Soma, T., Hayashi, R., Sugiyama, H., Tsujikawa, M., Kanayama, S., Oie, Y., and Nishida, K. (2014). Maintenance and Distribution of Epithelial Stem/Progenitor Cells after Corneal Reconstruction Using Oral Mucosal Epithelial Cell Sheets. *PLOS ONE* 9, e110987.
- [110] Kethiri, A.R., Raju, E., Bokara, K.K., Mishra, D.K., Basu, S., Rao, C.M., Sangwan, V.S., and Singh, V. (2019). Inflammation, vascularization and goblet cell differences in LSCD: Validating animal models of corneal alkali burns. *Experimental Eye Research* 185, 107665.
- [111] Garcia, I., Etxebarria, J., Boto-de-Los-Bueis, A., Diaz-Valle, D., Rivas, L., Martinez-Soroa, I., Saenz, N., Lopez, C., Del-Hierro-Zarzuelo, A., Mendez, R., *et al.* (2012). Comparative study of limbal stem cell deficiency diagnosis methods: detection of MUC5AC mRNA and goblet cells in corneal epithelium. *Ophthalmology* 119, 923-929.
- [112] Poli, M., Burillon, C., Auxenfans, C., Rovere, M.R., and Damour, O. (2015). Immunocytochemical Diagnosis of Limbal Stem Cell Deficiency: Comparative Analysis of Current Corneal and Conjunctival Biomarkers. *Cornea* 34, 817-823.
- [113] Holan, V., Trosan, P., Cejka, C., Javorkova, E., Zajicova, A., Hermankova, B., Chudickova, M., and Cejkova, J. (2015). A Comparative Study of the Therapeutic Potential of Mesenchymal Stem Cells and Limbal Epithelial Stem Cells for Ocular Surface Reconstruction. *Stem cells translational medicine* 4, 1052-1063.
- [114] Gao, Y., Li, Z., Hassan, N., Mehta, P., Burns, A.R., Tang, X., and Smith, C.W. (2013). NK cells are necessary for recovery of corneal CD11c+ dendritic cells after epithelial abrasion injury. *J Leukoc Biol* 94, 343-351.
- [115] Bock, F., Rossner, S., Onderka, J., Lechmann, M., Pallotta, M.T., Fallarino, F., Boon, L., Nicolette, C., DeBenedette, M.A., Tcherepanova, I.Y., *et al.* (2013). Topical

application of soluble CD83 induces IDO-mediated immune modulation, increases Foxp3⁺ T cells, and prolongs allogeneic corneal graft survival. *Journal of immunology* (Baltimore, Md : 1950) *191*, 1965-1975.

[116] Di Zazzo, A., Kheirkhah, A., Abud, T.B., Goyal, S., and Dana, R. (2017). Management of high-risk corneal transplantation. *Survey of ophthalmology* *62*, 816-827.

[117] Lin, M., Carlson, E., Diaconu, E., and Pearlman, E. (2007). CXCL1/KC and CXCL5/LIX are selectively produced by corneal fibroblasts and mediate neutrophil infiltration to the corneal stroma in LPS keratitis. *J Leukoc Biol* *81*, 786-792.

[118] Gan, L., Fagerholm, P., and Palmblad, J. (2004). Vascular endothelial growth factor (VEGF) and its receptor VEGFR-2 in the regulation of corneal neovascularization and wound healing. *Acta ophthalmologica Scandinavica* *82*, 557-563.

[119] Chang, L.K., Garcia-Cardena, G., Farnebo, F., Fannon, M., Chen, E.J., Butterfield, C., Moses, M.A., Mulligan, R.C., Folkman, J., and Kaipainen, A. (2004). Dose-dependent response of FGF-2 for lymphangiogenesis. *Proceedings of the National Academy of Sciences of the United States of America* *101*, 11658-11663.

[120] Liu, Y., Hamrah, P., Zhang, Q., Taylor, A.W., and Dana, M.R. (2002). Draining lymph nodes of corneal transplant hosts exhibit evidence for donor major histocompatibility complex (MHC) class II-positive dendritic cells derived from MHC class II-negative grafts. *The Journal of experimental medicine* *195*, 259-268.

[121] Hamrah, P., Huq, S.O., Liu, Y., Zhang, Q., and Dana, M.R. (2003). Corneal immunity is mediated by heterogeneous population of antigen-presenting cells. *J Leukoc Biol* *74*, 172-178.

[122] Yan, C., Gao, N., Sun, H., Yin, J., Lee, P., Zhou, L., Fan, X., and Yu, F.S. (2016). Targeting Imbalance between IL-1beta and IL-1 Receptor Antagonist Ameliorates Delayed Epithelium Wound Healing in Diabetic Mouse Corneas. *The American journal of pathology* *186*, 1466-1480.

[123] Robertson, D.M., Kalangara, J.P., Baucom, R.B., Petroll, W.M., and Cavanagh, H.D. (2011). A Reconstituted Telomerase-Immortalized Human Corneal Epithelium In Vivo: A Pilot Study. *Current eye research* *36*, 706-712.

[124] Kobayashi, T., Yoshioka, R., Shiraishi, A., and Ohashi, Y. (2009). New technique for culturing corneal epithelial cells of normal mice. *Molecular Vision* *15*, 1589-1593.

[125] Kawakita, T., Shimmura, S., Hornia, A., Higa, K., and Tseng, S.C.G. (2008). Stratified epithelial sheets engineered from a single adult murine corneal/limbal progenitor cell. *Journal of Cellular and Molecular Medicine* *12*, 1303-1316.

[126] Sun, C.-C., Chiu, H.-T., Lin, Y.-F., Lee, K.-Y., and Pang, J.-H.S. (2015). Y-27632, a ROCK Inhibitor, Promoted Limbal Epithelial Cell Proliferation and Corneal Wound Healing. *PLOS ONE* *10*, e0144571.

- [127] Okumura, N., Ueno, M., Koizumi, N., Sakamoto, Y., Hirata, K., Hamuro, J., and Kinoshita, S. (2009). Enhancement on primate corneal endothelial cell survival in vitro by a ROCK inhibitor. *Investigative ophthalmology & visual science* 50, 3680-3687.
- [128] Polack, F.M., and McNiece, M.T. (1982). The Treatment of Dry Eyes with Na Hyaluronate (Healon®). *Cornea* 1, 133-136.
- [129] Stuart, J.C., and Linn, J.G. (1985). Dilute sodium hyaluronate (Healon) in the treatment of ocular surface disorders. *Annals of ophthalmology* 17, 190-192.
- [130] Chung, J.H., Fagerholm, P., and Lindstrom, B. (1989). Hyaluronate in healing of corneal alkali wound in the rabbit. *Exp Eye Res* 48, 569-576.
- [131] Chung, J.H., Kim, W.K., Lee, J.S., Pae, Y.S., and Kim, H.J. (1998). Effect of topical Na-hyaluronan on hemidesmosome formation in n-heptanol-induced corneal injury. *Ophthalmic research* 30, 96-100.
- [132] Gomes, J.A.P., Amankwah, R., Powell-Richards, A., and Dua, H.S. (2004). Sodium hyaluronate (hyaluronic acid) promotes migration of human corneal epithelial cells in vitro. *The British journal of ophthalmology* 88, 821-825.
- [133] Ahmadiankia, N., Ebrahimi, M., Hosseini, A., and Baharvand, H. (2009). Effects of different extracellular matrices and co-cultures on human limbal stem cell expansion in vitro. *Cell biology international* 33, 978-987.
- [134] Kim, E.K., Lee, G.H., Lee, B., and Maeng, Y.S. (2017). Establishment of Novel Limbus-Derived, Highly Proliferative ABCG2(+)/ABCB5(+) Limbal Epithelial Stem Cell Cultures. *Stem cells international* 2017, 7678637.
- [135] Buentke, E., Mathiot, A., Tolaini, M., Di Santo, J., Zamoyska, R., and Seddon, B. (2006). Do CD8 effector cells need IL-7R expression to become resting memory cells? *Blood* 108, 1949-1956.
- [136] Krulova, M., Pokorna, K., Lencova, A., Fric, J., Zajicova, A., Filipec, M., Forrester, J.V., and Holan, V. (2008). A rapid separation of two distinct populations of mouse corneal epithelial cells with limbal stem cell characteristics by centrifugation on percoll gradient. *Investigative ophthalmology & visual science* 49, 3903-3908.
- [137] Chintakuntlawar, A.V., and Chodosh, J. (2009). Chemokine CXCL1/KC and its receptor CXCR2 are responsible for neutrophil chemotaxis in adenoviral keratitis. *J Interferon Cytokine Res* 29, 657-666.
- [138] Majo, F., Rochat, A., Nicolas, M., Jaoude, G.A., and Barrandon, Y. (2008). Oligopotent stem cells are distributed throughout the mammalian ocular surface. *Nature* 456, 250-254.
- [139] Di Girolamo, N., Bobba, S., Raviraj, V., Delic, N.C., Slapetova, I., Nicovich, P.R., Halliday, G.M., Wakefield, D., Whan, R., and Lyons, J.G. (2015). Tracing the Fate of Limbal Epithelial Progenitor Cells in the Murine Cornea. *Stem cells (Dayton, Ohio)* 33, 157-169.

- [140] Sun, T.-T., Tseng, S.C., and Lavker, R.M. (2010). Location of corneal epithelial stem cells. *Nature* *463*, E10-E11.
- [141] Schermer, A., Galvin, S., and Sun, T.T. (1986). Differentiation-related expression of a major 64K corneal keratin in vivo and in culture suggests limbal location of corneal epithelial stem cells. *The Journal of cell biology* *103*, 49-62.
- [142] Yeung, A.M., Schlotzer-Schrehardt, U., Kulkarni, B., Tint, N.L., Hopkinson, A., and Dua, H.S. (2008). Limbal epithelial crypt: a model for corneal epithelial maintenance and novel limbal regional variations. *Archives of ophthalmology (Chicago, Ill : 1960)* *126*, 665-669.
- [143] Qi, X., Xie, L., Cheng, J., Zhai, H., and Zhou, Q. (2013). Characteristics of Immune Rejection after Allogeneic Cultivated Limbal Epithelial Transplantation. *Ophthalmology* *120*, 931-936.
- [144] Özdemir, Ö., Tekeli, O., Örnek, K., Arslanpençe, A., and Yalçundağ, N.F. (2004). Limbal autograft and allograft transplantations in patients with corneal burns. *Eye* *18*, 241-248.
- [145] Alldredge, O.C., and Krachmer, J.H. (1981). Clinical types of corneal transplant rejection. Their manifestations, frequency, preoperative correlates, and treatment. *Archives of ophthalmology (Chicago, Ill : 1960)* *99*, 599-604.
- [146] Figueiredo, F.C., Nicholls, S.M., and Easty, D.L. (2002). Corneal Epithelial Rejection in the Rat. *Investigative ophthalmology & visual science* *43*, 729-736.
- [147] Abuzakouk, M., Feighery, C., and O'Farrelly, C. (1996). Collagenase and Dispase enzymes disrupt lymphocyte surface molecules. *Journal of immunological methods* *194*, 211-216.
- [148] Shultz, L.D., Ishikawa, F., and Greiner, D.L. (2007). Humanized mice in translational biomedical research. *Nature Reviews Immunology* *7*, 118-130.
- [149] Pepose, J.S., Nestor, M.S., Gardner, K.M., Foos, R.Y., and Pettit, T.H. (1985). Composition of cellular infiltrates in rejected human corneal allografts. *Graefe's archive for clinical and experimental ophthalmology = Albrecht von Graefes Archiv fur klinische und experimentelle Ophthalmologie* *222*, 128-133.
- [150] Frank, M.H., and Frank, N.Y. (2015). Restoring the cornea from limbal stem cells. *Regenerative Medicine* *10*, 1-4.
- [151] Pellegrini, G., Golisano, O., Paterna, P., Lambiase, A., Bonini, S., Rama, P., and De Luca, M. (1999). Location and clonal analysis of stem cells and their differentiated progeny in the human ocular surface. *The Journal of cell biology* *145*, 769-782.
- [152] Djalilian, A.R., Mahesh, S.P., Koch, C.A., Nussenblatt, R.B., Shen, D., Zhuang, Z., Holland, E.J., and Chan, C.C. (2005). Survival of donor epithelial cells after limbal stem cell transplantation. *Investigative ophthalmology & visual science* *46*, 803-807.
- [153] Chang, C.-Y., Green, C.R., McGhee, C.N.J., and Sherwin, T. (2008). Acute Wound Healing in the Human Central Corneal Epithelium Appears to Be

Independent of Limbal Stem Cell Influence. *Investigative ophthalmology & visual science* 49, 5279-5286.

[154] Saghizadeh, M., Kramerov, A.A., Svendsen, C.N., and Ljubimov, A.V. (2017). Concise Review: Stem Cells for Corneal Wound Healing. *Stem cells (Dayton, Ohio)* 35, 2105-2114.

[155] Carreño, E., Enríquez-de-Salamanca, A., Tesón, M., García-Vázquez, C., Stern, M.E., Whitcup, S.M., and Calonge, M. (2010). Cytokine and chemokine levels in tears from healthy subjects. *Acta Ophthalmologica* 88, e250-e258.

[156] Ebihara, N., Matsuda, A., Nakamura, S., Matsuda, H., and Murakami, A. (2011). Role of the IL-6 Classic- and Trans-Signaling Pathways in Corneal Sterile Inflammation and Wound Healing. *Investigative ophthalmology & visual science* 52, 8549-8557.

[157] Ghasemi, H. (2018). Roles of IL-6 in Ocular Inflammation: A Review. *Ocular Immunology and Inflammation* 26, 37-50.

[158] Arranz-Valsero, I., Soriano-Romaní, L., García-Posadas, L., López-García, A., and Diebold, Y. (2014). IL-6 as a corneal wound healing mediator in an in vitro scratch assay. *Exp Eye Res* 125, 183-192.

[159] van Gelderen, B.E., van der Lelij, A., Peek, R., Broersma, L., Treffers, W.F., Ruijter, J.M., and van der Gaag, R. (2000). Cytokines in Aqueous Humour and Serum before and after Corneal Transplantation and during Rejection. *Ophthalmic research* 32, 157-164.

[160] González, S., and Deng, S.X. (2013). Presence of native limbal stromal cells increases the expansion efficiency of limbal stem/progenitor cells in culture. *Experimental Eye Research* 116, 169-176.

[161] Baylis, O., Rooney, P., Figueiredo, F., Lako, M., and Ahmad, S. (2013). An investigation of donor and culture parameters which influence epithelial outgrowths from cultured human cadaveric limbal explants. *Journal of Cellular Physiology* 228, 1025-1030.

[162] James, S.E., Rowe, A., Ilari, L., Daya, S., and Martin, R. (2001). The potential for eye bank limbal rings to generate cultured corneal epithelial allografts. *Cornea* 20, 488-494.

[163] Sartaj, R., Zhang, C., Wan, P., Pasha, Z., Guaiquil, V., Liu, A., Liu, J., Luo, Y., Fuchs, E., and Rosenblatt, M.I. (2017). Characterization of slow cycling corneal limbal epithelial cells identifies putative stem cell markers. *Scientific Reports* 7, 3793.

[164] Ouyang, H., Xue, Y., Lin, Y., Zhang, X., Xi, L., Patel, S., Cai, H., Luo, J., Zhang, M., Zhang, M., *et al.* (2014). WNT7A and PAX6 define corneal epithelium homeostasis and pathogenesis. *Nature* 511, 358-361.

[165] Collinson, J.M., Chanas, S.A., Hill, R.E., and West, J.D. (2004). Corneal Development, Limbal Stem Cell Function, and Corneal Epithelial Cell Migration in the Pax6+/- Mouse. *Investigative ophthalmology & visual science* 45, 1101-1108.

